UNIVERSITY OF WARWICK

DEPARTMENT OF PHYSICS

HOLOGRAPHIC RECORDING IN COLOURED ALKALI HALIDE SINGLE CRYSTALS

BY

G.E. SCRIVENER

SEPTEMBER 1974

A B S T R A C T

This thesis characterises four alkali halide recording mediums which are suitable for holography. Holograms have been recorded with diffraction efficiencies of 4% and these show a marked wavelength sensitivity. Presented is an analysis that determines the wavelength variation of the diffraction efficiency and this is found to be in agreement with the experimental results.

CONTENTS

CONTENTS CONTINUED

CHAPTER ONE

1.1. INTRODUCTION

Photographic emulsions have a wider application than is often appreciated. Using currently available beam deflector and photodiode array technology it is possible to devise and construct optical computer memory elements using high speed, high resolution photographic films that store digitalised information employing direct or holographic techniques Systems have been designed and built that use photographic plates to store $\sim 10^8$ bits of information with a random access time of less than 1 μsec [1]. In general holographic systems are preferred because of the insensitivity of holograms to scratches and dust, also recording and reading the information is possible without the use of precision optics. Additionally holographic techniques are available such that exact optical alignment is unnecessary on readout. At present information cannot be updated or replaced at will, since to substitute information the photographic plates need to be replaced by new plates that have been prepared from a lengthy development procedure. These information stores are termed Read only optical memories - ROOM. A read/write store [2], where the information can be erased and then rewritten in real time, would require the photographic emulsion to be replaced by a photosensitive material that needs no development and is also reversible. That is, it can be exposed, interrogated and erased many times, i.e. a form of cyclicable photographic emulsion requiring no development.

At present there is a fairly intense research effort (reported in the literature) to produce a suitable reversible photosensitive material for fast holographic recording. Other possible applications, besides the more important data storage applications are for data processing techniques [3] and display purposes. Photochromic colour centre processes provide an extremely high resolution photosensitive medium, and in the final section of this chapter a review of reported holographic recording in alkalihalide colour centre photochromics is given, but firstly here, the important characteristics ideally required are listed [4]:-

a) The necessary recording exposure needs to be better than 4 mJoules/cm^2.

b) Erasure exposures of similar magnitude to the write exposure.

c) The resolution of the material needs to be adequate for typical holographic spatial frequencies i.e. 500-3,000 lines/mm.

d) Holographic diffraction efficiencies preferably greater than one percent.

e) A long fatigue free life time such that write-read-erase cycling does not noticeably alter the switching optical density. Life times of typically 10^5 cycles are ideally required.

f) Minimal scattering effects, and linear response (see section 1.2.3.)

g) Non destructive readout (N.D.R.O.). A fault with many reversible holographic recording mediums is that readout slowly erases the recording. For data processing and some display purposes D.R.O. may not prove to be a disadvantage. For data storage, frequent memory refreshment could occur; however, N.D.R.O. is ideally required.

At present there are no photosensitive materials suitable for holographic recording that have all the above stated features. This thesis investigates the possible application of colour centre photochromic processes to holographic recording. The experimental chapters consider four different colour centre processes which have been used to record holograms. Initially relatively insensitive cathodochromic potassium bromide and potassium chloride are examined, and included in their comparison is proof of a diffraction efficiency phase enhancement when the reconstruction wavelength differs from the wavelength of peak absorption. Chapter four uses dichroic absorption of M centres in sodium fluoride for recording and chapter five analyses the particularly sensitive F centre to F' centre photochromic process. This first chapter introduces separately the concepts of holography and colour centre phenomenon. Holograms have previously been recorded in alkali halide colour centre photochromics and a brief review of these is given in the final section of this chapter. A comparison of these photochromics (section 1.4) and the cathodochromics and photochromics studied in the experimental chapters two to five will finally be reviewed together with all other known reversible holographically sensitive media in chapter six.

1.2. HOLOGRAPHY

1.2.1. Introduction

Photography records in two dimensions the intensity distribution of an object as it is seen imaged through a lens. In the case of holography the object wave itself is recorded in amplitude and phase. This is achieved by recording on a high resolution photosensitive film the interference between the object wave and a coherent reference wave. The developed plate (if development is necessary) called a hologram, when illuminated by the original reference beam reproduces a diffracted wave identical to the original object wave. This holographic process is discussed in the following section. Originally the concept of this, two step method of optical imagery was conceived by Gabor [5] in 1949 and developed by Rogers [6] but not until the recent advent of the laser has holography made any significant scientific impact. Much of the basic and original work on holography was done by Leith and Upatnieks [7] and they were the first to record off axis reference beam holograms thus removing the double imaging effects of the early 'in line' holographic recordings. This had been necessary because of the unavailability of coherent light sources. Later in time the same two authors demonstrated the technique of redundant holographic recording. By using diffuse illumination it is possible to record at each point on the hologram all the object information and this means that partial damage to the hologram does not result in a loss of object information.

1.2.2. Basic Holography

As reported in the previous introduction, holography records specific wavefronts in amplitude and phase by their interference with a coherent reference wave. Consider the situation of Fig. 1.1 where an object scatters light into a region where a photosensitive plate is located, such that the object wave complex amplitude at the photosensitive plate is O. Illuminating the plate simultaneously is a reference wave of complex amplitude R. In each case, for the general analysis the amplitude and phase are functions of the spatial coordinates in the hologram plane. The intensity of the interference pattern is:-

$$(O + R)\ (O + R)^* \qquad (1)$$

where the term * represents the complex conjugate. We assume here that the photosensitive plate records in a linear fashion such that the resulting amplitude transmission of the plate after development (if necessary) is directly proportional to the initial incident exposure. It is also assumed that the recording medium is capable of resolving the interference pattern. Reconstruction of the hologram takes place with the same reference wave which now becomes modulated by the amplitude transmission of the hologram to take the form proportional to:-

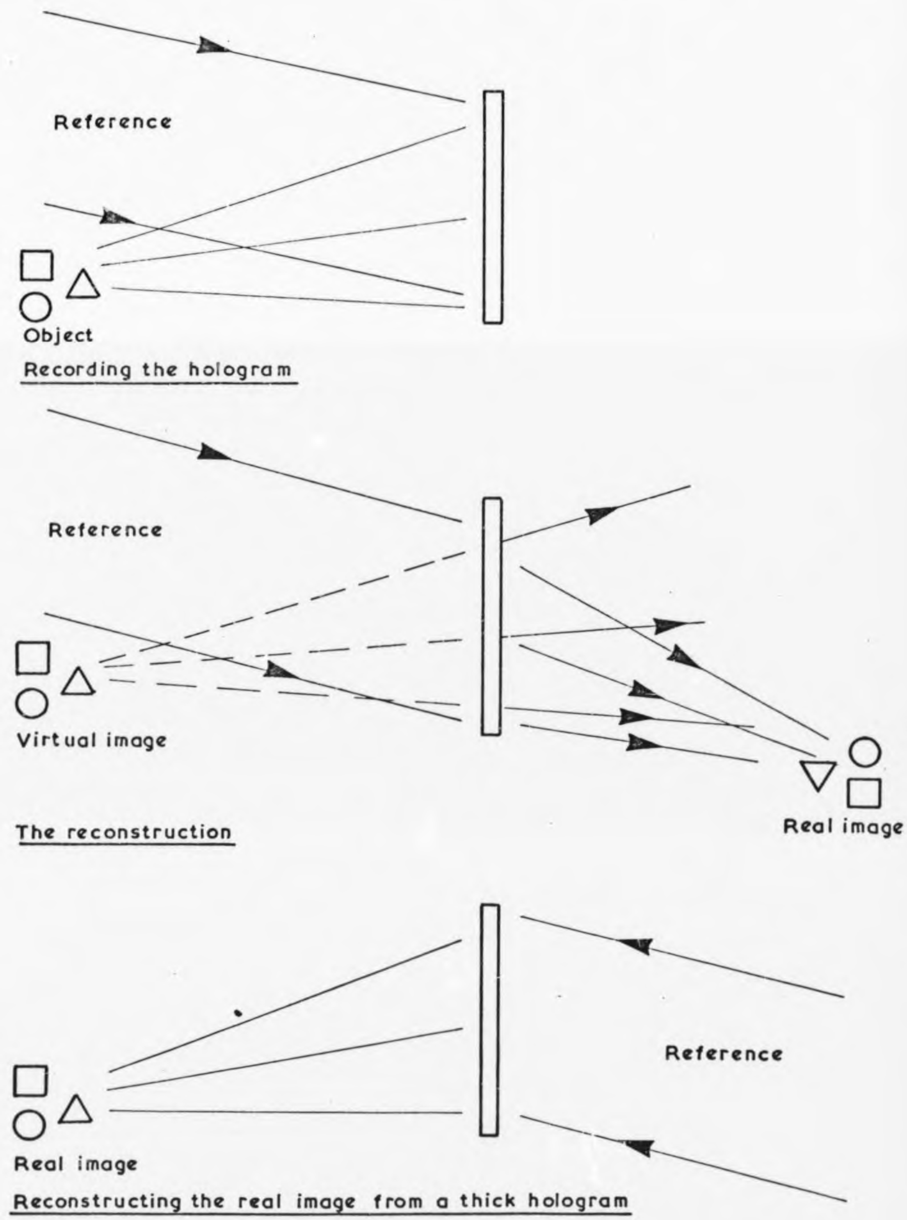

FIG.1.1. BASIC HOLOGRAPHY

$$R\,(O + R)\,(O + R)^*$$
$$= R\,OO^* + RRR^* + RRO^* + RR^*O \qquad \ldots\ldots \qquad (2)$$

Each term represents a wave emerging from the hologram. The first two terms correspond to the directly transmitted light while the last two terms refer to the diffracted light. Provided R is sufficiently uniform such that R^2 is approximately constant across the hologram, and this normally arranged by making R a plane wave, the object is reconstructed as a virtual image represented by the term RR^*O in equation (2). In the case of a thin hologram (where the fringe spacing is very much larger than the holograms thickness) the term RRO^* would refer to a real image formed in front of the hologram's plane, and the two reconstructions are shown graphically in Fig. 1.1. For thick holograms (where the fringe spacing is much less than the holographic thickness) only the virtual image is reconstructed [8]. In order to reconstruct a real image from a thick hologram it is necessary to illuminate the hologram by the original reference wave's complex conjugate, with the hologram rotated through 180^o, resulting in the 'imaging' shown in Fig. 1.1.

Transmission holographic diffraction can take place in one of four ways, the hologram can be thick (volume hologram) or thin (plane hologram) and diffraction may be due to absorption or refractive index variations. Replacing the absorption variations that give rise to diffraction in an absorption hologram by refractive index variations results in what is termed a phase hologram. Because there is no inherent absorption, phase holograms can produce large diffraction efficiencies and in some cases 100% diffraction is predicted [9] and 90% has been observed experimentally [10].

No attempt will be made here to analyse the process of diffraction as this is well covered in the literature [8, 11 and 12] for all types of holograms. A brief review of the coupled wave analysis [9] approach is given at the end of chapter two in order to clarify the interpretation of the experimental results therein.

In conclusion to this subsection it is worthwhile to comment briefly on the various experimental optical arrangements suitable for holographic recording. When the two interfering wavefronts in the hologram plane have the same curvature the hologram formed is called a Fourier Transform (F.T.) hologram. The reason for this is apparent from Fig. 1.2(a) where the object

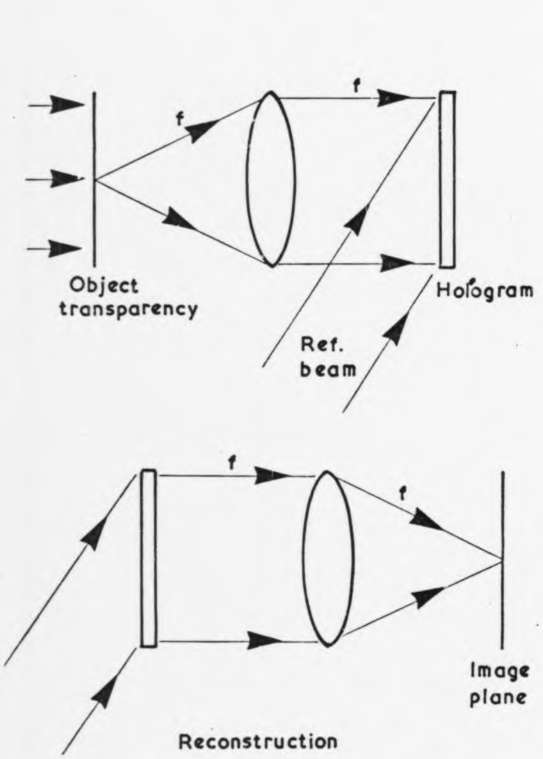

FIG.1.2(a) FOURIER TRANSFORM HOLOGRAM RECORDING.

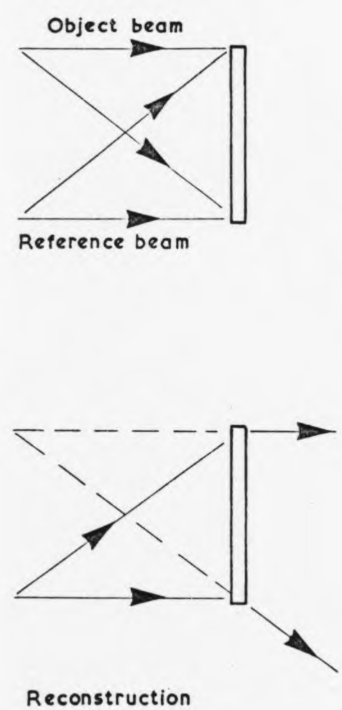

FIG.1.2(b) LENSLESS FOURIER TRANSFORM RECORDING

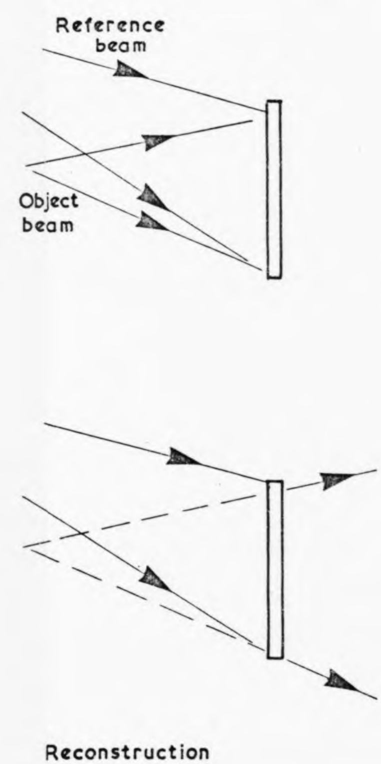

FIG. 1.2(c) FRESNEL RECORDING

is Fourier Transformed into the hologram plane, by use of the lens shown. Fig. 1.2(b) shows a lensless F.T. holographic recording and likewise results from the interference of two identical wavefronts. When the recording is made with two dissimilar wavefront curvatures the hologram is termed Fresnel (Fig. 1.2(c)). For two similar wavefronts the interference pattern consists of straight line fringes perpendicular to the plane containing the two interfering beams. In the case of interference between two dissimilar wavefronts the resulting pattern is considerably more complex. The properties of these two types of holograms are very different.

1.2.3. Characterisation of Recording Mediums

In general holographic recording mediums can only resolve a finite range of spatial frequencies, and care must be taken in the design of a holographic recording system not to exceed the resolution capability. For Fourier Transform holography the reconstructed field of view is limited by the high frequency cut off normally associated with many types of recording media. In the case of Fresnel recording object spatial frequencies are resolved only if the medium can resolve their interference with the reference wave. Resolution is normally referred to in terms of the modulation transfer function where the diffraction efficiency is expressed in terms of the spatial frequency for the particular medium in question.

Another important characteristic feature of any recording medium is that of its amplitude transmittance variation with exposure. In holography the diffraction properties are controlled by the amplitude transmittance of the recording medium and this is an important parameter in linear holographic recording. The reconstruction must have a one to one correspondence with the object intensity distribution in the same way a photographic film has when operated within the linear region of the Hurter and Driffield curve. Consequently care must be taken to ensure linear operation such that a faithful representation of the object is produced on reconstruction. A typical photographic emulsion transfer curve is shown in Fig. 1.3. To operate in the linear region it is necessary to record with an uneven beam ratio intensity such that the d.c. biasing associated with a visibility less than unity 'centres' the exposure onto the linear region. This is illustrated schematically in Fig. 1.3. Because of this a reduction in diffraction efficiency results.

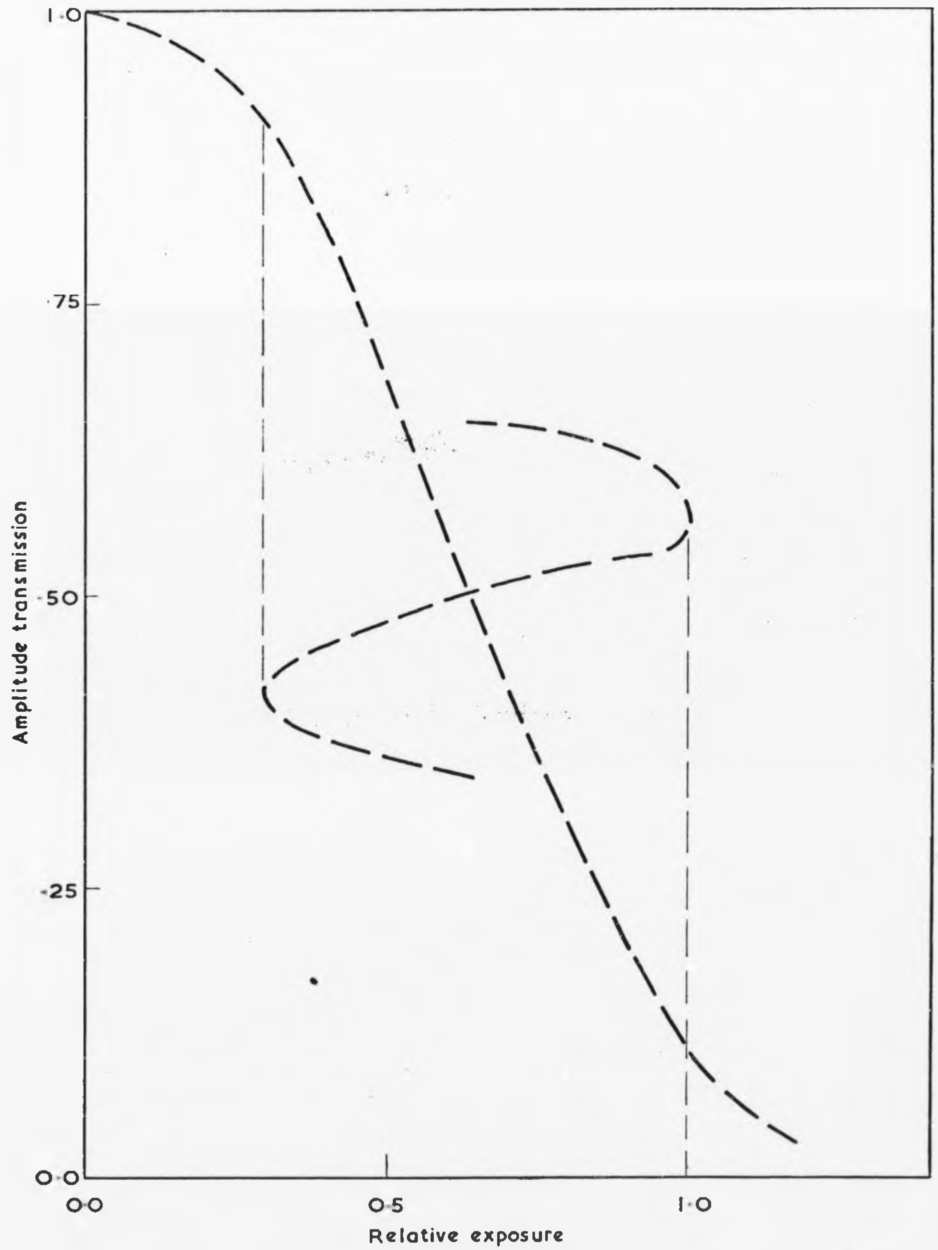

FIG.1.3. TYPICAL EMULSION TRANSFER CURVE SHOWING LINEAR OPERATION WITH INCIDENT FRINGE VISIBILITY OF LESS THAN UNITY

1.3. COLOUR CENTRE PHENOMENON

1.3.1. Introduction

For the greater part of this century the phenomenon of colour centres in insulating solids has been a subject of intense interest. Within the literature are many extensive reviews of the topic [13, 14 and 15]. The alkali halides of interest here are all of the sodium chloride structure and are easily obtainable, commercially, in single crystal form with a reasonable degree of purity, typically better than 20 p.p.m. At normal temperatures the alkali halides are highly insulating solids with a large window in their absorption spectrum in the visible region. In the ultra violet (usually $>$ 6 ev) there is the fundamental absorption edge.

By far the most common defect centre produced in the alkali halides is the F centre [15] and this consists of an electron trapped at a negative ion vacancy. The absorption resulting from the 1s - 2 p electron transistion is known as the F band, and this normally, although not always, occurs in the visible region. Shown in Fig. 1.4 is the F centre configuration schematic. It is possible to produce with relative ease large F centre concentrations and for this reason cathodochromic and photochromic F centre systems have an obvious application to direct or holographic image retention. Room temperature bleaching of the F band usually results in the formation of the M, N and R aggregate centres and these are also shown schematically in Fig. 1.4.

None of the above mentioned defect centres, nor indeed any of the other centres involved in the colour centre processes used for holographic recording in the experimental chapters of this thesis are dealt with in depth here, since they are not, for this thesis, of interest from a solid state physics view point. Generally their spectroscopic behaviour is the important relevance to the holographic characterisation and this is dealt with separately at the beginning of each of the experimental chapters. However an introductory appraisal of photochromic and cathodochromic effects is given in the following two subsections.

1.3.2. Photochromic Effects

Photochromics have the property of changing colour reversibly under visible or ultraviolet illumination. This effect occurs in many forms of organic and inorganic compounds, although only colour centre effects in alkali halide crystals

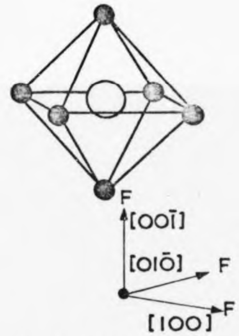

(a) F centre

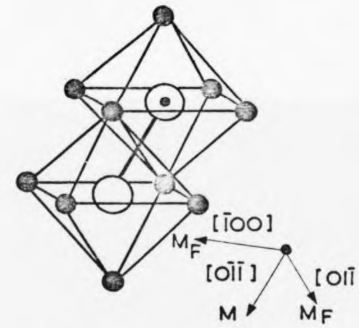

(b) M centre

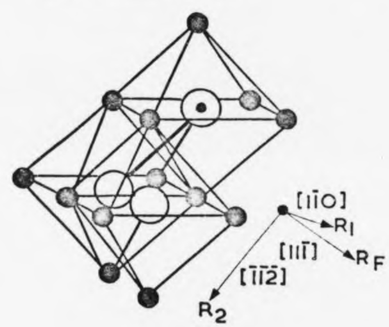

(c) R centre

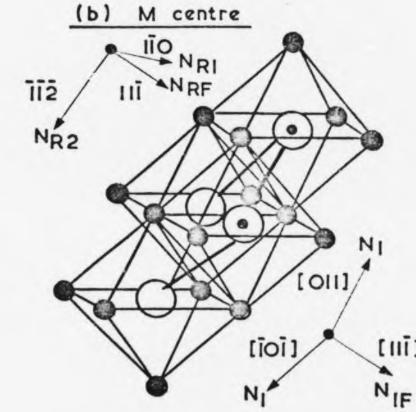

(d) N centre

FIG. 1.4.

are of interest here. The two photochromic systems of interest in this thesis involve absorption that can be reduced by exposure in that absorption band, and this results in the formation of another centre and associated absorption. By selective exposure the concentration of the various centres can be altered and consequently the absorption in each of the bands is changed.

There are three basic techniques for the production of defect centres in the alkali halides and these are:-

1. Additive colouration
2. Electrolytic colouration
3. Colouration by ionising radiation

Relevant to the following experimental chapters are the additive colouration techniques which essentially consist of heating the alkali halide close to its melting point in the presence of the metal vapour. Fairly large F centre concentrations are easily achieved for relatively short colouration times using a technique originally suggested by Van Doorn [16]. This is explained more fully in chapter five. At low temperatures it is possible to reduce the F centre concentration by an F $\longrightarrow$ F' centre conversion, and the reverse reaction is possible under suitable conditions.

Electrolytic colouration is accomplished by the application of an electric field to the pure crystal at high temperatures. Usually the cathode is pointed and at the flat anode halogen gas is evolved leaving the crystal with an stoichiometric excess of alkali metal. A colouration is produced characteristic of F centre absorption. At temperatures such that ionic motion occurs, electric fields of approximately 100 volts/cm are adequate to produce dense colourations, although the main disadvantage of this technique is that inhomogenous defect concentrations are produced.

Colouration is also possible by ionising radiation. Exposure to ultraviolet radiation, soft x-rays, gamma rays and electron beams produce colour centres. Cathodochromism, where electron beam colouration can be bleached optically is considered separately in the following subsection since two experimental chapters involve this effect. The commonest technique used in experimental colouration is that using x-ray sources and this topic is well covered in the literature [13]. Two prominent absorption bands are produced after irradiation at all temperatures from 4^{o}K to 300^{o}K and these are due to F and V centres.

It is generally accepted that an homogenous 'photochromic' concentration is required for holographic recording since this enables a consistant characterisation relative to other recording mediums. Because of the difficulty in obtaining homogenous defect concentrations using electrolytic and x-ray colouration techniques, only electron beam and additive colourations were used as a source of cathodochromic and photochromic material.

1.3.3. Cathodochromic Effects

For the purposes of this discussion, cathodochromic crystals are those which colour when bombarded with electrons. It is then possible by visible irradiation to bleach the induced colouration. Although this effect is observed in many types of compounds [17,18] only the alkali halides will be considered briefly here. For many of these, colouration can occur for electron energies of as little as 5 keV, and this produces complimentary F and V centres (which are displaced halogen atom clusters), the stability of which depends on the temperature of electron irradiation. Large F centre concentrations of 10^{17} - 10^{19} per cm^3. are obtainable in the potassium halides for incident electron doses of $\sim 10^{20}$ keV/cm^3.

Although there is not an excessive amount of documentation on defect production by fast electrons, it is thought that the generation processes and defect centres produced are very similar to those for x-ray production. There were many early theories proposed for defect production by ionising radiation [13], and it is now thought that the model proposed by Pooley [19] and Hersh [20] provides the most satisfactory explanation. F centre generation takes place via an electron-hole pair (exciton) recombination. Initial excitation of the negative ion forms an excited halogen ion - halogen atom combination (^{V}K centre) and this is considered as a 'hole' coupled to the electron which now occupies the vacancy generated by the ^{V}K centre production. Radiationless transitions take place from the exciton giving energy to the two halogen ions, but due to lattice interactions this is divided unequally. The more energetic ion may then start a $\langle 110 \rangle$ crystal axis collision sequence resulting finally in the formation of the interstitial centre separated from the F centre.

Clusters of these interstitial centres give rise to the ^{V} band and its stability depends on the electron irradiation temperature. For low temperature colouration ($\sim 77^{o}K$) it is found that on F band illumination the crystal returns to its virgin state and this results from the recombination of the F and V centres, which during the irradiation were unable to separate to any distance. At room temperature electron irradiations the V band formed is unaltered by F band illumination since considerably more stable V centre clusters were generated during the irradiation. In this case F band illumination results in the formation of M, N and R band which are generated by F centre aggregation.

1.4. REVIEW OF HOLOGRAPHIC RECORDING IN ALKALI HALIDE CRYSTALS

1.4.1. Introduction

This section summarises research previously reported on holographic recording in photochromic and cathodochromic colour centres in alkali halide single crystals. Invariably use is made of F centre reduction because of the large optical density changes associated with this absorption. From a holographic view point it is desirable to utilise photochromic systems that can be totally modulated. This means that the colour centre absorption at the operating wavelength can be reduced to zero by optical bleaching, enabling more efficient holographic diffraction gratings to be produced.

1.4.2. Holographic Recording in Electron Coloured Sodium Chloride

Large F centre concentrations are obtained in single sodium chloride crystals when irradiated with an electron beam. The F centre concentration is reduced by exposure to 476.2 nm laser light resulting in the generation of aggregate centres. It is possible to cycle the F centre concentration (and hence the crystals absorption to Krypton Ion laser 476.2 nm. light) by progressive electron irradiation and optical bleaching. Holograms have been recorded in this cathodochromic material [21] and a system devised for reversible holographic information storage [22]. Although this recording medium has the advantage of high resolution and reversibility without any development stages; it has a poor holographic performance. Reported diffraction efficiencies of .04% have been achieved at spatial frequencies of 1000 lines/mm. This low diffraction efficiency is probably due to the residual 476.2 nm. absorption of the aggregate bands. Destructive readout is experienced by reconstruction at the writing wavelength but this can be eliminated by interrogation in the relatively stable R and M bands.

1.4.3. Holographic Storage Using F $\longrightarrow$ X centre Conversion in Potassium Chloride and Potassium Bromide

It is well known [13] that F band illumination at temperatures ~200°C leads to a reduction in F centre concentration and the formation of another absorption band - called the X band - which absorbs to the lower energy side of the F band. This X band is due to the formation of non scattering metal colloidal centres of size less than 5 μm. Using this photo thermal chemical process low diffraction efficiency holograms have been formed in electro-lytically and additively coloured single crystals of potassium bromide and chloride [23,23 and 25]. The holographic recording takes place at high temperature and this enables non destructive readout at room temperature, although this then means rather lengthy write-read-erase cycling times. Write exposures of between 1 and 10 Joules/cm^2 are required and diffraction efficiencies of 0.03% have been reported on crystals coloured electrolytically during growth.

Recently [26] direct and holographic image retention has been reported using F $\longrightarrow$ X conversion in coloured sodium chloride which when heated to 140°C requires incident exposures of typically 1 Joule/cm^2.

1.4.4. Storage Properties of F_A centre Holograms

When one of the alkali ions adjacent to an F centre is replaced by a foreign alkali cation of smaller size than the host cation, the resulting centre is called an F_A centre. The reduction in symmetry of the cubic F centre to the tetragonal F_A centre gives a dichroic absorption spectrum. That is, there is a polarisation dependence of absorption. The three-fold degenerate F centre transistion is split into two, one polarised in the direction of the impurity ion (110 direction) and a two-fold degenerate transistion perpendicular to the impurity direction. By suitable polarisation of the incident illumination it is possible to switch centres with transistion moments parallel to the incident polarisation to other possible orientations, and this dichroism can be used for direct or holographic recording [27 - 30]. For sodium doped potassium chloride, holographic storage has been reported using a helium neon laser with incident exposures of 10 mJoules/cm^2. Holographic diffraction efficiencies of 0.1% have been measured and non-destructive readout is possible because of the decreased quantum efficiency of the reorientation process on cooling.

1.4.5. Holographic Storage in Hydrated Additively Colour Potassium Bromide

Hydration of additively coloured potassium bromide produces a colour centre absorption, at room temperature, in the ultraviolet at 228 nm.in addition to the F centre absorption at 625 nm. The ultra-violet absorption is due to the substitution of an hydrogen ion in place of the bromide lattice ion. Using U $\longrightarrow$ F centre conversion, holographic recording has been reported [31] in this medium and this is reversible since regeneration of the original U centre concentration is possible by heating. Although the writing process is very insensitive, non destructive readout is possible by interrogation of the F band modulation with 630 nm. light.

1.5.1. Conclusion

This introductory section has reported on holographic recording in photochromic and cathodochromic alkali halides, none of which appear to be particularly satisfactory in view of the ideal properties required of a recyclable holographic recording medium (section 1.1.1). In the following experimental chapters this thesis presents a detailed study of holographic recording in several types of photochromic and cathodochromic alkali halide crystals with many advantages over the materials surveyed here.

REFERENCES

[1] P. Waterworth D.C.J. Reid, Proceedings of the First European Electrooptics Markets and Technology Conference.

2 W. Stewart, L.S. Cosentino, App. Opts. Vol. 9 No. 10 2271.

3 E.M.I. Tech. Lt. No. 1839 issue 1.

4 M. R. Tubbs, Optics and Laser Techn. Aug. 1973 155.

5 D. Gabor, Proc. Royal Soc. Ser. A 1977, 454.

6 G.L. Rogers, Proc. Roy. Soc. Edin, 63A, 193, 1952.

7 E.N. Leith, J. Upatnieks, J. Opt. Soc. America 54, 1295.

8 Principles of Holography, H.M. Smith, Wiley.

9 H. Kogelnik, Bell Syst. Techn. J. 48, 2909.

10 L.H. Lin, App. Opts. No. 18, No. 5, 963.

11 Optical Holography, Collier et al, Academic Press.

12 E.G. Ramburg, R.C.A. Review 27 467.

13 Colour Centres in Solids, Schulman and Compton, Pergamon.

14 Physics of Colour Centres, Fowler (Editor), Academic Press.

15 F. Centres in Alkali Halides, J.J. Markham, Academic Press.

16 C.Z. Van Doorn Review of Scient. Instruments, 32, 755.

17 Z.J. Kiss, W. Phillips, Phys. Review 180, No. 3, 924.

18 K.C. Duncan Jr., B.W. Faughnam, W. Phillips, App. Opts. Vol.9, No. 10 2236.

19 D. Pooley, Proceedings Physical. Soc. Vol. 87, Pt.1, 245.

20 H.N. Hersh, Phys. Review Vol. 148, No. 2, 928.

21 A.S. Mackin, App. Opts., Vol. 9 No. 7, 1658.

22 A.S. Mackin, U.S.A. Patent No. 3671096.

23 B. Stadnik, Z. Tronner, Optics Communication Vol. 6, No. 2, 199.

24 B. Stadnik, Z. Tronner, Nouv. Rev. Optique Applique t.3, No. 6, 347.

25 B. Stadnik, Z. Tronner, Laser, No. 4, 46.

26 Brighton Electrooptics Conf. 1974 to be published.

27 Y. Shono, T. Luuzuka, T. Hoshino, App. Phys. Letts. Vol. 22, No. 6, 299.

28 N. Roder, Optics Com. Vol. 6, No. 3, 270.

29 H. Blume, T. Bader, Paper G 136, International Conf. on Colour Centres in Ionic Crystals, 1971.

30 F. Lanzl, N. Roder, W. Waidelich, Paper G 137, International Conf. on Colour Centres in Ionic Crystal 1971.

31 D. Huhn, W. Martienssen, Opto Electron. No. 2, 47.

CHAPTER TWO

HOLOGRAPHIC RECORDING IN ELECTRON COLOURED SINGLE CRYSTALS OF POTASSIUM BROMIDE

2.1.1. Introduction

The F band absorption of potassium bromide peaks at 625 nm.and has a half width of 0.36 eV. at room temperature. A convenient form of defect production in the alkali halides is by fast electron irradiation. This method of colouration is advantageous since large and homogenous defect concentrations are obtainable in coloured layers between 0.5 µm. to 500 µm. thick for 5-400 keV. electrons. The F band in potassium bromide is readily reduced by absorption in any part of the band and the effect may be utilised to record holograms using the 632.8 nm. output from a helium neon laser. Shown in Fig. 2.1 is the F band absorption and matching laser wavelength. Because the resolution is limited only by the F centre separation it is not difficult to record the spatial frequencies necessary for holography which are of the order of 10^3 - 10^4 lines/mm. For a typical F centre concentration of 10^{18} centres/cm^3 the F centre separation would be 10^{-5} mm.and this is clearly much smaller than that necessary to achieve a resolution of 10^3 - 10^4 lines/mm. There are none of the resolution problems associated with other holographic recording materials for example, photographic emulsions where granularity limits resolution to below 2000 lines/mm. Thick holograms have previously been recorded in potassium bromide as reported in section 1.4 of chapter one, although defect production by electron irradiation at liquid nitrogen temperatures followed by warming to room temperature for recording, to give high modulation recording conditions has not before been used for holography.

2.2.1. Sample Preparation

For the following holographic experiments crystal surfaces of good optical quality are required and there are three alternative preparation procedures:-

(a) Polishing of the crystal prior to colouration
(b) Polishing after colouration
(c) Index matching of cleaved crystals in a suitable non-reactive fluid.

The first two preparations are experimentally inconvenient, for (a) a conductive layer would need to be deposited on to the polished flat, since

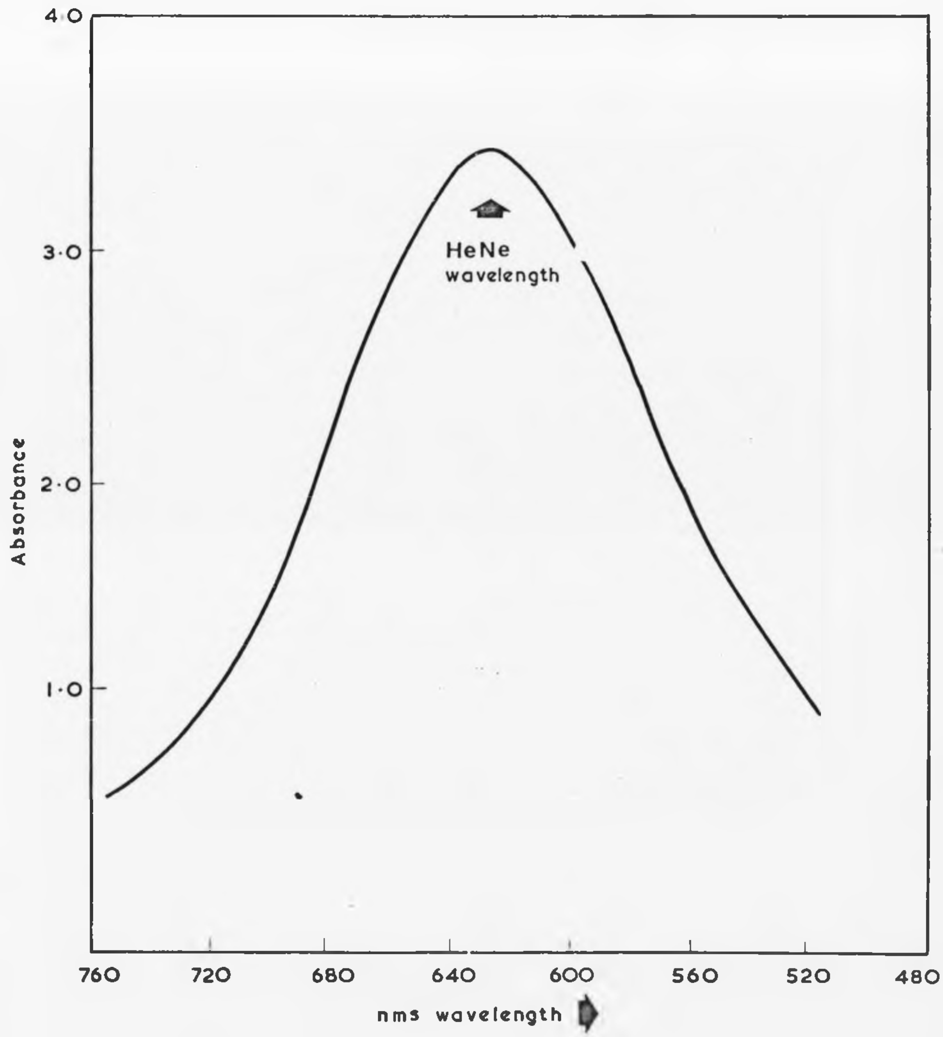

FIG. 2.1. F-BAND ABSORPTION IN KBr RELATIVE TO HeNe WAVELENGTH

surface damage is otherwise induced by the discharge of non-penetrating electrons collecting on the surface of the crystal during irradiation. Also the presence of a conducting layer would reduce the holographic performance of the coloured layer by attenuating the incident light and hence lowering the effective diffraction efficiency. In the case of (b) polishing would have to be performed in a safe light and sufficiently quickly such that thermochromic effects do not reduce the F centre concentration. Unavoidably some of the centres would be lost during polishing although an allowance could be made for this by over colouration of the crystal. Index matching of cleaved coloured crystals was found to be an extremely useful technique and for potassium bromide of refractive index 1.56, bromobenzene was used, a clear colourless unpleasant liquid with a matching refractive index to within 0.5% at the laser wavelength (630 nm).

2.2.2. <u>Electron Irradiation</u>

Relatively pure single crystals of potassium bromide grown by Messrs. Hilger and Watts (Rank Precision Industries) are cleaved, using a specially designed cleaving device, for mounting into the low temperature cryostat shown in Fig. 2.2. The crystal is maintained in intimate contact with the copper tail of the cryostat by means of a copper plate aperture and clamp which also restricts the electron irradiation to a sample area of 1 cm^2. This ensures an even colouration across the sample. Surrounding the cryostat tail and crystal mounting assembly is a copper x-ray shield with suitable apertures. An undesirable feature of x-ray colouration is that it produces a non uniform concentration of defects, as explained in section 1.3.2. A thermocouple was fitted to the cryostat's inner component to ensure correct temperature operation. The cryostat assembly was attached to the target end of a Van Der Graaf electron accelerator manufactured by the High Voltage Engineering Corporation, which is capable of generating electron energies between 20 keV and 400 keV at currents of up to 150 μ amps. An aluminium foil of thickness, 10 μm, was situated between the target crystal and electron gun to protect the sample from filament light which would otherwise effect the growth of the F band during irradiation. Electron penetration in potassium bromide is a function of accelerating voltage and for low energies at room temperature follows the form:-

$$d = 0.35 \ V^{1.7} \qquad \ldots\ldots \qquad [1]$$

where d is the penetration depth in μm, and V the accelerating voltage in K Volts. This does not hold true for higher voltages ($>$25 kV) and here d was determined

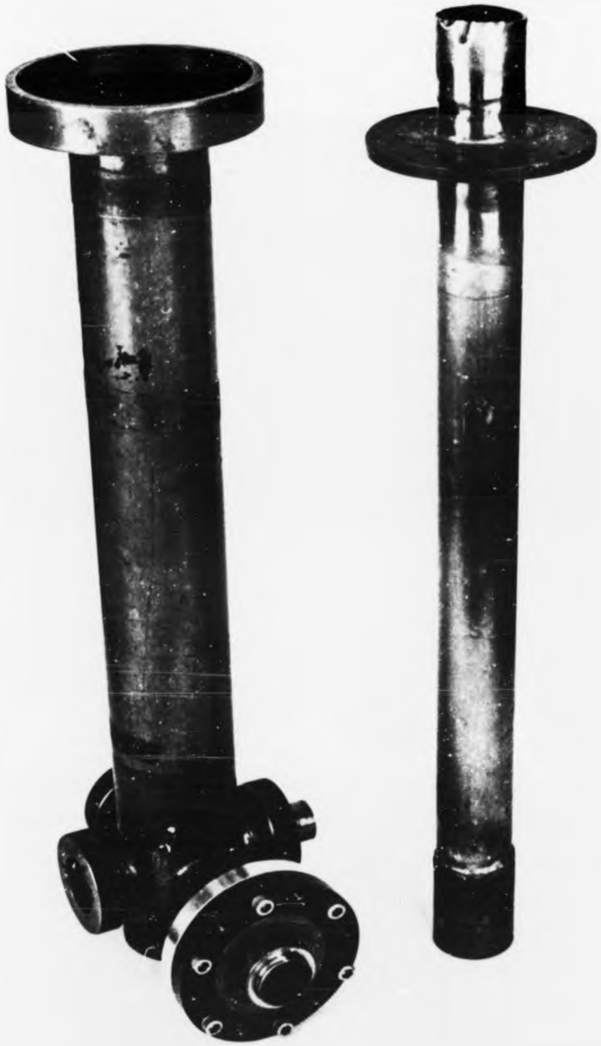

FIG. 2.2. LOW TEMPERATURE ELECTRON IRRADIATION CRYOSTAT.

experimentally by taking calibrated optical micrographs of the coloured crystal cross-section. The F centre concentration appears to be uniform in depth until the last 10% of penetration where it falls gradually to zero. Measured penetration depths were to the end of the even colouration, and for 350 keV irradiations at liquid nitrogen temperatures were found to be 500 μm. In order to produce large F band optical densities most irradiations were performed at 350 keV and 20 μ amps. Although higher electron fluxes could easily be achieved the small current was necessary to ensure that the crystal did not heat up during irradiation. A typical irradiation lasting 1-5 minutes at 350 keV would produce an F band absorption at 632.8 nm.of between approximately 3.0 and 8.0 optical density.

2.2.3. Optical Characterisation [2]

Two systems were considered for holographic recording, firstly room temperature (R.T.) electron irradiation of the alkali halide followed by R.T. optical bleaching, and secondly liquid nitrogen temperature (L.N.T.) electron irradiation followed by R.T. optical bleaching. The spectral changes in absorption after extensive F band bleaching are shown in Fig. 2.3 and Fig. 2.4 for R.T. and L.N.T. irradiations respectively. Also shown is the absorption spectrum of an uncoloured crystal. Present in each case prior to optical bleaching is a broad V band in the ultra-violet (due to clusters of interstitial centres), an F band at 625 nm.and a small M band at 917 nm. resulting from F centre aggregation during the electron irradiation. For R.T. electron irradiations, optical bleaching of the F band generates new absorption bands to the low energy side of the F band. The new absorption is due to the aggregation of F centres to form M, N and R centres. In the case of L.N.T. colouration the bleaching mechanism is quite different, here the V centres take an active part and recombine with F centres to produce a total reduction of all visible absorption. The two different bleaching mechanisms occur because of the different size of the V centres produced in each case. During R.T. colouration the Frenkel defects formed have greater mobility and thus are able to form large clusters of interstitial defects, while during L.N.T. colourations the interstitials are unable to move far from the lattice site from which they originate to form relatively small clusters. The larger V centres formed at R.T. are considerably more stable, because of their size, and are unaffected by either F or V band illumination, whereas the V centres formed at L.N.T. are sufficiently small and unstable for F centre combination to occur.

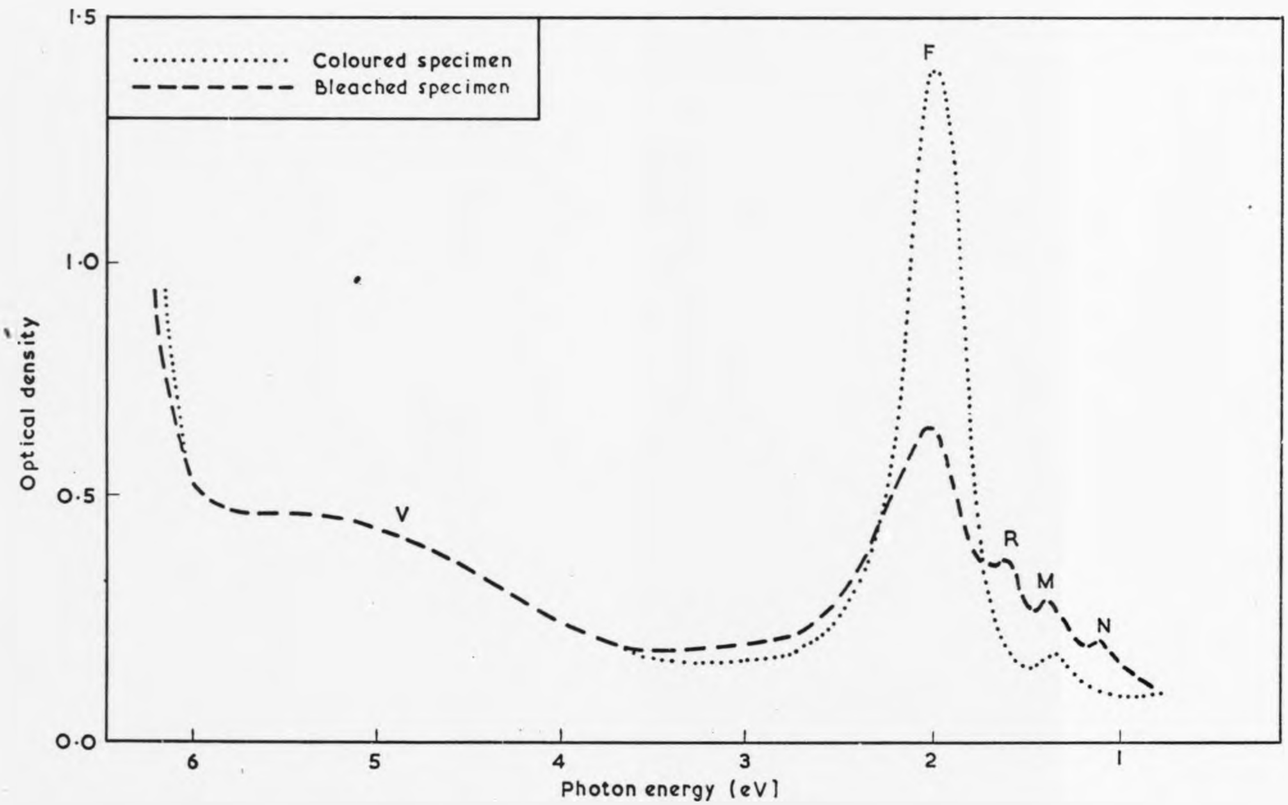

FIG.2.3. R.T. BLEACHING OF R.T. COLOURED POTASSIUM BROMIDE.

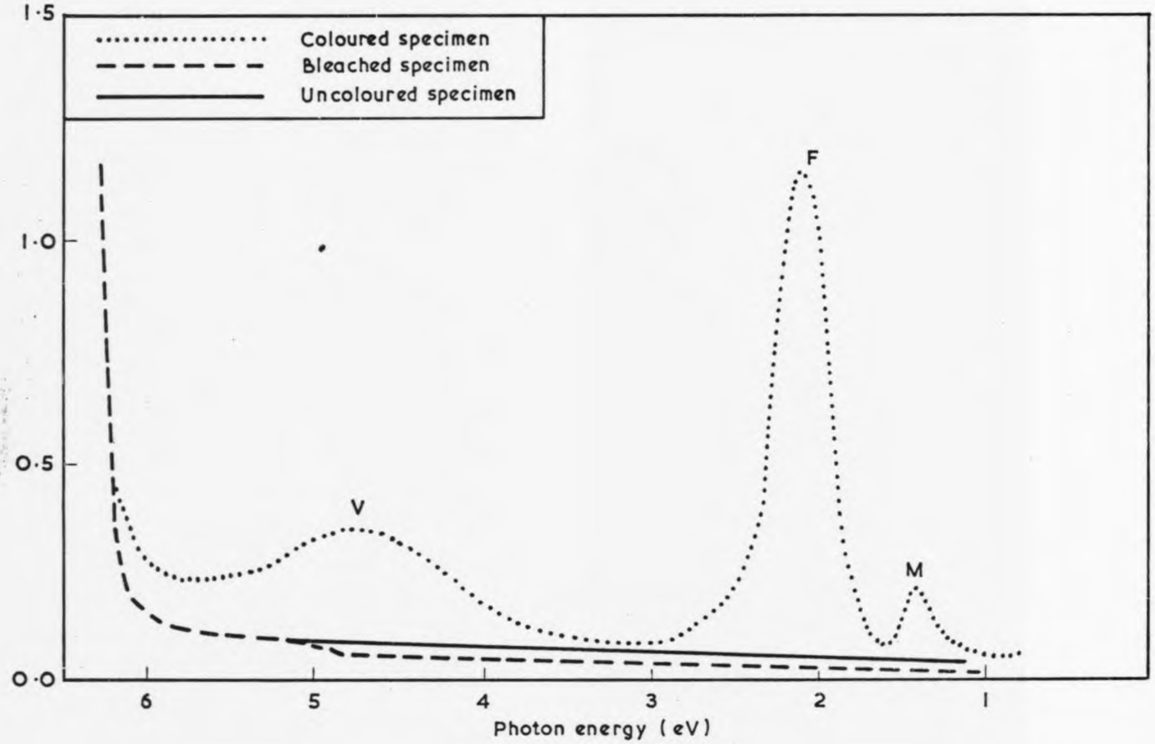

FIG.2.4. R.T. BLEACHING OF L.N.T. COLOURED POTASSIUM BROMIDE

The L.N.T. electron colouration is more advantageous for holography. This is because a holographic grating produced in this cathodochromic medium will not suffer any residual absorption common to both bleached and unbleached parts of the diffraction grating. For R.T. colourations this could never be the case since total modulation of the optical density is impossible (see Fig. 2.3), due to the presence of M_F and R_F centre absorption in the same spectral region as the F band.

2.3.1. Holographic Techniques

It is essential to achieve good fringe stability when recording a hologram. Movement in excess of one quarter fringe spacing during recording will lead to a washing out of the recorded incident fringe pattern. Instability arises from two sources, building vibration transmitted through the mountings to the optical components of the holographic arrangement, and small fluctuations in path length difference of the two interfering beams due to air currents arising from draughts or small temperature differences present in the system.

To minimise vibration all holographic components were mounted, using magnetic clamps, onto a heavy iron table which in turn rested on four anti-vibration pneumatic supports. These supports are shown diagrammatically in Fig. 2.5 and consist of an inflated rubber inner tube inside a metal cylinder. The table feet sit on steel plates supported by the inner tubes. Thermally induced effects were reduced by the use of cardboard box covers enclosing the optical arrangement, and finally the fringe stability was tested by inspection using a simple Michelson Interferometer arrangement built from the holographic optical components.

In the following holographic experiments a 30 mWatt B30 helium neon laser manufactured by Scientifica and Cook Ltd. was used. The helium neon laser is ideal for holography since it has a long coherence length and uniphase output is possible without difficulty.

2.4.1. Two Beam Interference Experiments

In general, practical recording media are not always able to resolve all the spatial frequencies present when two complex wavefronts interfere. A measure of the capability of a medium to resolve fine detail is called its modulation transfer function (M.T.F.) and this is expressed as the diffraction efficiency determined as a function of the spatial frequency spectrum. Because for colour centre materials the limiting resolution is governed only by the F centre separation no M.T.F. limitations are to be expected. Although this is solely dependent on the F centre concentration, for typical concentrations used

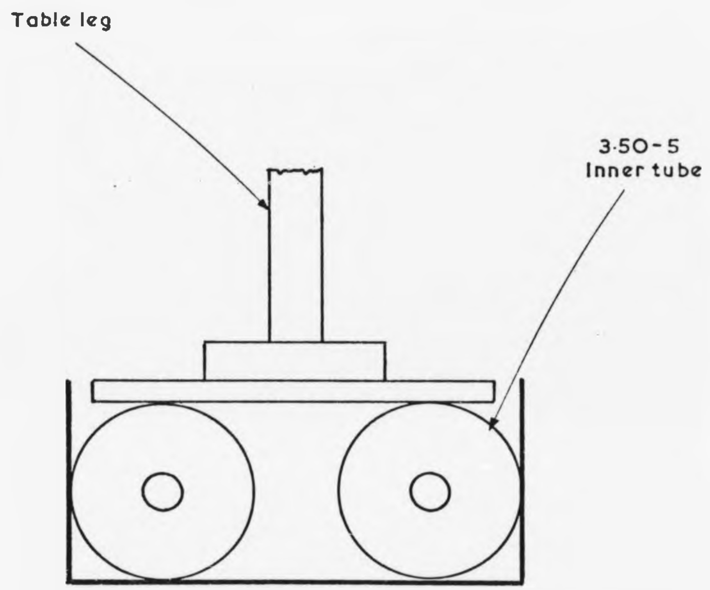

FIG. 2.5. CROSS-SECTION OF ANTIVIBRATION PNEUMATIC TABLE LEG SUPPORT.

in the following experiments spatial frequencies of 10,000 lines/mm.will be resolved without difficulty. For the two beam interference experiments reported in the following subsection a beam separation angle of 30° was used which gave a grating spacing of approximately 1 μm. calculated from the Bragg equation for interference between two plane waves:-

$$d' = \frac{\lambda}{2 \sin \theta/2}$$

where θ is the angle between beams and λ the wavelength of light.

In order to characterise the properties of holograms recorded in electron irradiated potassium bromide two beam interference experiments were performed using the optical arrangement shown schematically in Fig. 2.6,with this optical arrangement it was possible to determine variations of diffraction efficiency with exposure, initial F band optical density and deviation from the Bragg angle. The output from the laser is spatially filtered and then divided into two. In one beam are two polarisers set to ensure that the two incident beams are polarised in the vertical direction and are of equal intensity. A photodiode monitors the laser output continuously and a photocell is used to measure the diffracted signal which in some cases is very low. When recording the hologram the photocell was protected from high light levels by means of the neutral density filters shown. Exposure intensities were measured absolutely on a calibrated laser power monitor, also the two detectors used to determine the diffraction efficiency were calibrated although not absolutely since only relative intensities were required.

2.4.2. Holographic Diffraction Efficiency

Using the optical configuration of Fig. 2.6, initially the variation of diffraction efficiency with exposure was determined for a selection of colouration optical densities. The F band absorbance at the laser wavelength of 632.8 nm.was determined by use of a Perkin Elmer 450 spectrophotometer, which is capable of measuring optical densities to an upper limit of 4.0. When the optical density of a coloured crystal was in excess of 4.0 the absorbance at the laser wavelength was determined by extrapolation of the available data obtained, below the maximum optical density level of 4.0, assuming a Gaussian curve shape. The accuracy of this technique was checked by comparison of the F band halfwidth extracted from the Gaussian plot and values quoted in the literature [3].

A Helium Neon Laser

B Spatial Filter

C Lens

D Beam Splitter

E Shutter

F Polarisers

G Aperture

H Hologram

J N.D. Filters

K Photocell

L Photodiode

M Mirrors

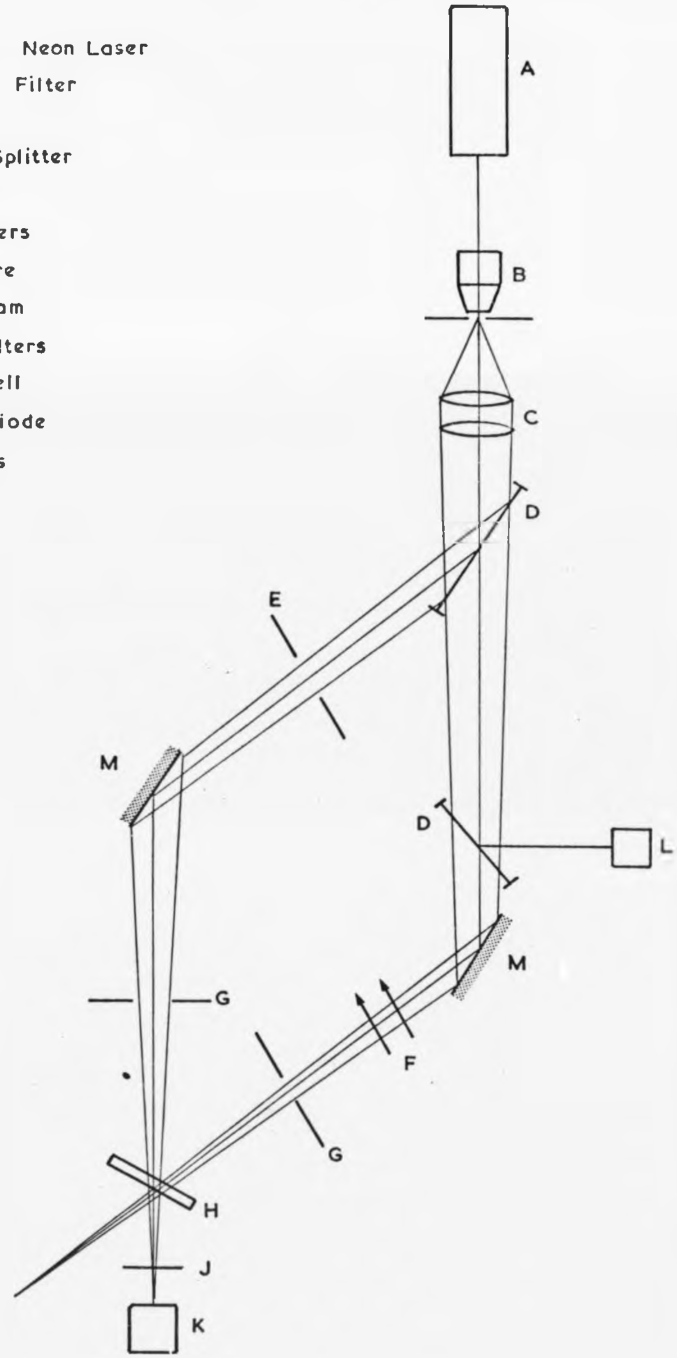

FIG. 2.6. TWO-BEAM INTERFEROMETER ARRANGEMENT.

In the hologram plane the crystal is mounted inside the holder assembly illustrated in Fig. 2.7 which consists of a spring loaded crystal grip fitted rigidly to the overhead support. A fused silica spectroscopic cell containing the index matching liquid fits over the crystal holder and is kept in place by means of a spring loaded seat.

The crystal was exposed to the two beam interference pattern for periods of approximately one minute in duration, the exact period of time being determined from the estimated total exposure required in each case. At the end of each period the diffracted intensity was measured by obstructing one of the incident beams and detecting the resulting diffracted intensity at the photocell. Each time the hologram is 'read' it suffers a short damaging exposure of approximately 1 sec., since the material exhibits destructive readout, although relative to the overall exposure this was not considered to alter the exposure characteristics significantly. For a series of coloured optical densities (measured at 632.8 nm.) the diffraction efficiency as a function of exposure is shown in Fig. 2.8 and the variation of peak diffraction efficiency with coloured optical density is plotted in Fig. 2.9.

2.5.1. Off Axis Recording

The calculated off axis variation of diffraction efficiency (or rocking curve) for thick holograms takes the form [4]:-

$$\frac{\eta}{\eta_{max}} = \frac{\mathrm{Sin}^2 \chi}{\chi^2} \qquad \ldots\ldots \quad 1$$

where $\chi = \dfrac{\pi d.\ n\ \mathrm{Sin}\,\theta\ \Delta\theta}{\lambda}$

and
- d is the holographic thickness
- n the refractive index of the medium
- θ the angle between the beams
- $\Delta\theta$ the deviation from the Bragg angle

From equation 1 the hologram's thickness can be expressed in terms of the rocking curve's halfwidth:-

$$\frac{3}{4\pi} = \frac{\mathrm{Sin}\,\theta\ \ \theta_{\frac{1}{2}}.}{n\lambda}\ d \qquad \ldots\ldots \quad 2$$

where $\theta_{\frac{1}{2}}$ is the deviation from the Bragg angle for the diffraction efficiency to fall by one half. Colouration depths used were 130 μm (corresponding to a colouration voltage of 150 KV) giving an expected $\theta_{\frac{1}{2}}$ of 30'.

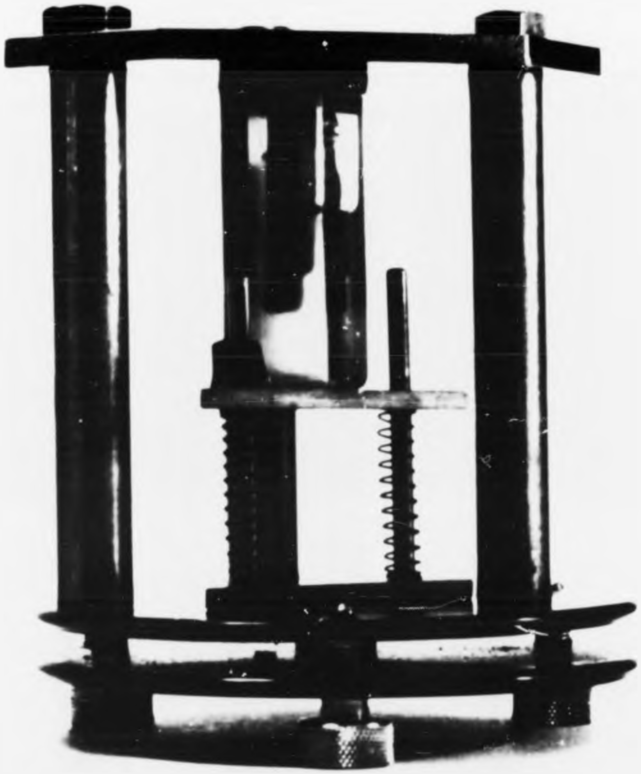

FIG. 2.7. CRYSTAL MOUNTING FOR HOLOGRAPHIC RECORDING IN ELECTRON COLOURED KBr.

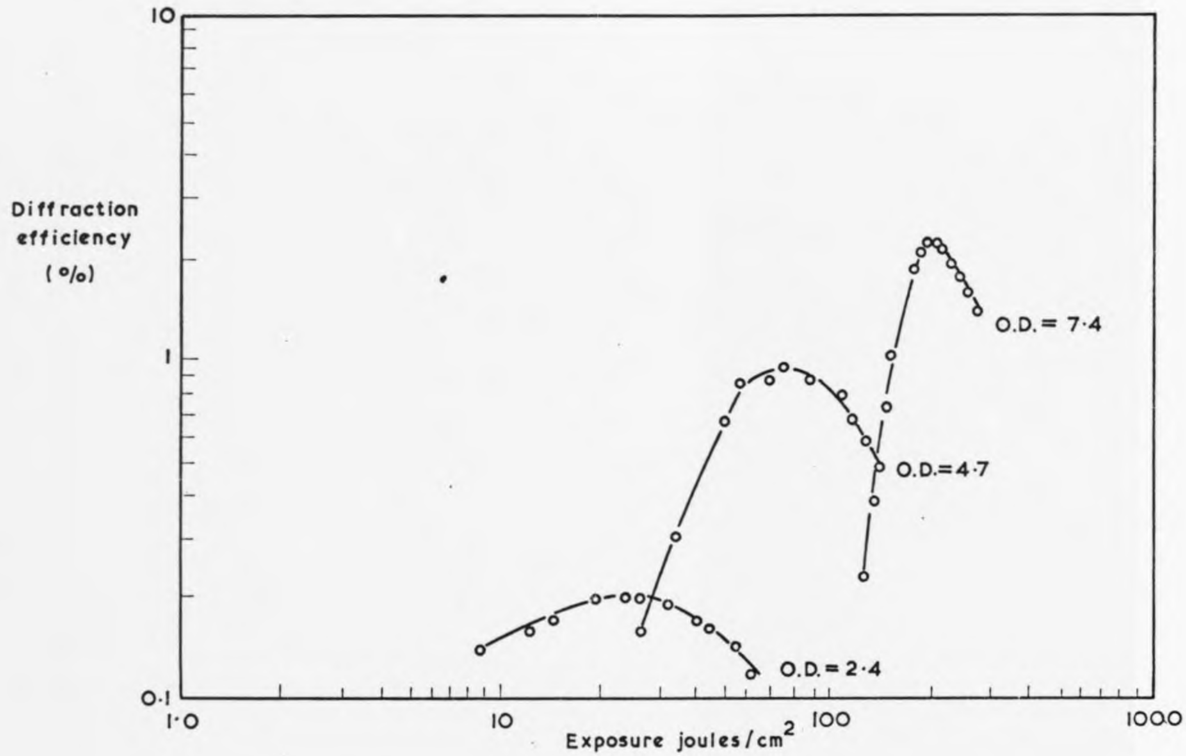

FIG. 2.8. DIFFRACTION EFFICIENCY VS EXPOSURE FOR A SERIES OF COLOURED O.D.'s (MEASURED AT 630 mns)

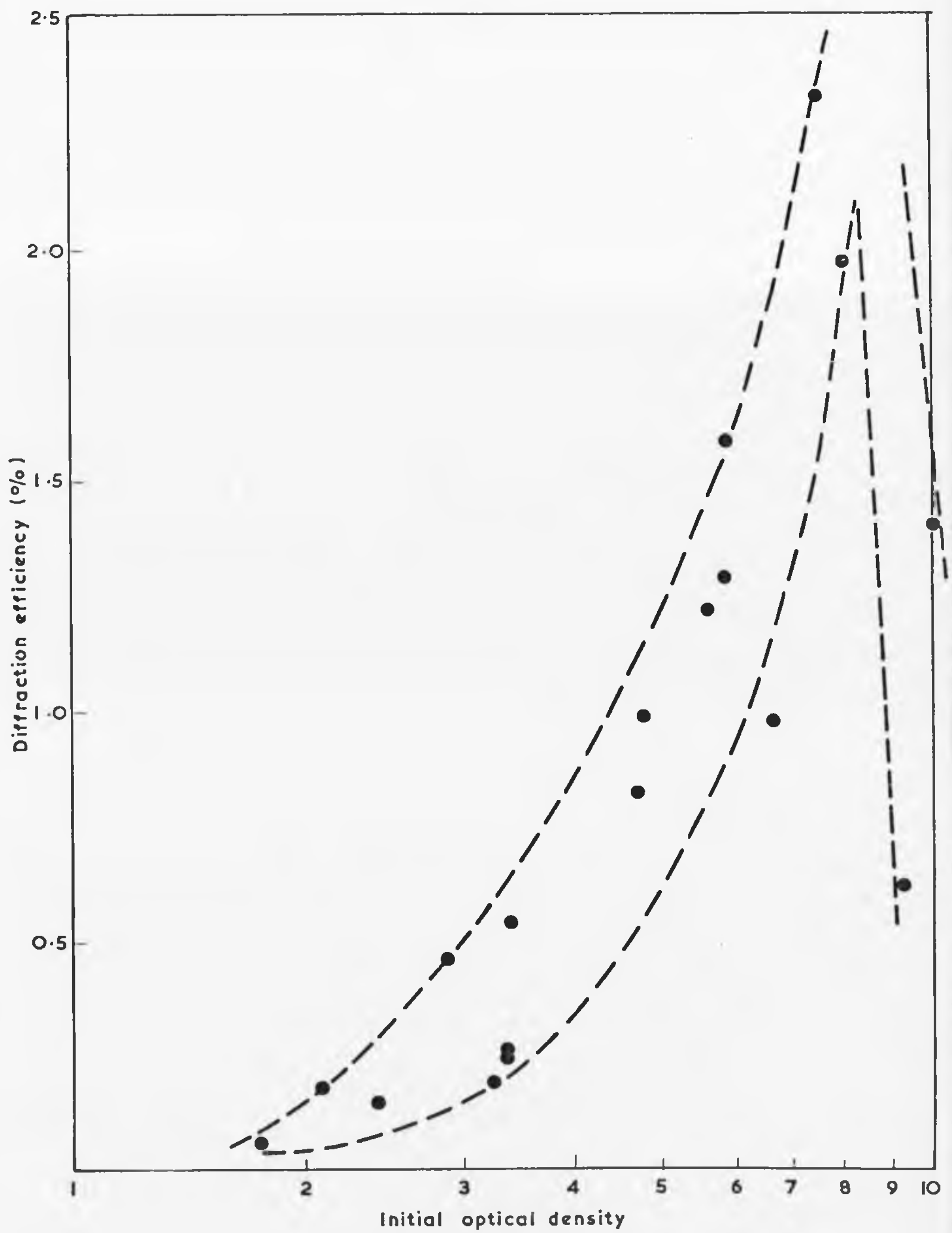

FIG. 2.9. PEAK DIFFRACTION EFFICIENCY AS A FUNCTION OF INITIAL OPTICAL DENSITY.

The experimental arrangement was that of Fig. 2.6 with the crystal and mounting assembly set onto the table of a vernier optical spectrometer, and this enabled accurate measurements to be made of the exact misorientation from the Bragg condition. Holograms were recorded until peak diffraction efficiency and then readout at angles away from the Bragg angle with a reduced beam intensity. Relative off axis efficiency is shown in Fig. 2.10, with an estimated halfwidth of 33' which from equation 2 indicates an effective holographic thickness of only 90 μm. A reduction in thickness of the original coloured layer is to be expected because of the uneven incident exposure through the gratings depth. At the optimum exposure, the front of the hologram is severely over exposed and does not contribute proportionally to the diffraction process. For these particular experiments a coloured layer thickness of 130 μm gave an effective holographic thickness of 90 μm.

An interesting feature of Fig. 2.10 is that no secondary maxima are present although they are predicted by equation 1 . It is thought that this again arises from the uneven exposure within the coloured layer, and a schematic representation is shown in Fig. 2.11 of a typical grating's cross-section. At the front surface it is over exposed whereas at the rear it is clearly under exposed. For each section through the depth of the grating it is apparent that the fringe modulation alters in the manner shown in Fig. 2.11. It has been shown before [5] that the rocking curve is related proportionally to the Fourier Transform of the variation of fringe modulation with depth. Although this function is not actually known it certainly will have an apodising effect on the rocking curve.

2.6.1. Recording a Transparency

The optical arrangement for recording the hologram of a transparency is shown in Fig. 2.12. Output from a helium neon laser is split into two, one beam is used directly as the reference, while the object beam is spatially filtered and focused through the hologram plane by means of a lens. The transparency is inserted between the spatial filter and lens such that an 'infocus' image is located on the otherside of the hologram. Since in the hologram plane interference takes place between a plane and complex wavefront the hologram is categorised as Fresnel.

After a suitable exposure the crystal was interrogated by the reference plane wave and the reconstructed wavefront viewed in focus after the hologram plane, where it was photographed. Fig. 2.13 shows the reconstruction together

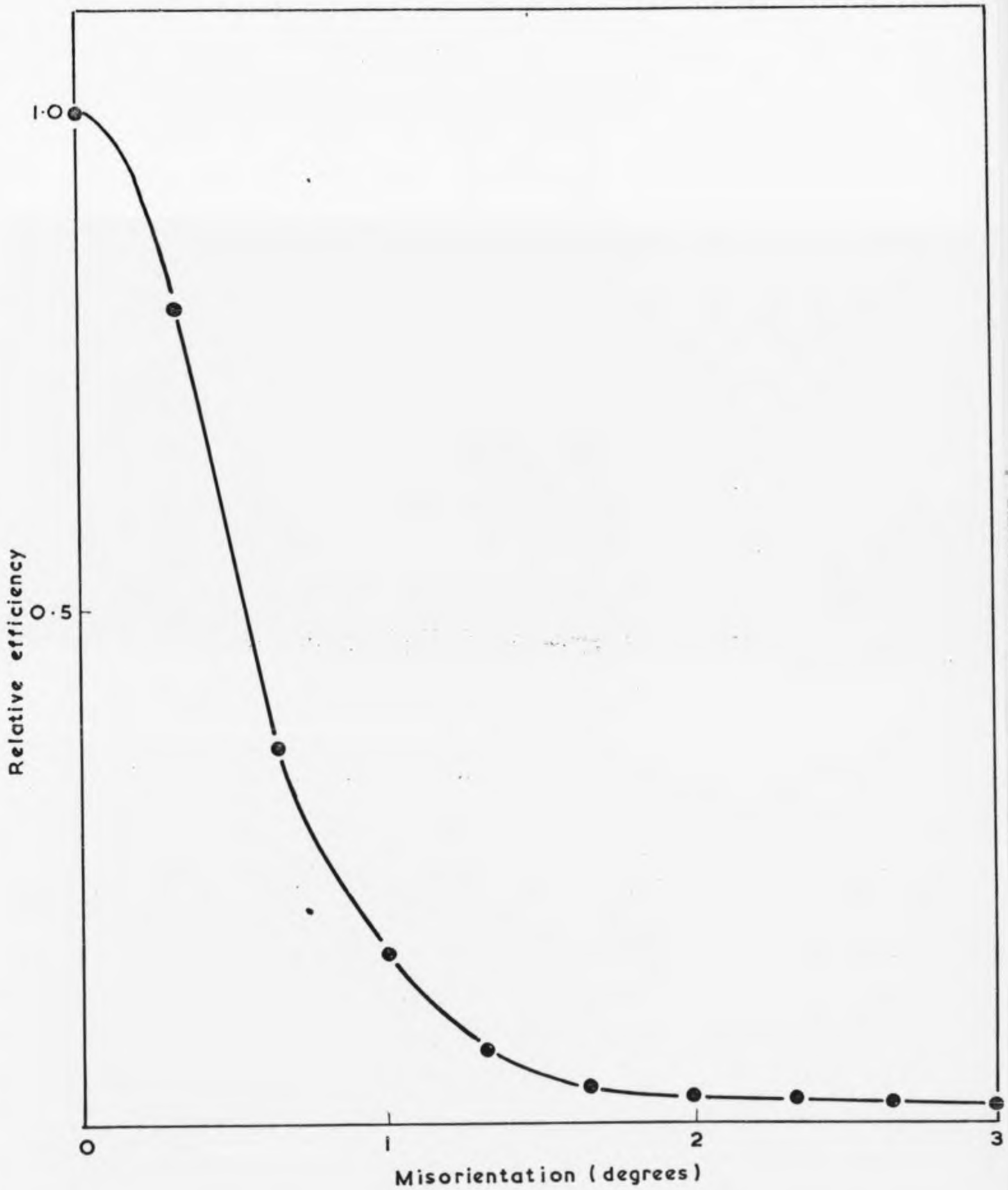

FIG. 2.10. OFF AXIS DIFFRACTION EFFICIENCY FOR A THICK KBr HOLOGRAM.

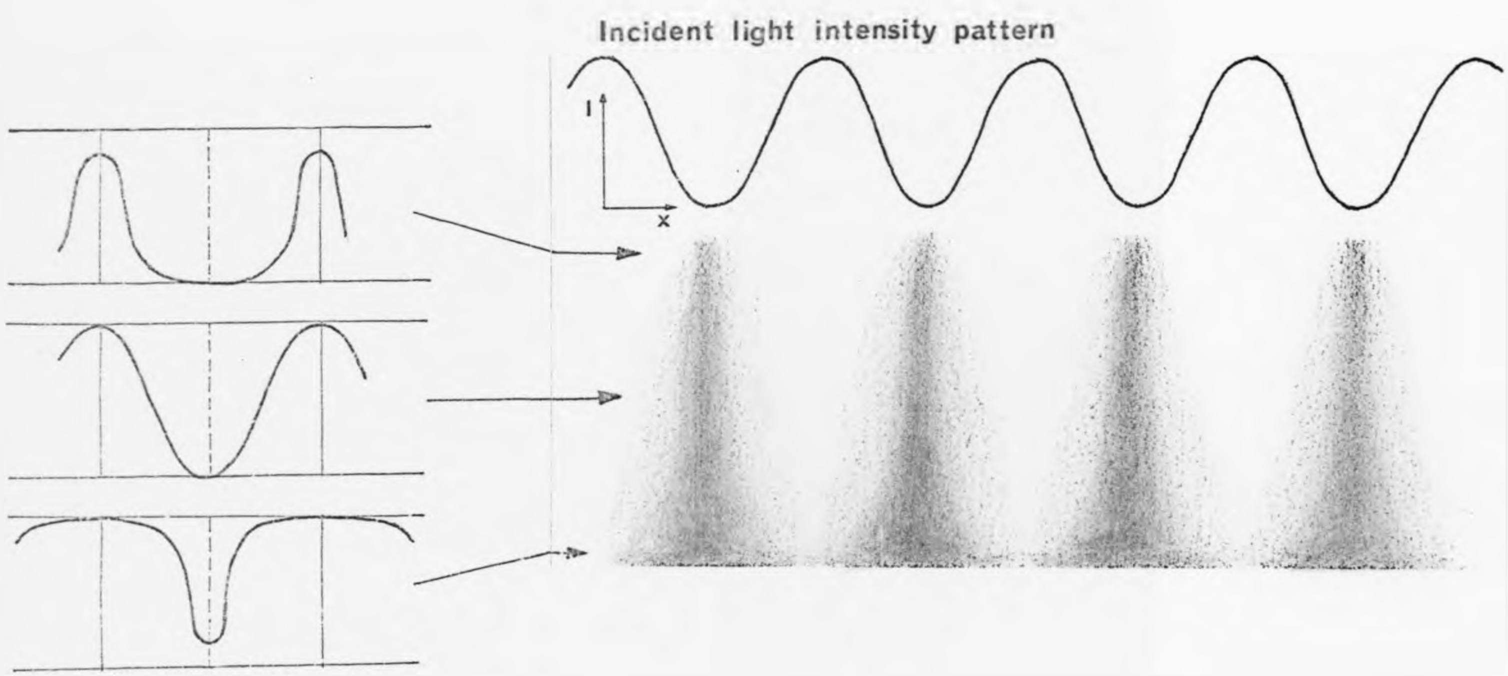

FIG. 2.11. SCHEMATIC REPRESENTATION OF GRATING CROSS-SECTION SHOWING VARIATION OF MODULATION WITH DEPTH

A Helium Neon Laser
B Beam splitter
C Shutter
D Mirror
E Spatial filter
F Transparency
G Lens
H Hologram

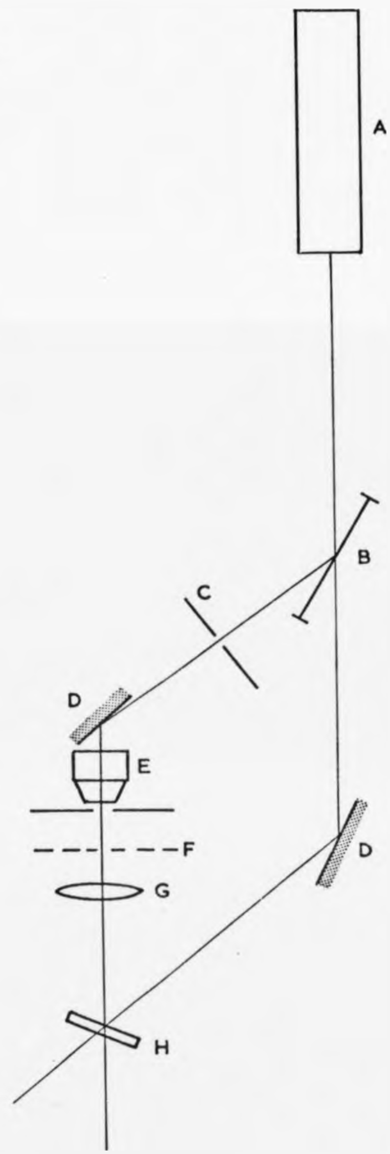

FIG.2.12. HOLOGRAPHIC RECORDING OF THE TRANSPARANCY

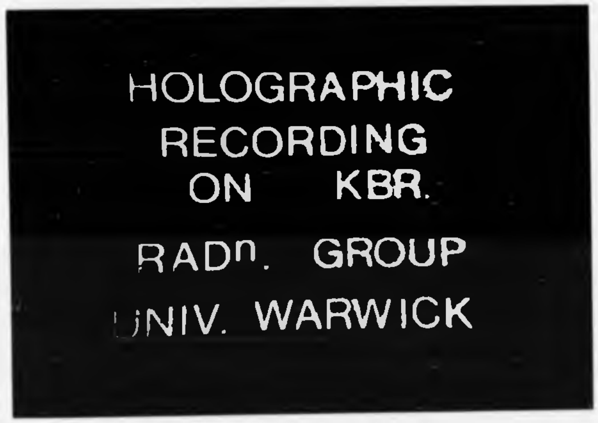

RECONSTRUCTION OF HOLOGRAM RECORDING IN POTASSIUM BROMIDE

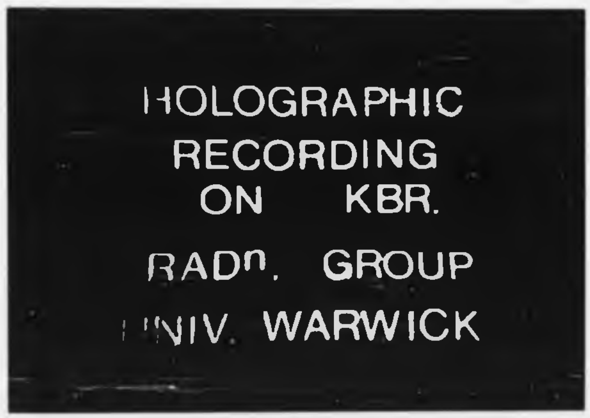

OBJECT IMAGED THROUGH CRYSTAL

FIG. 2.13.

with the object imaged through the crystal.

2.7.1. Non-Linear Effects

It has previously been explained that the customary representation of a recording medium's response is in terms of its amplitude transmittance. This follows from the consideration of the holographic reconstruction process, only when the amplitude transmittance of the hologram is linearly related to the original incident exposure is the reconstruction a faithful representation of the original object.

In Fig. 2.14 is shown the absorbance variation with exposure of a coloured potassium bromide crystal and from this the intensity and amplitude transmission changes have been determined. Because for liquid nitrogen temperature coloured KBr the bleaching process is two stage [2] there are two linear portions of the amplitude transmission curve. Unfortunately this could lead to difficulty in some holographic applications because of the reduced effective range of linear amplitude transmission with exposure. It is not however foreseen here that this presents any major obstacle for use as a holographic recording medium.

2.8.1. Theoretical Interpretation

Perhaps the best and most comprehensive treatment of thick diffraction gratings it that of Kogelnik [6, 7 and 8] which gives a coupled wave analysis of the diffraction process and this allows for cases where large diffraction efficiencies result in a sizeable depletion of the incident beam in passage through the recording medium. This is not true for a Fresnel - Kirchoff diffraction approach [9,10] which sums the effect of many diffracting elements through the depth of the hologram each receiving the same incident intensity This analysis is valid only for weak diffraction. The coupled wave analysis assumes a grating with spatial modulation of either α, the amplitude attenuation or n, the refractive index (in the treatment of phase holograms) or both (for mixed holograms) and solves the wave equation inside the medium for the coupled incident and diffracted waves. Predicted in the theory is the diffraction efficiency at, or near the Bragg condition for transmission or reflection holograms. In the treatment of thick, transmission absorption gratings, the situation for coloured potassium bromide, the diffraction efficiency is given by:-

$$= 100 \exp\left[- \frac{2\alpha_o d}{\cos \theta} \right] \sinh^2 \frac{\alpha_1 d}{2 \cos \theta} \ \% \qquad \ldots\ldots \quad 1$$

where α_o is the mean and α_1 the modulating amplitude attenuation such that

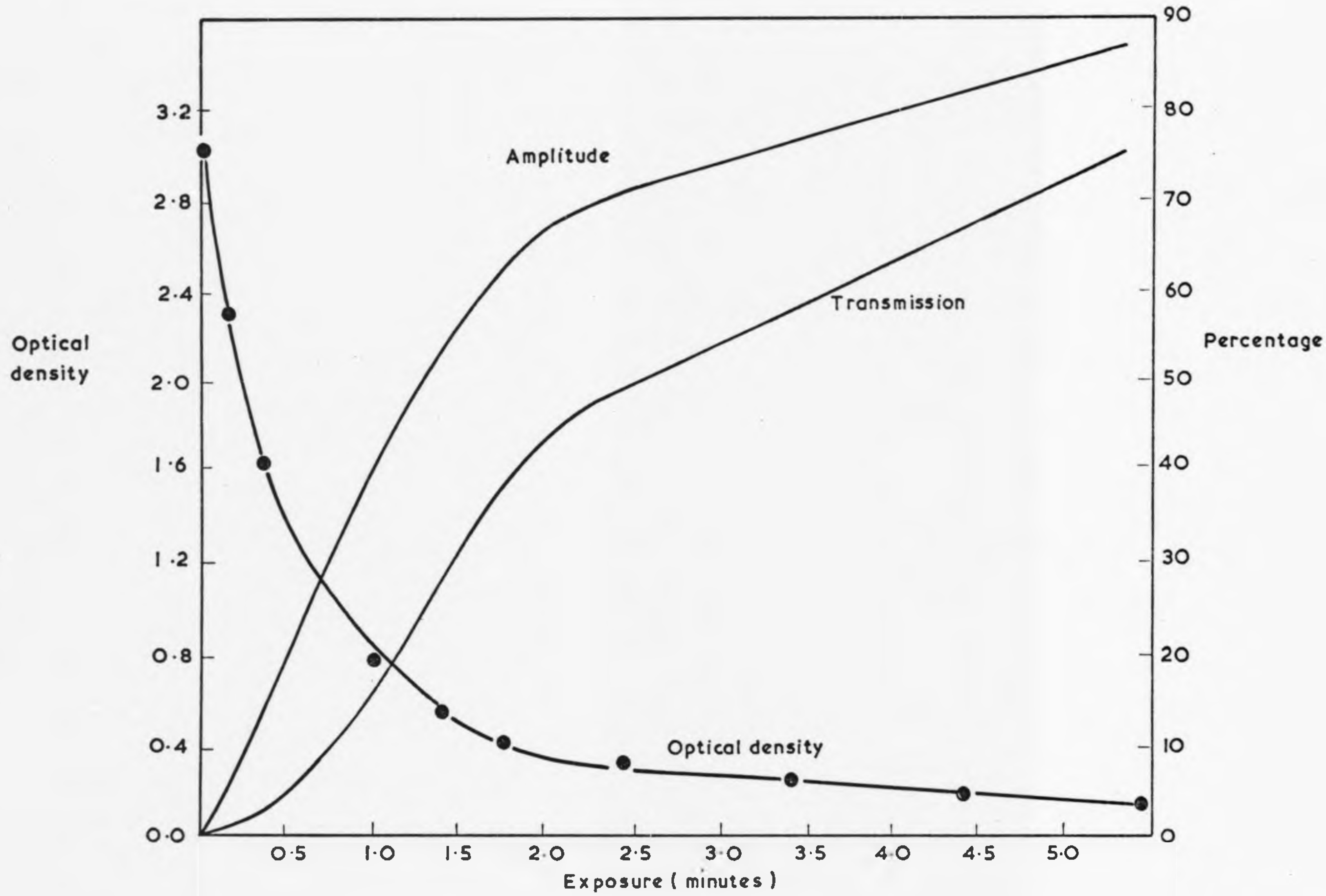

FIG. 2.14. OPTICAL DENSITY/TRANSMISSION/AMPLITUDE TRANSMISSION VS EXPOSURE

at any position x, on the grating the amplitude attenuation is given by:-

$$\alpha = \alpha_0 + \alpha_1 \sin Kx \qquad \ldots\ldots \quad 2$$

where K the grating vector, equals 2π/wavelength and θ and d are defined as in section 2.5.1. The variable α, is confusingly defined as the amplitude attenuation (as opposed to the intensity attenuation) to make the intensity transmission T, as follows:-

$$T = \exp - 2\alpha d$$

Fig. 2.15 shows the function of equation 1 for different values of α_0/α_1, and clearly the maximum efficiency is obtained when $\alpha_0/\alpha_1 = 1$. This now clarifies the preferred use of L.N.T. coloured potassium bromide as reported in section 2.2.3, since R.T. coloured KBr would give a value of α_0/α_1, greater than unity resulting in a reduction in diffraction efficiency.

The highest diffraction efficiency reached with gratings recorded in potassium bromide was 2.3%, considerably less than the maximum value expected from Fig. 2.15 for $\alpha_0/\alpha_1 = 1$ which is 3.7%. In general experimentally observed values do not exactly agree with those predicted by the theory and this can be seen from the comparisons below:-

Mode of Diffraction	Transmission		Reflection	
Property Modulated	α	n	α	n
Theoretical Maximum	3.7%	100%	7.2%	100%
Maximum obtained by experiment	3.0%	90%	3.8%	90%
References	[11]	[12]	[13]	[12]

The observed maximum of 3.0% for thick amplitude transmission holograms was obtained on Kodak 649F emulsion which is 10^5 times more sensitive than the cathodochromic material used in this chapter. This probably accounts for the higher efficiencies because of the reduced instability problems associated with a shorter exposure. Another contributing advantage of photographic film is that there is possibly a small phase contribution to the diffraction efficiency due

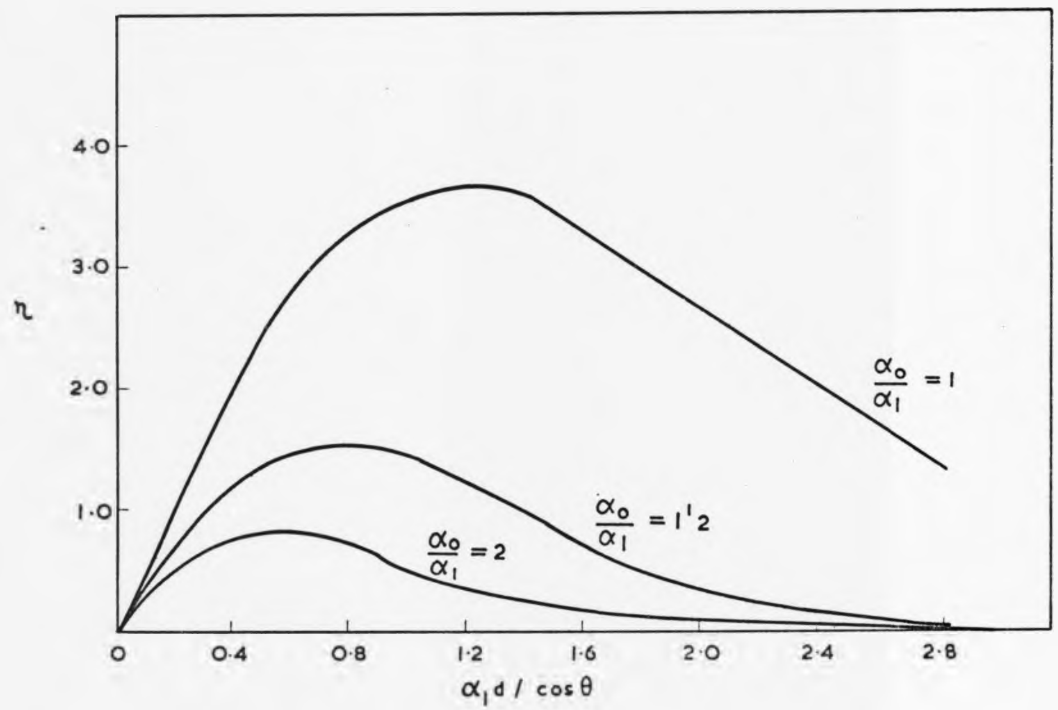

FIG. 2.15. DIFFRACTION EFFICIENCY VS $\alpha_1 d / \cos\theta$

to emulsion thickness variations after development. The efficiency observed in electron coloured potassium bromide exceeds the best value reported in the literature for holographic recording in photochromic and cathodochromic absorption materials. Diffraction efficiencies of 1.2% have been achieved in doped strontium titanate [14] although for electron coloured sodium chloride [15] efficiencies were found to be two orders of magnitude lower than the theoretical maximum.

The coupled wave analysis does not allow for a non-linear medium response nor does it include the possibility of non-uniform fringe modulation throughout the depth of the hologram. For cathodochromic KBr both of these effects are prominent. The effect of non-linear recording in thick amplitude holograms is well documented [16 and 17] for photographic emulsions and shows theoretically and experimentally that efficiencies in excess of 3.7% are obtainable.

Kermisch [18] calculates the effect of non-uniform exposures in photochromic recording mediums and concludes that provided the reconstruction is at the Bragg angle the effective modulation to be used in equation 1 is the average value of the modulation variation throughout the depth of the hologram. The same author goes on to consider the efficiency enhancement from the refractive index changes associated with absorption. At 632.8 nm in the F band of KBr this is very small and consideration of mixed gratings (i.e. with absorption and phase components) will be studied in depth in the following chapter.

REFERENCES

[1] A Schulman, E.P. Eel, Fizika Tverd, Tela, 2, 524, (translation in Soviet Phys. Solid State; 2, 489).

2 M.J. Redman, M.R. Tubbs, Phil. Mag. Vol. 24, No. 191, 1059.

3 E. Mollwo, Z. Physik, 85, 56.

4 D.R. Bosomworth, H.J. Gervitsen, App. Opts. Vol. 7 No. 1, 95.

5 C.F. Quate, D.W. Wilkinson, D.K. Winslow, Proc. I.E.E.E. 53, 1604.

6 H. Kogelnik, Bell Syst. Techn. J. 48, 2909.

7 Optical Holography, Collier, Burckhardt and Lin, Academic Press.

8 H. Kogelnik, Microwaves, Vol. 6, No. 11, 69.

9 E.G. Ramburg, R.C.A. review No. 27, 469.

10 Principles of Holography, H.M. Smith, Wiley.

11 N. George, J.W. Mathews, App. Phys. Letts., Vol.9, 212.

12 L.H. Lin, App. Opts. Vol. 8, No. 5, 963.

13 L.H. Lin, C.V. LoBianco, App. Opts. Vol. 6, 1255.

14 J.J. Amodei, D.R. Bosomworth, App. Opts. Vol. 8, 2473.

15 A.S. Mackin, App. Opts. Vol. 9, No. 7, 1658.

16 C.R. Bendak, B.D. Guenther, R.C. Hartman, App. Opts. Vol. 1, 2992.

17 Yu. A. Pryakin, F. Kh. Safinllin, Opt. and Spectrosc. Vol. 33 No. 2, 170.

18 D. Kermisch, Journal Opt. Soc. Amer. Vol 59, No. 11. 1409.

CHAPTER THREE

HOLOGRAPHIC RECORDING IN ELECTRON IRRADIATED POTASSIUM CHLORIDE SINGLE CRYSTALS

3.1. Introduction

In the last chapter experiments were described on the performance of holograms produced by bleaching the F band of electron beam coloured potassium bromide with a helium neon laser. The visible output wavelength of which is to within 1% of the wavelength peak of the F band absorption. The refractive index change associated with a Gaussian shaped F centre absorption band is largest at the half power points and use can be made of this to record holograms away from the centre of absorption with a phase enhanced diffraction efficiency. Very little enhancement was to be expected in electron irradiated potassium bromide because of the close matching of laser wavelength and peak absorption where the associated refractive index change is zero.

For cathodochromic potassium chloride a selection of argon and krypton ion laser wavelengths are available which span the region of F band absorption, and these are shown in Fig. 3.1 superimposed onto the F centre absorption band. Also displayed in this figure is the associated refractive index change. This data was obtained by modifying the calculations performed by Dexter [1] on the refractive index change associated with the F band in potassium chloride at liquid nitrogen temperatures.

Simple holographic gratings have been recorded in electron coloured potassium chloride and these show a marked wavelength sensitivity in diffraction efficiency, which does not peak at the centre of absorption. This indicates the presence of a significant phase contribution to the diffraction efficiency. Holograms that have both a phase and absorption component are known as mixed gratings and these have been discussed in the literature [2]. In this chapter an analysis is given based on the single oscillator approximation for the F centre to express the diffraction efficiency of a mixed grating in terms of wavelength and holographic fringe modulation. Fairly good agreement is found with experimental wavelength sensitivity although the theory predicts diffraction efficiencies in excess of 10% whereas only 4% was observed in practice.

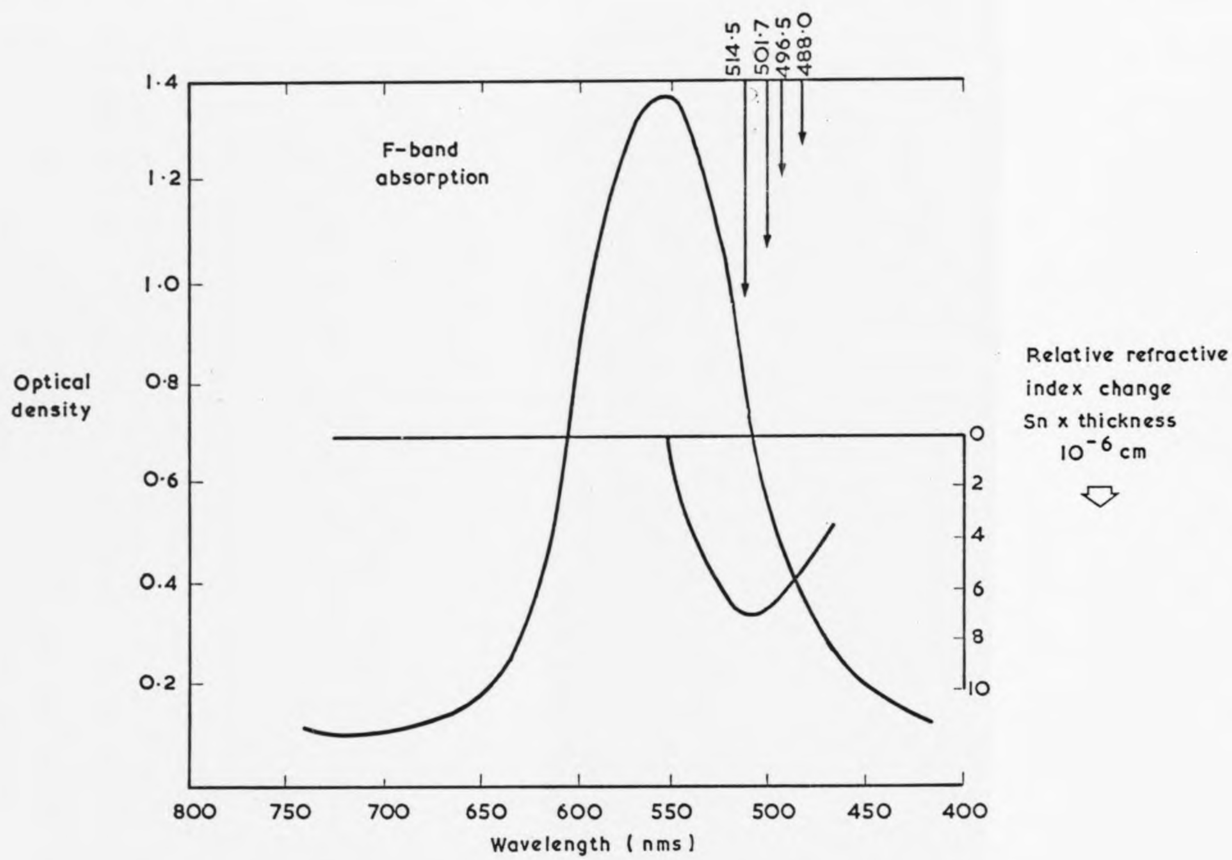

FIG. 3.1. F-BAND OF POTASSIUM CHLORIDE RELATIVE TO ARGON LASER WAVELENGTHS AND ASSOCIATED REFRACTIVE CHANGE

3.2.1. Cathodochromic Effects in Potassium Chloride

Electron coloured potassium chloride differs little in cathodochromic performance from electron coloured potassium bromide. Coloration was achieved as before with slightly smaller electron doses. For the following holographic characterisation experiments, 400 kV. irradiations were used giving a penetration depth of 800 μm.

The F band absorption occurs in the green, with a peak at 555 nm and has a half width of 0.36 eV. at room temperature. As for KBr, room temperature bleaching of liquid nitrogen temperature coloured crystals leads to a total reduction of the F band. The absorption spectrum in the visible region is shown in Fig. 3.2 both before and after extensive room temperature bleaching.

3.3. Two Beam Interference Experiments and Analysis

3.3.1. Experimental Results

The variation of diffraction efficiency with exposure and initial optical density was investigated by techniques identical to those reported in the previous chapter. Using the same optical arrangement as before the efficiency as a function of exposure, and peak efficiency as a function of colouration optical density measured at 514.5 nm, are shown in Fig. 3.3, and Fig. 3.4 respectively. In both cases the response is similar to that for potassium bromide except for the magnitude of the diffraction which has increased two-fold.

The relative diffraction efficiency was determined at various reading wavelengths for the argon and krypton ion lasers using the optical configuration of Fig. 2.6, but without the spatial filter and condensing lens. These components were removed because of the difficulty experienced in aligning accurately the two lasers to the same optical system. The hologram was initially written at 514.5 nm (Argon Ion Laser) and then interrogated with a reduced incident light intensity (to effectively eliminated destructive readout) for nine laser wavelengths from 587.4 nm.(Krypton Ion laser) in the yellow to 457.9 nm.(Argon Ion Laser) in the violet. For each readout wavelength it was necessary to reorientate the crystal to the correct Bragg angle, and then adjust the detector for maximum signal. The relative diffraction efficiency as a function of wavelength is shown later in Fig. 3.7 with the results of the analysis presented in the following section.

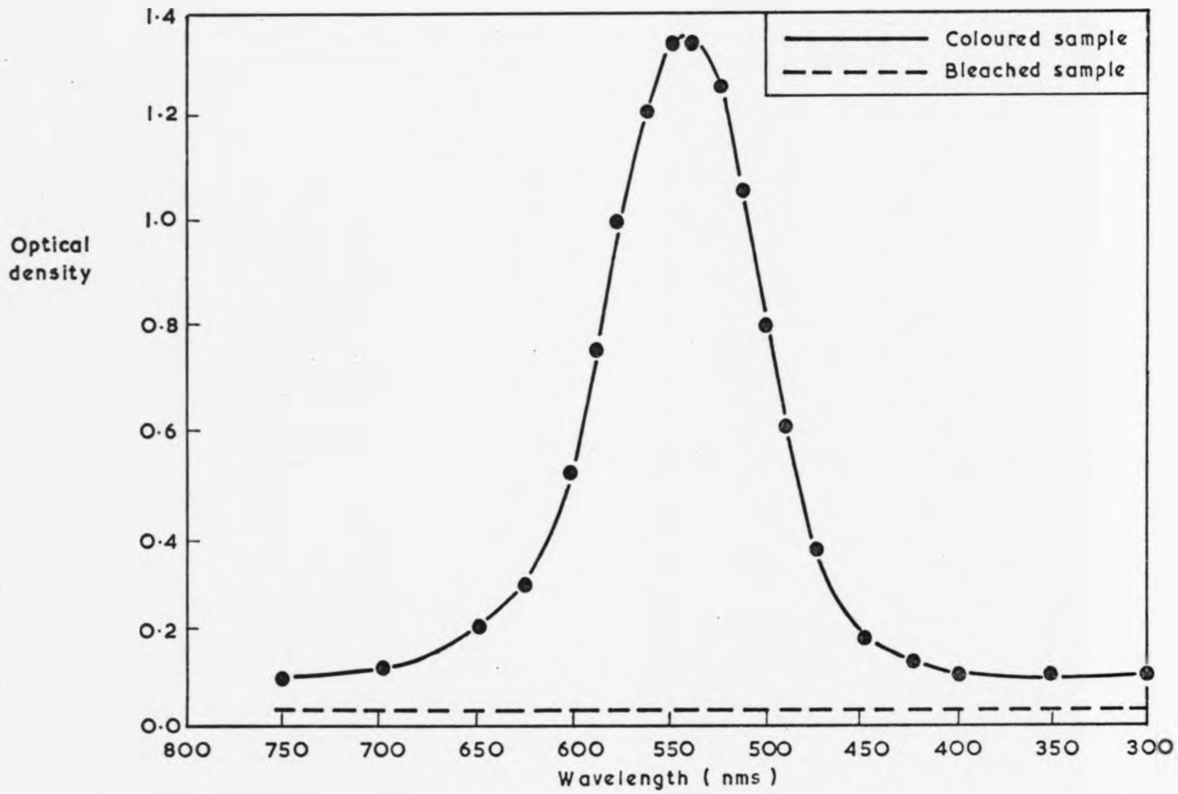

FIG.3.2. R.T. BLEACHING OF L.N.T. COLOURED POTASSIUM CHLORIDE (F-BAND)

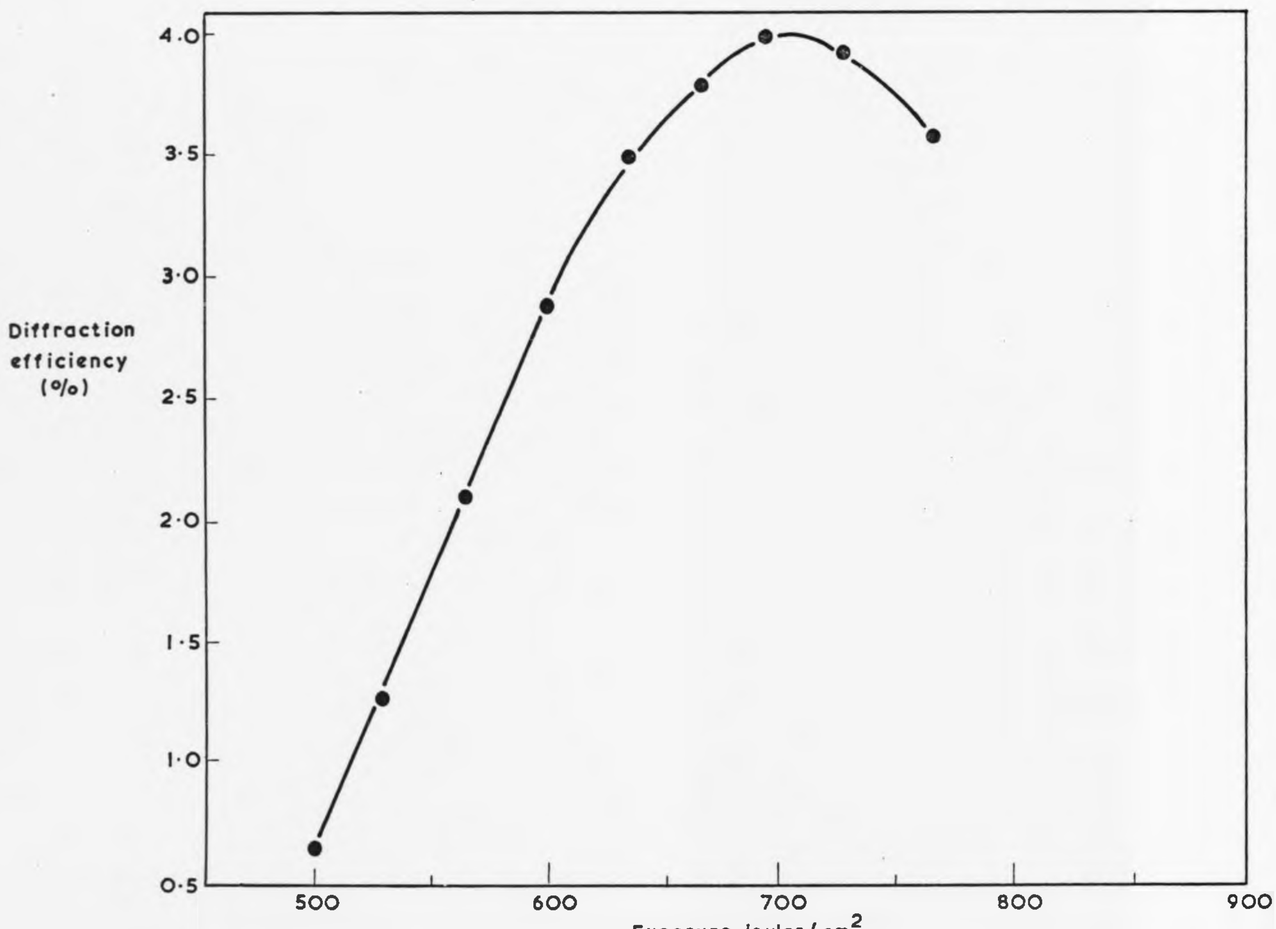

FIG. 3.3. DIFFRACTION EFFICIENCY AS A FUNCTION OF EXPOSURE FOR ELECTRON COLOURED KCl

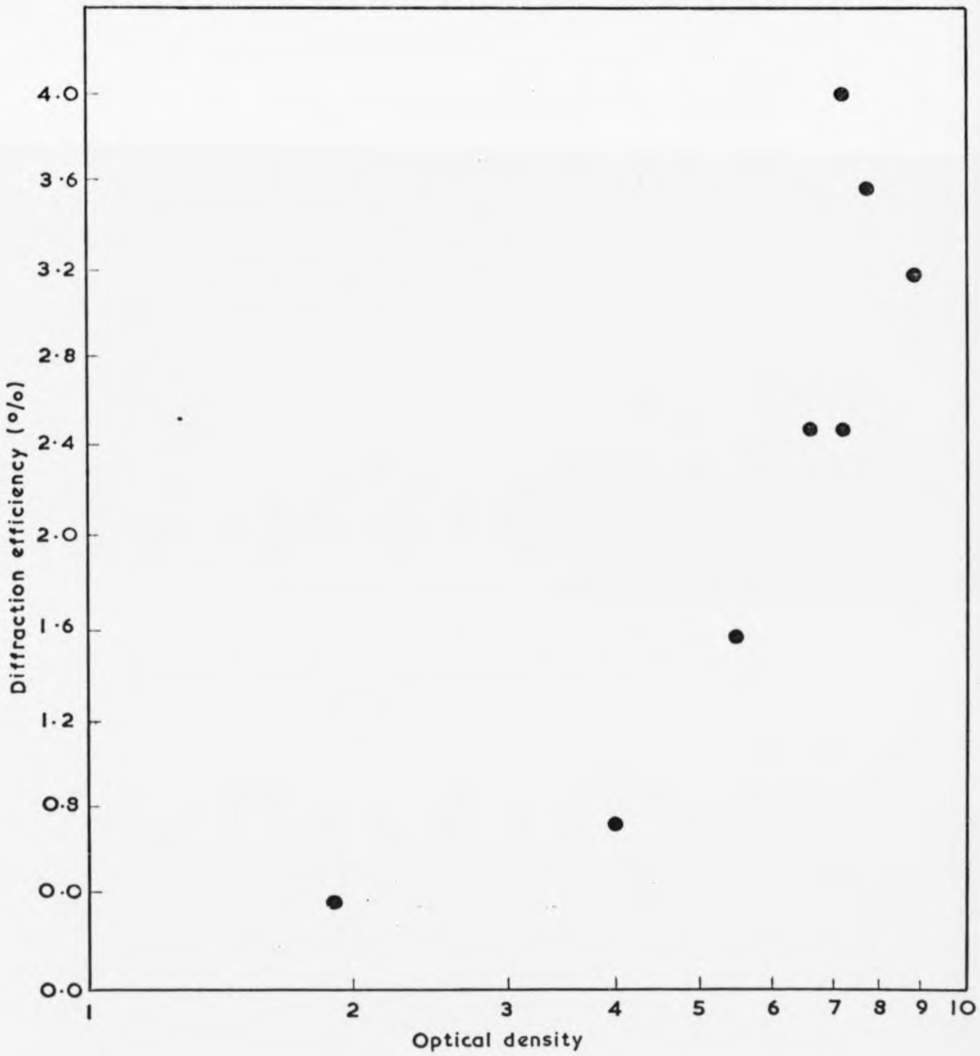

FIG.3.4. DIFFRACTION EFFICIENCY AS A FUNCTION OF INITIAL OPTICAL DENSITY

3.3.2. Mixed Diffraction Gratings from a Single Oscillator Absorption

The preceeding experimental results can conveniently be interpreted using the absorption due to a single classical oscillator to which the F centre absorption approximates. This approach enables a relatively easy mathematical analysis to be performed to give the phase contribution present in a mixed diffraction grating in terms of the amplitude absorption modulation [3]. The final equation presents the diffraction efficiency in terms of the wavelength for different values of the grating's amplitude modulation. In the following section this is then compared to the experimental data.

The optical constants of a single classical oscillator, k, the extinction coefficient, and n, the refractive index are related by the equation [4].

$$n^2 - n_0^2 - k^2 = \frac{2 n_0 k_{max} \nu_0 W_{1/2} (\nu_0^2 - \nu^2)}{+ W_{1/2}^2 \nu^2} \qquad \ldots\ldots \quad 1$$

where ν = the frequency
n_0 = the bulk refractive index
k_{max} = peak extinction coefficient when $\nu = \nu_0$
$W_{1/2}$ = the half width of the absorption band.

The extinction coefficient k, is related to the intensity attenuation, K, by the equation:-

$$K = \frac{4\pi k}{\lambda}$$

where λ is the wavelength

For an F centre peak absorption of 2.0 optical density in 400 keV electron coloured potassium chloride K is approximately 10^{-2} cm^{-1} and thus k^2 approximately equals 10^{-7} which can be neglected in comparison to the other terms on the left-hand side of equation 1 .

By approximating:-

$n^2 - n_0^2$ to $2 n_0 \delta n$ Since $\delta n / n_0 \ll 1$

and $\nu^2 - \nu_0^2$ to $2 \nu \delta\nu$ where $\delta\nu = \nu - \nu_0$
since $\delta\nu / \nu$ will be much less than unity.

Equation 1 can now be written as the refractive index change n associated with the absorption:-

$$\delta n = \frac{2 W_{1/2} \, \delta\nu \, k_{max}}{4\delta\nu^2 + W_{1/2}^2} \qquad \ldots\ldots 2$$

The attenuation constant, K, is related to the optical density D, and the colouration thickness, d, by:-

$$Kd = 2.3D \qquad \ldots\ldots 3$$

and therefore 2 becomes:-

$$\delta n d = \frac{1.15\lambda}{\pi} D_{max} W_{1/2} \frac{\delta\nu}{4\delta\nu^2 + W_{1/2}^2} \qquad \ldots\ldots 4$$

It can be determined by differentiation of 4 ; that the induced phase change for the single oscillator absorption (Lorentizian line shape) of maximum size ($\nu_o = \nu$) Dmax has a peak at $2\delta\nu = W_{\frac{1}{2}}$, and is zero at the centre of absorption. We note that $\delta nd/\lambda$ has a maximum value of 0.09 Dmax (for $W_{\frac{1}{2}} = 0.36$ eV and $\lambda = 5.1 \times 10^{-5}$ cm) and this compares favourably with the calculation of Dexters [1], for an assumed Gaussian F band absorption, which gives a maximum value of $\delta nd/\lambda$ with the same constants,of 0.11 Dmax.

The band shape for the classical oscillator in terms of the optical density, D, takes the form:-

$$D = D_{max} \frac{\nu^2 W_{1/2}^2}{(\nu_o^2 - \nu^2)^2 + W_{1/2}^2 \nu^2} \qquad \ldots\ldots 5$$

All the information is now available to substitute into the coupled wave equation [2] for mixed gratings. This equation is an extension of the thick absorption grating equation for the diffraction efficiency, discussed in section 2.8.1. of the previous chaper. It divides into separate absorption and phase components which are shown respectively in the following equation for η (the diffraction efficiency):-

$$\eta = \exp - \frac{2.3 D_o}{\cos\theta} \left[\sinh^2 \frac{2.3 D_1}{4\cos\theta} + \sin^2 \frac{\pi \delta n d}{\lambda \cos\theta} \right] \ldots\ldots 6$$

where Do is the average, and D_1 the modulating optical densities of the grating(although previously expressed as α the amplitude attenuation related to the optical density by:- $2.3D = 2\alpha d$) and θ is the Bragg angle. In this instance, as for electron irradiated potassium bromide, $Do = D_1$, although generally this must be written as $Do = (1+b)D_1$ since $Do/D_1 \gg 1$.

For convenience we define:- $x = \frac{\delta\nu}{W_{1/2}}$ with $\delta\nu$ in units of eV.

and using the approximation $\nu_0^2 - \nu^2 = 2\nu\delta\nu$ 4 and 5 become respectively:-

$$\delta n d = \frac{2.3\lambda}{2\pi} D_{1max} \cdot \frac{x}{4x^2+1}$$

$$D_1 = D_{1max} \frac{1}{4x^2+1} \qquad \ldots\ldots \quad 7$$

Such that D_{1max} is the optical density at the centre of the absorption band, for the modulating absorbance, and δnd is the phase change associated with this optical density.

Substitution of 7 into 6 and defining B as $\frac{2.3D_{1max}}{\cos\theta}$ gives

$$\eta = \exp - \frac{(1+b)B}{4x^2+1}\left[\sinh^2 \frac{B}{4(4x^2+1)} + \sin^2 \frac{Bx}{2(4x^2+1)}\right] \qquad \ldots\ldots \quad 8$$

This function is plotted in Fig. 3.5 for fixed values of B and with b = 0. As the modulation B increases the peak of η moves further from the centre of absorption since the phase component of equation 8 becomes increasingly more significant. For values of B below 1.4, the phase component does not manifest itself as the characteristic dip at the centre of absorption. Differentiation of 8 assuming $\sinh z = \sin z = z$ (for fairly small values of η) enables the peak of the M shaped efficiency curve to be determined for various values of B as shown by:-

$$x^2 = \frac{B(1+b) - 1}{4} \qquad \ldots\ldots \quad 9$$

Alternatively, for a fixed wavelength, a, the peak efficiency would oocur at a value of B given by:-

$$B = \frac{2\ (4\ a^2 + 1)}{1+b} \qquad \ldots\ldots \quad 10$$

The efficiency at the peak varies as $\frac{(4x^2+1)}{(1+b)^2}$ and clearly high efficiencies are obtained for large x values and small b values. Shown in Fig. 3.6. is the variation of x with B at which the peak diffraction efficiency occurs for b = 0 and b = 1. This is illustrated with the relative absorption and normalised phase change, $\delta nd/\lambda$, as a function of x taken from equations 5 and 4

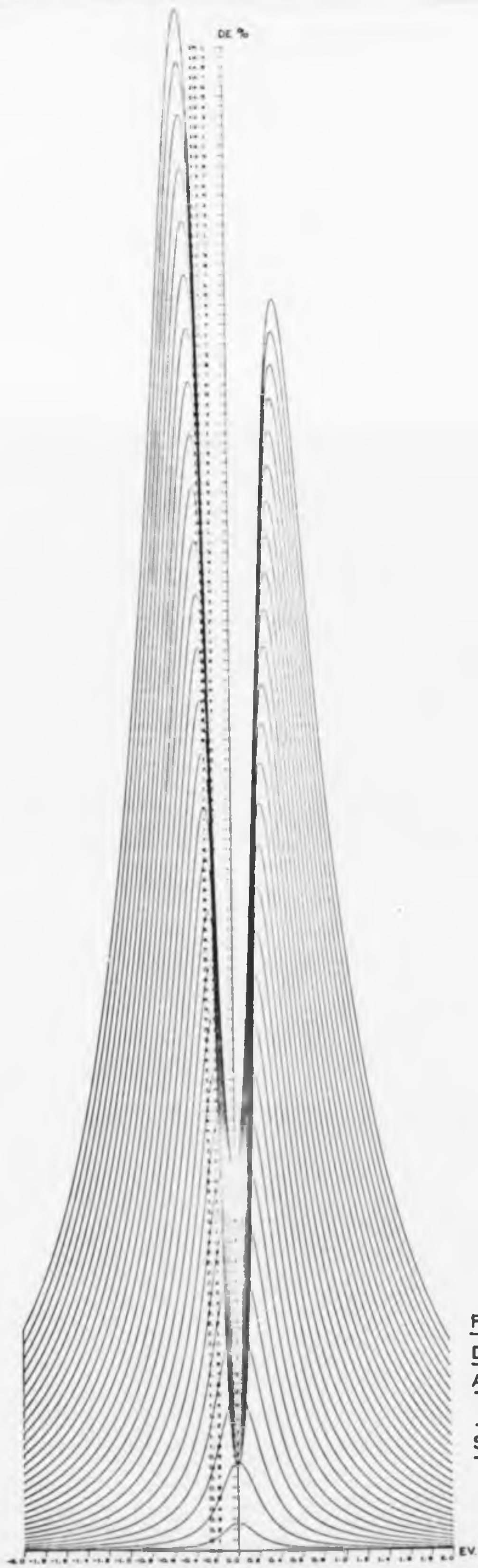

FIG.3.5.
DIFFRACTION EFFICIENCY AS A FUNCTION OF δ^{ν} $(x = \delta^{\nu} / W1/_2)$ FOR A SERIES OF B VALUES

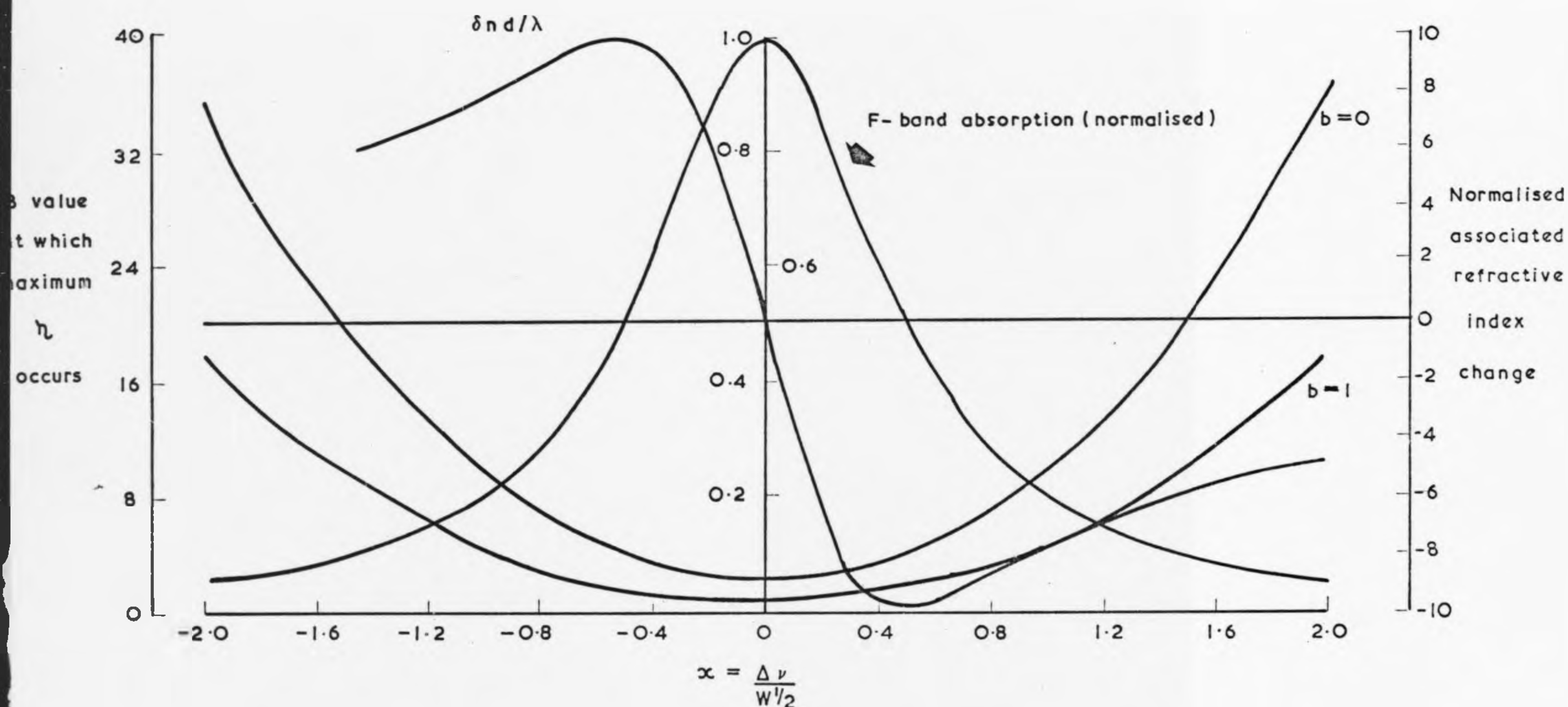

FIG. 3.6. B VALUE VS WAVELENGTH FOR WHICH MAXIMUM DIFRACTION OCCURS

respectively.

3.3.3. Comparison of Results

The results of section 3.3.1. were fitted to the analysis of the previous section with the values $b = 0$ (because $D = Do$ since a total reduction of the F band is possible) and $B = 4.6$. Determination of B was achieved by simple bleaching experiments on samples with an estimated dark fringe intensity, I_{min}, measured in the following way. The beam ratio was altered of the holographic recording arrangement for each of a series of sample holograms. For an ideal holographic recording material it can be shown [5] that the relationship between V^2 (where V is the fringe visibility equal to $2\sqrt{R} / R+1$, and R is the beam ratio) and the diffraction efficiency is linear. Experimentally however as a V value of unity is approached the diffraction efficiency levels off to a constant value because of the non-linear response of the medium. The visibility at this point of departure from straight line variation enables one to determine the effective bright to dark fringe intensity actually achieved experimentally, The dark fringe intensity is then given by:-

$$I_{min} = I_1 + I_2 - 2\sqrt{I_1 I_2} \qquad \text{and} \qquad I_1/I_2 = R$$

By bleaching a sample with Imin for an equivalent exposure necessary for optimum diffraction efficiency, gives a resulting optical density equivalent to twice the effective modulating optical density which is then expressed as B.

Shown in Fig. 3.7 is equation 8 for $B = 4.6$ and $b = 0$, also the experimental data, normalised to the predicted maximum, and this agrees with the theory to a fair degree of accuracy. Equation 9 predicts a maximum efficiency for $x = 0.9$ which is in good agreement with the experimentally observed peak at 476.5 nm. The calculated efficiency at 514.5 nm was 7.3% although only 4% was found by experiment. It appears that the maximum diffraction efficiency achieved in practice rarely exceeds 50% of the theoretically predicted maxima and this was also shown to be the case for potassium bromide in the previous chapter.

3.4.1. Low Temperature Readout

The previous calculations can easily be extended to include the temperature variation of η, the diffraction efficiency. Two of the

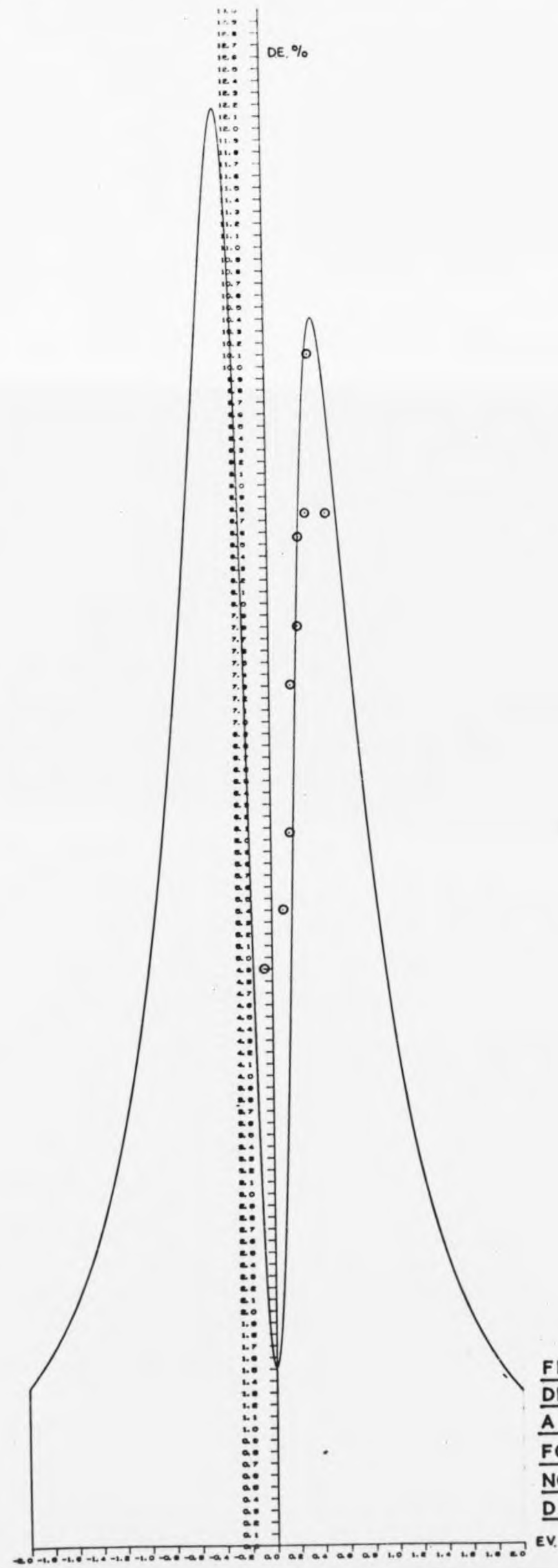

FIG.3.7.
DIFFRACTION EFFICIENCY AS A FUNCTION OF δ^V $(x=\delta^V/WI/_2)$ FOR B=4·6. b=O WITH NORMALISED EXPERIMENTAL DATA

variables of equation 8 section 3.3.2. i.e. B and x are a function of temperature because of induced changes in the halfwidth, peak height and position of the F band absorption. The optical density at the peak of the F band, expressed as B, can be written in terms of the temperature dependent halfwidth, $W_{\frac{1}{2}}$, since they are related by Smakula's [6] equation as:-

$$B = \frac{B^1 W_{\frac{1}{2}}^{1}}{W_{\frac{1}{2}}} = \frac{Bo}{W_{\frac{1}{2}}}$$

where $W_{\frac{1}{2}}^{1}$ and B^1 are the room temperature values of $W_{\frac{1}{2}}$ and B respectively and Bo now has the units of optical density per eV. Both of the terms in the quotient $\delta\nu/W_{\frac{1}{2}}$ defined before as x, are functions of temperature and can be expressed analytically by computer fitting. However although the expression for $\bar{\nu}_o$ is accurate to within 10% of the observed value this can lead to a large inaccuracy in $\delta\nu$ because of the $\delta\nu/\nu < 1$ condition. An alternative approach is to use the experimentally observed variations of ν_o and $W_{\frac{1}{2}}$ with temperature. A plot of η versus T^oK is shown in Fig. 3.8 using equation 8 of the previous section with b = 0 and $W_{\frac{1}{2}}$, ν_o data from the literature [7], with an estimated Bo = 1 (corresponding to a room temperature B value of 2.8). It can be seen that there is a low temperature enhancement of the diffraction efficiency, although this is untrue for high Bo values.

3.4.2. Experimental Results

The basic arrangement for two beam interference recording was used. For low temperature operation index matching was impractical, and hence polished flats were used. Because of surface damage induced on electron irradiation the samples were initially coated with a thin film of gold of approximately 60-70% transmission. After colouration, the coated crystal was mounted into the stainless steel cryostat shown in Fig. 3.9 designed for low temperature holographic recording, and evacuated by means of a combination of adsorption and diffusion pumps, such that vibrationless operation was possible during holographic writing.

The hologram was recorded and readout at 514.5 nm, at various temperatures between 90^oK and room temperature. For each 'readout' it was necessary to maximise the diffraction by crystal reorientation because of the fringe spacing variation with temperature.

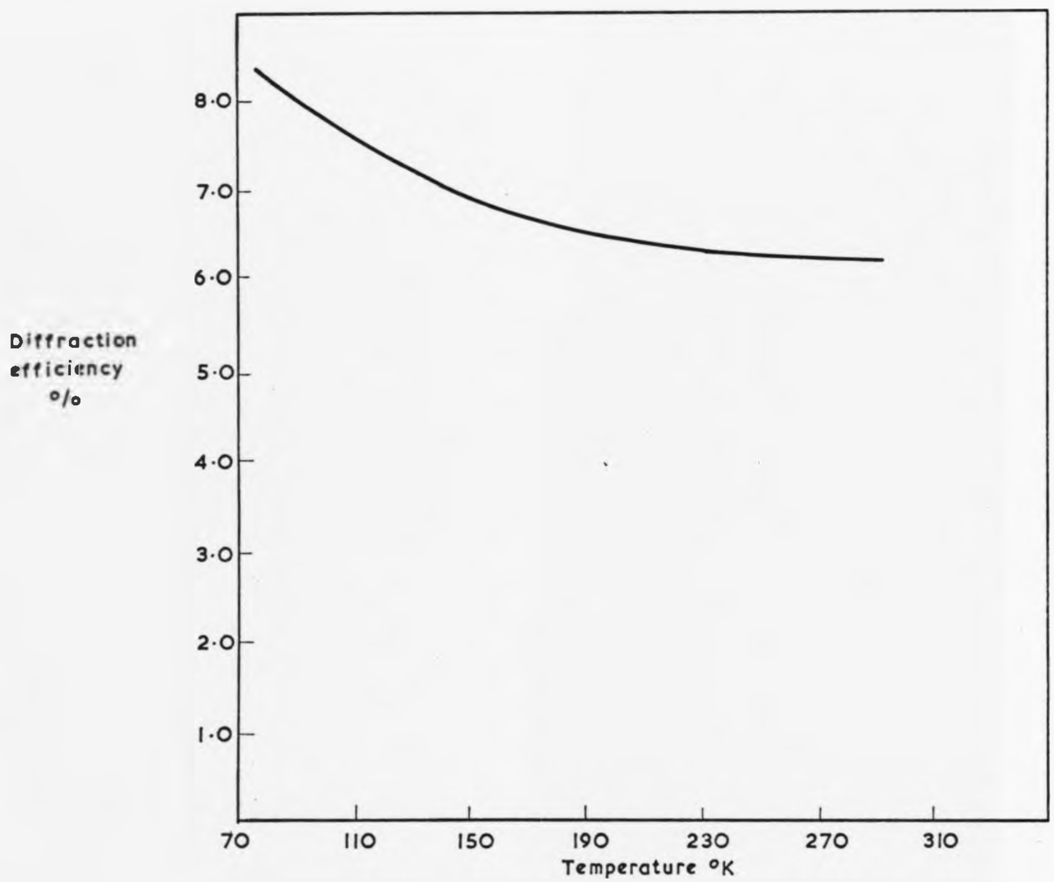

FIG. 3.8. CALCULATED DIFFRACTION EFFICIENCY VARIATION WITH TEMPERATURE ($B_o = 1$)

FIG. 3.9. LOW TEMPERATURE CRYOSTAT FOR HOLOGRAPHIC RECORDING.

Shown in Fig. 3.10 is the temperature sensitivity of diffraction efficiency with values of 0.24% and 0.17% at 90°K and 270°K respectively. In general it was not possible to achieve the high diffraction efficiencies obtainable with index matched crystals, however the trend found experimentally agrees with the variation determined in the previous subsection for an estimated Bo = 1. The ratio of efficiencies at liquid nitrogen temperature and room temperature was found experimentally to be 1.3 whereas theoretically it was 1.5.

3.5.1. Off Axis Recording at 514.5 nm and 488 nm

The off axis recording in electron coloured potassium chloride was experimentally similar to that previously reported in section 2.5.1. for potassium bromide. Here 514.5 nm. generated holograms were readout away from the Bragg angle with the 514.5 nm. and 488 nm. lines of the argon ion laser. The halfwidths of these two rocking curves shown in Figs. 3.11 and 3.12 indicate effective holographic thicknesses of 130 µm and 120 µm. A colouration depth of 140 µm was determined by microscopy of the coloured cross-section for 150 keV electron irradiations. Again the non-uniform exposure with depth gave an effective thickness of only 80-90% of the coloured layer thickness.

3.6.1. Summary of Chapter Three

It has been shown that it is possible to record high efficiency holograms in electron coloured potassium chloride, because of the advantages of readout away from the centre of F centre absorption. A two-fold increase in diffraction efficiency has been observed relative to readout at the centre of absorption (as in chapter two). The analysis given in section 3.3.2. based on the assumption that the F centre absorption approximates to a classical oscillator, agrees with the experimentally observed wavelength sensitivity, and readout at various temperatures, and indicates the presence of a phase component in the diffraction efficiency.

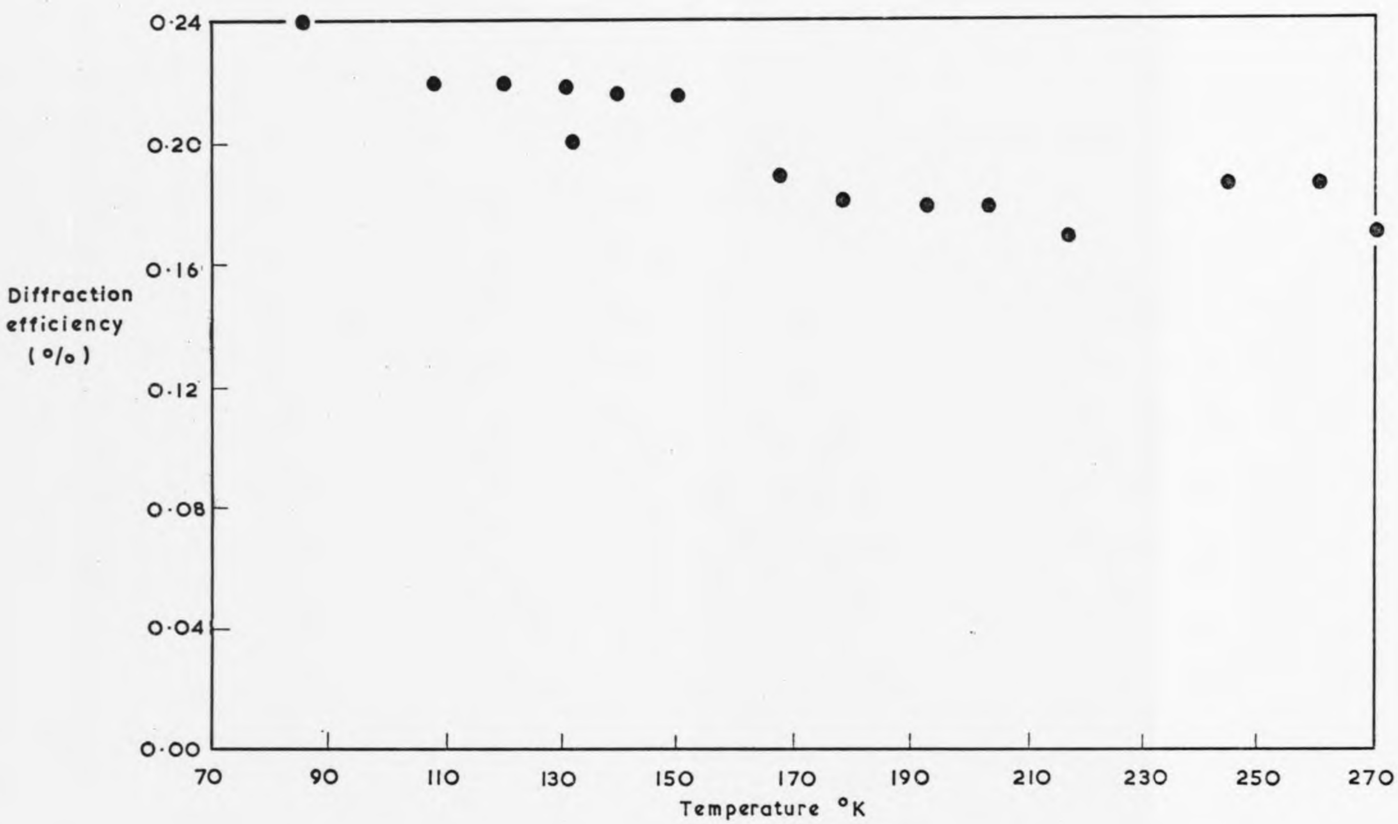

FIG. 3.10. EXPERIMENTAL TEMPERATURE VARIATION OF DIFFRACTION EFFICIENCY

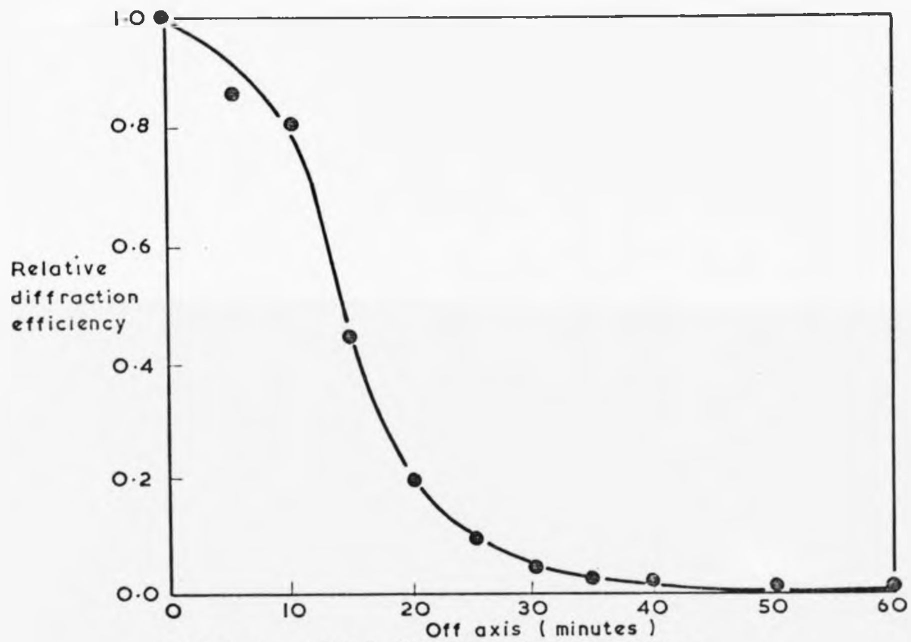

FIG. 3.11. WRITE 514·5 nm READ 514·5 nm

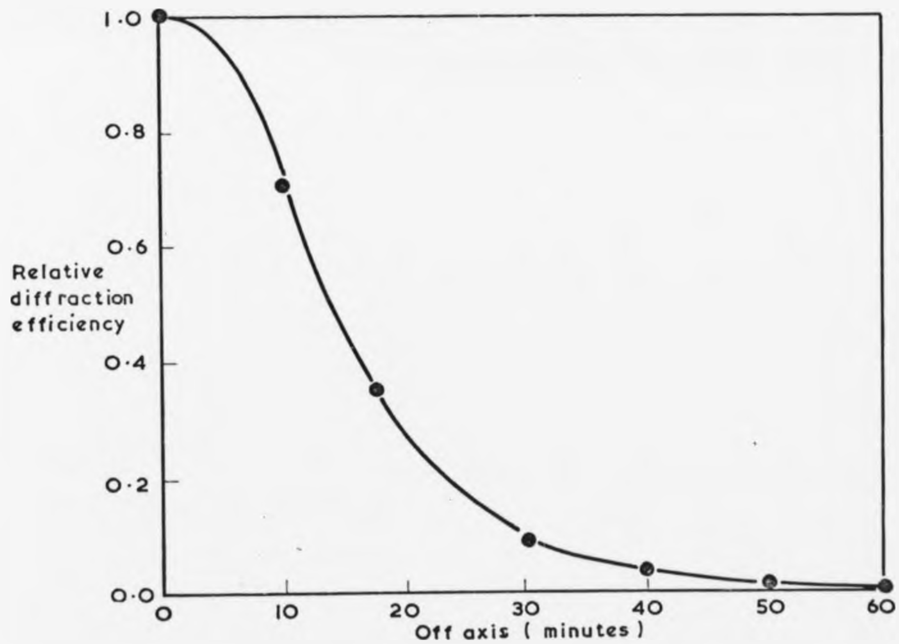

FIG. 3.12. WRITE 514·5 nm READ 488·0 nm

REFERENCES

[1] D.L. Dexter, Phys. Review, Vol. 111, No. 1, 119.
2 H. Kogelnik, Bell Syst. Techn. J. Vol. 48, 2909.
3 H. Kogelnik, Microwaves, Vol. 6, No. 11, 68.
4 Optical Properties of Semiconductors, Moss, Butterworths.
5 L.H. Lin, J. Opt. Soc. America, Vol. 61, No. 2, 203.
6 D.L. Dexter, Phys. Review, 101, 48.
7 G.A. Russel, C.C. Lick, Phys. Review, 101, 1473.

CHAPTER FOUR

USE OF M BAND DICHROISM IN SODIUM FLUORIDE FOR HOLOGRAPHIC RECORDING

4.1. Introduction

The previous two chapters have reported on holographic recording in various cathodochromic alkali halide crystals where the writing process involves the annihilation of complementry defect centres by diffusion. The sensitivity of the process is inherently low, and destructive readout is inevitable since the reading beam continues to bleach the hologram. Storage time can be lengthened, although not indefinitely, by using a reduced read beam intensity. An alternative method of storing holograms which would not suffer destructive readout is that using the dichroism shown by anisotropic colour centres such as the M centre. Sodium Fluoride was selected as a favourable alkali halide because of the availability of laser wavelengths to match the absorption bands. The absorption of polarised light depends on the relative orientation of the M centre and E vector, and it is possible to orient M centres using light in the ultra violet which is absorbed by the M_F band. Green light in the M band is unable to effect the induced dipole orientations and therefore may be used for non-destructive readout. The sensitivity of this process is considerably higher than that of the cathodochromic processes reported in the previous two chapters. In electron irradiated sodium fluoride the M_F and M centre absorption occurs at 340 nm. and 507 nm. respectively. Thus a system may be envisaged that uses the 351 nm. krypton ion laser line to initially orient the M centres in one direction, and then write the hologram with interfering beams polarised perpendicularly to the original aligning polarisation. Non-destructive readout is then achieved in the M band using the 514.5 nm. argon line.

Use of the dichroic absorption in M centres in both potassium chloride and sodium fluoride as a basis for direct information storage in two and three dimensions has been reported in the literature [1,2 and 3]. However these techniques do not offer the same advantages as that for holographic systems, and for this reason the holographic characterisation of sodium fluoride is of some interest.

4.2.1. M Centre Dichroism in Electron Irradiated NaF

The M centre consists of two electrons trapped at a negative ion vacancy pair orientated along the ⟨011⟩ crystal direction. Associated with the M centre are three absorption bands, one at 507 nm. and two others of near equal energy corresponding to higher excited states of the M centre, at approximately 340 nm. There is a distinct dipole moment associated with each of these absorption bands. The 507 nm. absorption is called the M band and is the absorption associated with the ⟨011⟩ dipole moment. Absorption at ~340 nm. relates to the two other dipole moments in the ⟨100⟩ and ⟨0$\bar{1}$1⟩ crystal directions and this is called the M_F band although in fact this consists of two narrowly separated bands. Large M centre concentrations (without the presence of other aggregate centres) can be obtained by the aggregation at 273°K of F centres produced by electron irradiation. Illustrated in Fig. 4.1(a) is the room temperature visible absorption spectrum of sodium fluoride after 400 KeV. electron irradiation at liquid nitrogen temperature. There is a large F band at 340 nm. and a small M band at 507 nm. due to aggregation during irradiation. Fig. 4.1(b) shows the same crystal (absorption) after extensive F band bleaching at 273°K by the combined 351 nm. and 356 nm. krypton ion laser lines. The M band growth at the expense of the F centre concentration is clearly shown.

By exposure to polarised light in the M_F band it is possible to align the M centres and this results in a polarisation dependence of absorption, known as dichroism. In Fig. 4.2 is shown the absorption between 350 nm. and 750 nm. of the two perpendicular light polarisations aligned to the crystal ⟨011⟩ and ⟨0$\bar{1}$1⟩ directions and propagating in the crystal ⟨100⟩ direction. This occurs after considerable exposure to M_F band light polarised in the direction of which the M_F band absorption is now a minimum. If initially the M_F band exposure was polarised in the ⟨0$\bar{1}$1⟩ crystal direction then this will maximise the absorption to ⟨011⟩ (M_F) polarised light (orientating the M centres along the ⟨0$\bar{1}$1⟩ axis) and minimise the absorption of M_F polarised light in the ⟨0$\bar{1}$1⟩ crystal direction. Experimentally it has so far only been possible to achieve an M band dichroic absorption ratio of between 3 and 4 to one and this is due to the presence of R centre absorption at approximately the same wavelength.

It has been reported [4] that the reorientation of an M centre takes place via an M^+ centre [5]. The M^+ centre ground state has an absorption close in

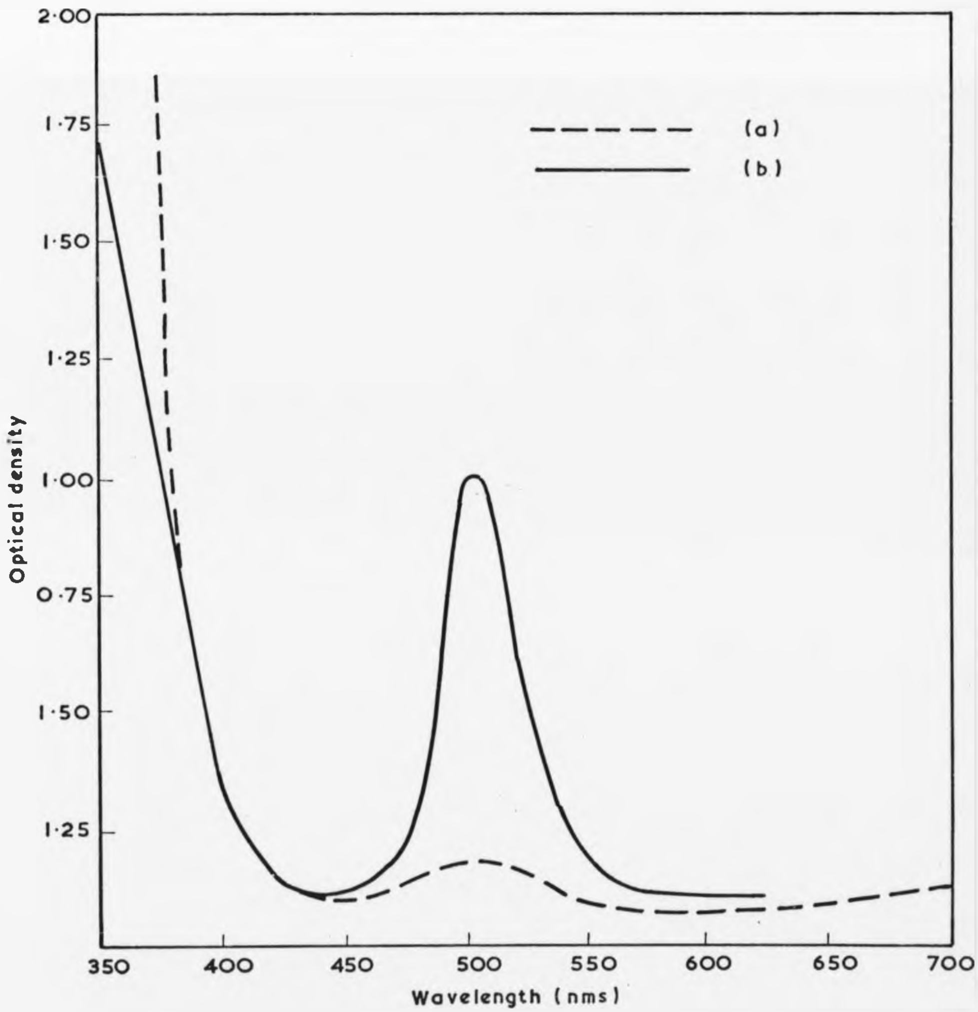

FIG.4.1 M-BAND GROWTH IN SODIUM FLUORIDE

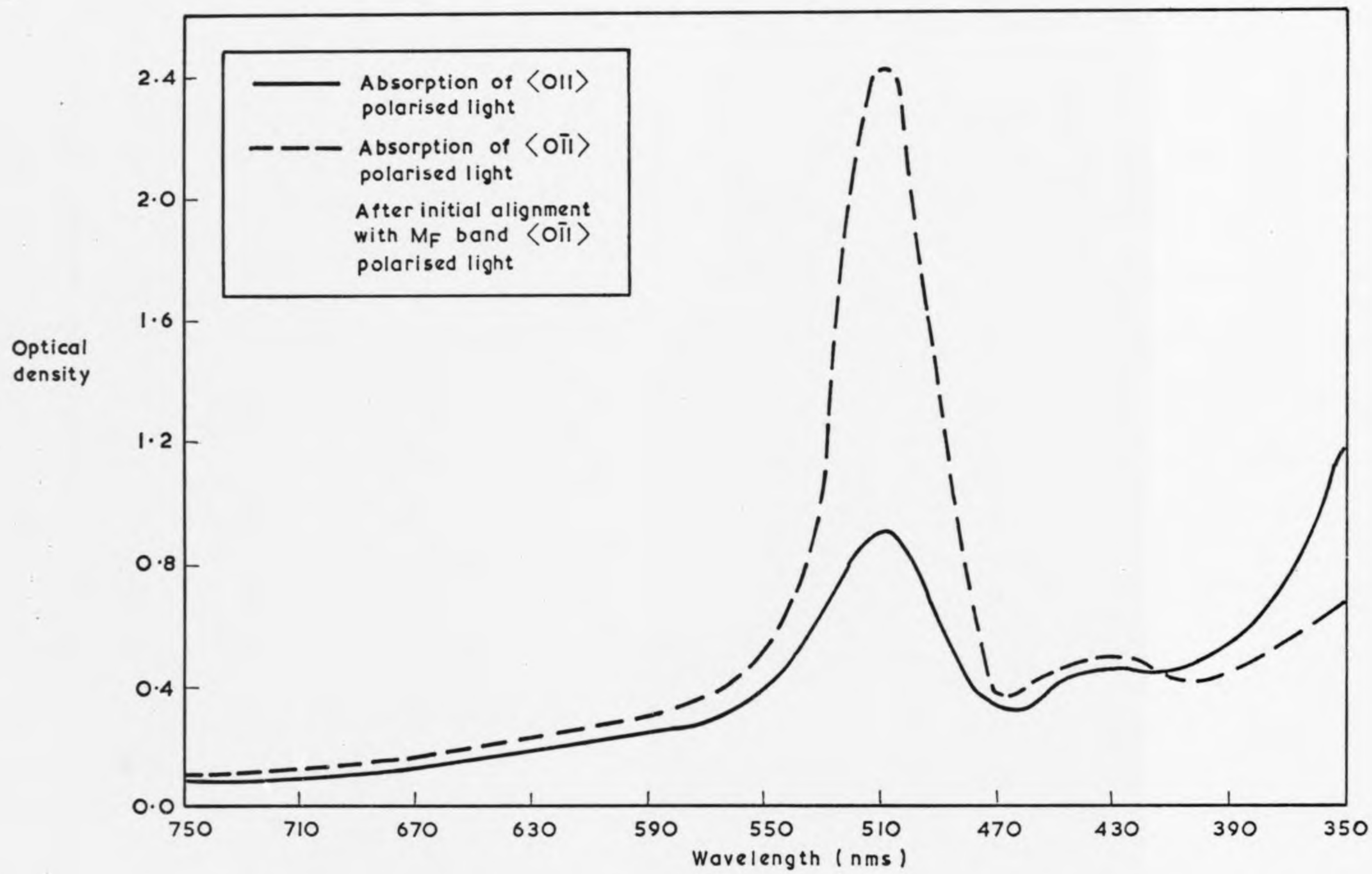

FIG. 4.2. THE DICHROIC SPECTRUM OF THE M-BAND IN SODIUM FLUORIDE

energy to that of the M_F absorption, and it is thought that initially the M centres ionise (with the free electron trapped by an F centre to form an F' centre) to form an M^+ centre, which reorients during de-excitation between M^+ high states. The presence of an F centre concentration is likely even after F band bleaching, although it is not immediately identifiable because of the overlapping M_F band absorption. Finally the M centre is reformed by the reaction:-

$$M^+ + F' \longrightarrow M + F$$

This mechanism for M centre reorientation is based on the experimental observation that orientation will not occur if by bleaching the unstable F' centre concentration is suppressed. Because it is not possible to ionise the M centre with lower energy light from the M band the orientation is unaffected by interrogation with green light.

To illustrate the dichroic effect a contact print was prepared in the following way. Initially the M centres were aligned using M_F light propagating in the crystal $\langle 100 \rangle$ direction and polarised parallel to either the crystal $\langle 011 \rangle$ or the $\langle 0\bar{1}1 \rangle$ direction. The printing exposure was then taken with the incident M_F light polarised at right angles to the original aligning polarisation. Using a microscope with crossed polarisers on either side of the crystal two micrographs were taken in green light of the print corresponding to the two crystal orientations for maximum contrast and these are shown in Fig. 4.3.

4.3.1. Holographic Recording

Using M centre dichroic absorption in electron coloured sodium fluoride a hologram was recorded using the optical configuration of Fig. 2.12 for transparency recording in coloured potassium bromide. An external prism was used to separate the 351 nm.and 356 nm.lines from the krypton ion laser, because of its greater intensity the 351 nm. output was used for recording. Readout was achieved with the 514.5 nm. argon ion laser line. Prepared samples of coloured sodium fluoride containing fairly large M centre concentrations (M band peak optical densities of 2.0 where easily obtainable for coloured penetration depths of 400 μm. corresponding to 400 KeV electrons) were index matched in methanol, contained in a silica spectrophotometer cell and mounted

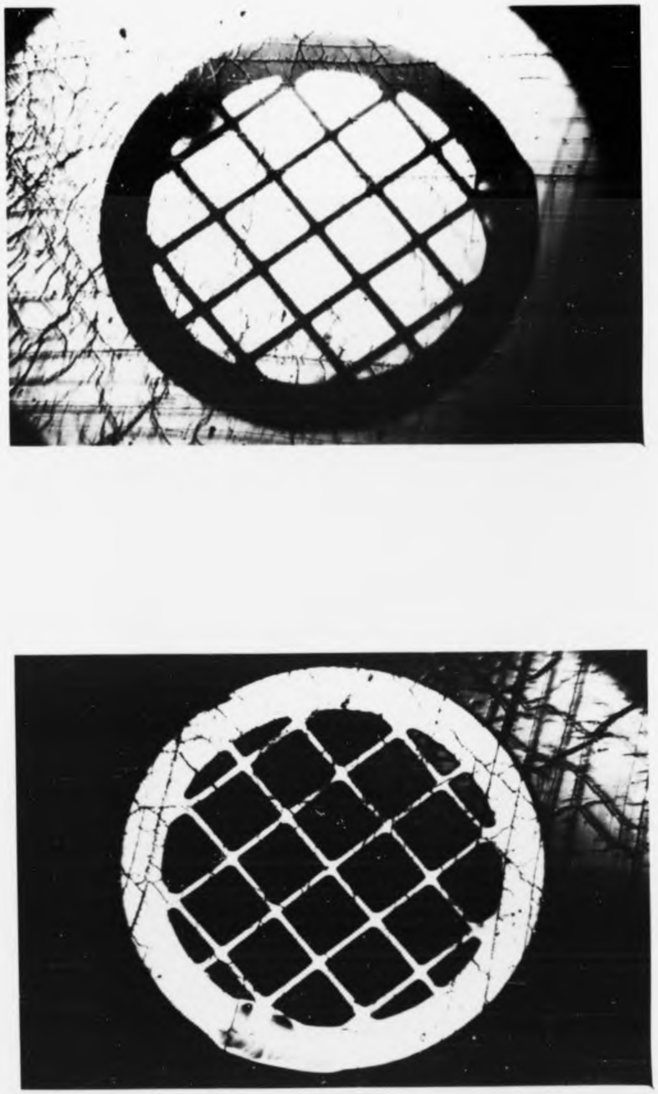

FIG. 4.3. CONTACT PRINTS TAKEN IN SODIUM FLUORIDE (USING THE M-BAND DICHROISM)

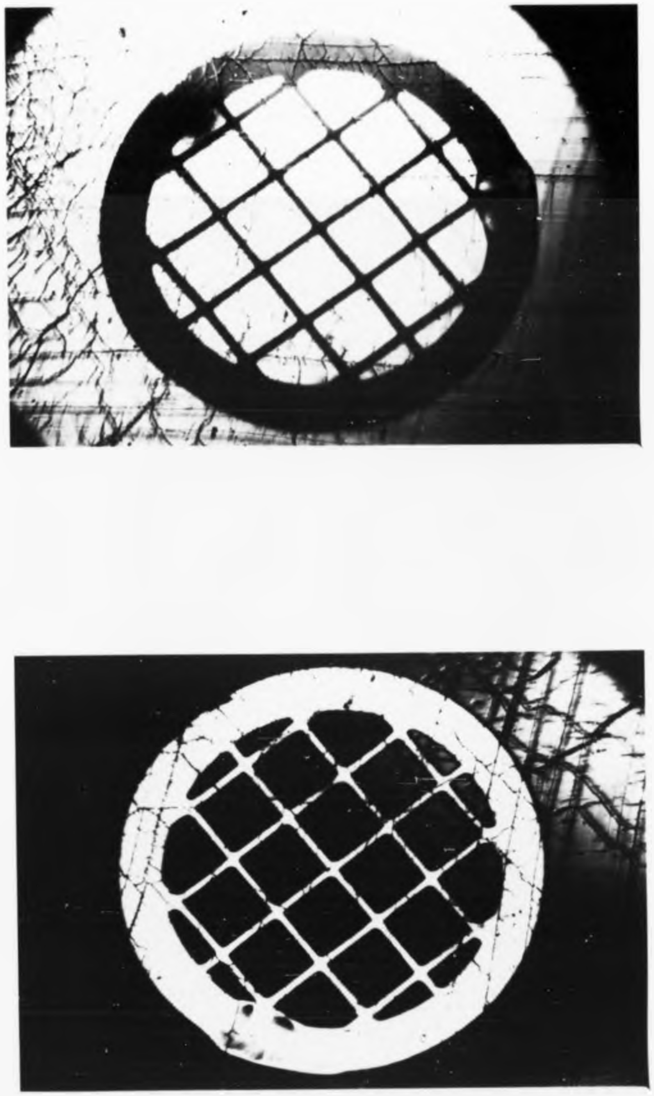

FIG. 4.3. CONTACT PRINTS TAKEN IN SODIUM FLUORIDE (USING THE M-BAND DICHROISM)

such that the crystal in the $\langle 100 \rangle$ direction was at 45° to the vertical. Both the 351 nm. write beam and 514.5 nm. read beam were polarised in the vertical direction. An initial alignment of M centres was effected, using the reference beam only, by prolonged ultra violet exposure. The hologram was then recorded, after the crystal had been reorientated through 90° about an horizontal axis which corresponded to the crystal's normal axis equi-angular between the two holographic interference beams. Incident bright fringes would again reorientate the M centres, whereas dark fringes would not effect the initial alignment. Readout can now be achieved at 514.5 nm. without further change of crystal orientation. Where bright fringes were incident on the crystal the absorption for vertically polarised green light would be high and for dark fringes the absorption would be low. Readout is therefore possible with either vertical or horizontally polarised light.

It is not always possible to reconstruct the entire image when a change of wavelength occurs between write and read stages in holography. This becomes apparent by differentiation of the Bragg condition for thick holograms:-

$$d \cos \frac{\theta}{2} \, \delta\theta = \delta\lambda$$

The reorientation of the reference beam, $\delta\theta$, necessary to satisfy the Bragg condition for readout at a new wavelength, $\lambda + \delta\lambda$, depends on the angle, θ, between the reference and object beam. When a complex object is recorded there is a spread of θ values and consequently the new Bragg condition cannot be simultaneously satisfied for all object points. The reconstruction illustrated in Fig. 4.4 was photographed in two parts corresponding to two reference beams - crystal orientation angles. Elimination of this effect can be achieved by reduction of the object beam divergence which allows the above equation to be approximately satisfied for all θ values.

4.3.2. Wavelength Sensitivity of Holographic Efficiency

The wavelength variation of holographic diffraction efficiency for sodium fluoride was determined in the same way as that reported in section 3.3.2. for the wavelength sensitivity of potassium chloride.

For the range of krypton and argon laser lines available, the variation of relative diffraction efficiency shows the characteristic M shape associated with

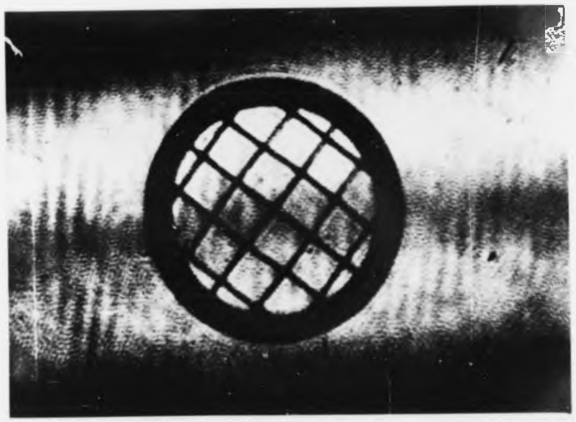

FIG. 4.4. RECONSTRUCTION OF HOLOGRAM RECORDED IN SODIUM FLUORIDE (USING M-BAND DICHROISM).

phase holograms. The hologram was initially written until a peak of diffraction efficiency with exposure was located (at 351 nm). Non-destructive readout with laser lines between 457.9 nm. and 568.1 nm. was possible with low read intensities, and the relative diffraction efficiencies are shown as the data points in Fig. 4.5. Because of the absence of laser lines between 530.9 nm. and 568.1 nm. the expected second peak at $\sim$ 550 nm. could not be confirmed experimentally.

It is possible to fit this data to the general analysis given in section 3.3.2. of the previous chapter, in particular to fit these results to equation (8) of that section. For sodium fluoride $D_o = 2D_1$, giving a b value of unity. This follows from consideration of Fig. 4.2 of section 4.2.1. which shows the two dichroic absorption states to be in the ratio 3:1. Hence the modulating optical density of the grating i.e. from $D_o + D_1$ to $D_o - D_1$, having the same ratio gives a D_o to D_1 ratio of 2. A higher absorption value of 2.4 (again take from Fig. 4.2) gives a D_1 value of 0.8 and hence a B value of 1.7. Using these derived values for b and B, equation (8) is plotted as the solid line in Fig. 4.5 with the variable $x = \frac{\delta\nu}{W_{\frac{1}{2}}}$ rewritten directly as $\delta\nu$, the energy separation from the absorption peak. The experiment data of Fig. 4.5 have been normalised to the calculated peak value since the values observed experimentally were below the calculated peak value.

4.4.1. Summary

Holographic recording using dichroic M centres in electron coloured sodium fluoride has not been fully characterised in this chapter, to the same extent as reported for electron coloured potassium bromide and potassium chloride in the previous two chapters. This chapter essentially supports the evidence of a phase contribution present in holograms reconstructed at a wavelength well separated from the peak of the absorption band. The analysis presented in chapter three for mixed gratings has been successfully extended to sodium fluoride.

A major advantage of dichroic holographic recording in sodium fluoride is the possibility of non-destructive readout with visible light. From the experimentation performed for this chapter it would appear that this is not strictly true for room temperature operation. It would seem that there is a small amount of reorientation due to visible absorption but it is thought that this could be eliminated by operation at a lower temperature.

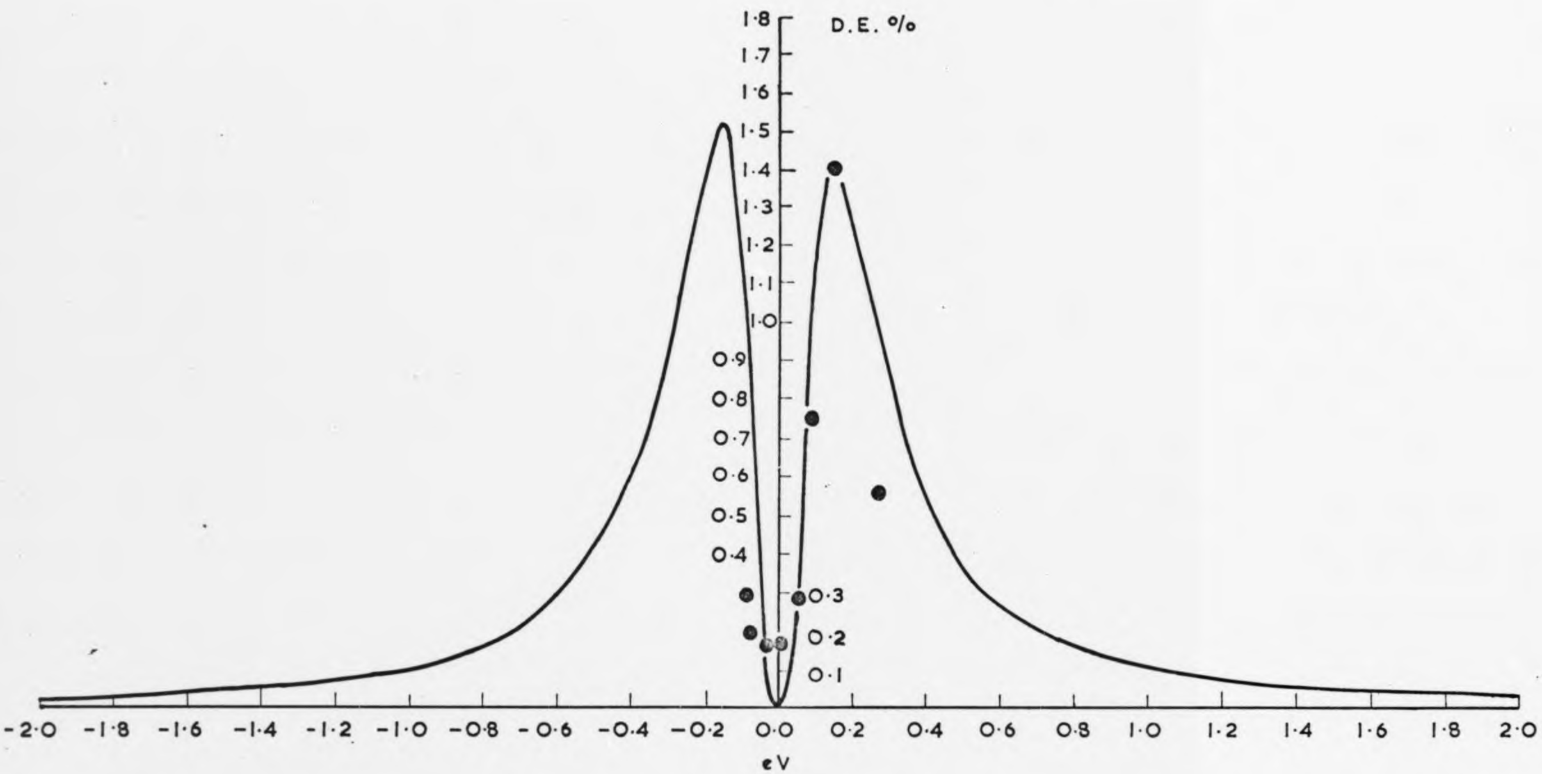

FIG. 4.5. WAVELENGTH SENSITIVITY OF DIFFRACTION EFFICIENCY

REFERENCES

[1] I. Schneider: App. Opts. Vol. 10, No. 4, 980.

2 I. Schneider, M. Marrone, M.N. Kabler: App. Opts. Vol. 9 No. 5, 1163.

3 I. Schneider: App. Opts. Vol. 6, No. 12, 2197.

4 I. Schneider: Phys. Review Letts. 10/24, 1295.

5 An M^+ Centre is a singlely ionised M Centre.

CHAPTER FIVE

BLEACHING KINETICS AND HOLOGRAPHIC CHARACTERISATION OF AN IDEAL PHOTOCHROMIC SYSTEM IN ADDITIVELY COLOURED POTASSIUM CHLORIDE

5.1. Introduction

Previously, photochromics have been considered that have a sensitivity which is less than that which can be achieved ideally in a reversible photochromic system. The most sensitive photochromic process is that which involves electron transfer only, an example of which is the F $\rightarrow$ F' conversion in additively coloured potassium chloride. At low temperatures by exposure to green light the F centre traps another electron to form an F' centre, and this absorbs to the lower energy side of the F band. Under suitable temperature conditions this process can be made reversible. The reaction, either way can have a quantum efficiency of two and this process is analysed in the following section. For a typical F centre concentration of 10^{17} per cm^3 in a crystal 1 mm. thick for F band light of energy 2 eV, the sensitivity can approximately be determined as 1mJoule/cm^2 (assuming a quantum efficiency of two) and this is observed experimentally.

The F $\rightleftharpoons$ F' system approaches an ideal photochromic and in this chapter it is investigated as a fast holographic storage medium. After a preliminary discussion of the process and sample preparation, experiments are described which determine its holographic speed, diffraction efficiency and readout stability. Finally a modified arrangement is considered that involves an electric field assisted F $\rightleftharpoons$ F' process and this will be properly introduced in section 5.4.1.

5.2.1. The Photochromic Material

The F band before and after F band bleaching at 170^{o}K is shown in Fig. 5.1 for additively coloured potassium chloride. Appearing to the low energy side of the F band is the F' band, which is poorly resolved from the F band and is thermally unstable. This process has been extensively covered in the literature [1,2,3]. Shown in Fig. 5.2. are the relative quantum efficiencies for the two reactions - F' $\rightarrow$ F and F $\rightarrow$ F' - as a function of temperature. The F' $\rightarrow$ F conversion takes place in two steps, ionisation of the F' centre to form an F centre, and a free electron which is trapped by an anion vacancy to form

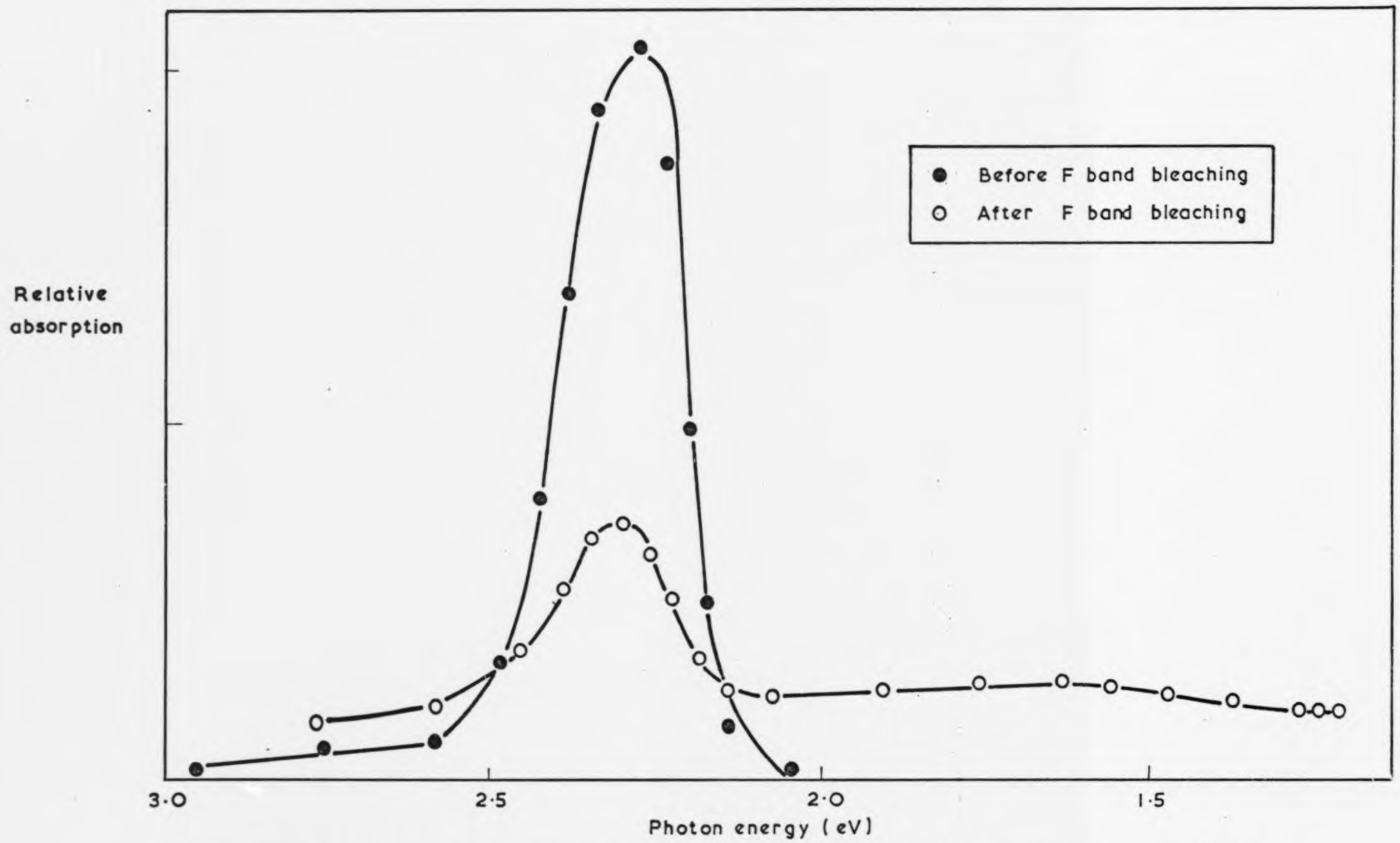

FIG.5.1. THE $F \rightarrow F^{1}$ TRANSITION AT 170°K IN KCℓ FOR $1 \cdot 6 \cdot 10^{16}$ F CENTRES PER cm^3 [2]

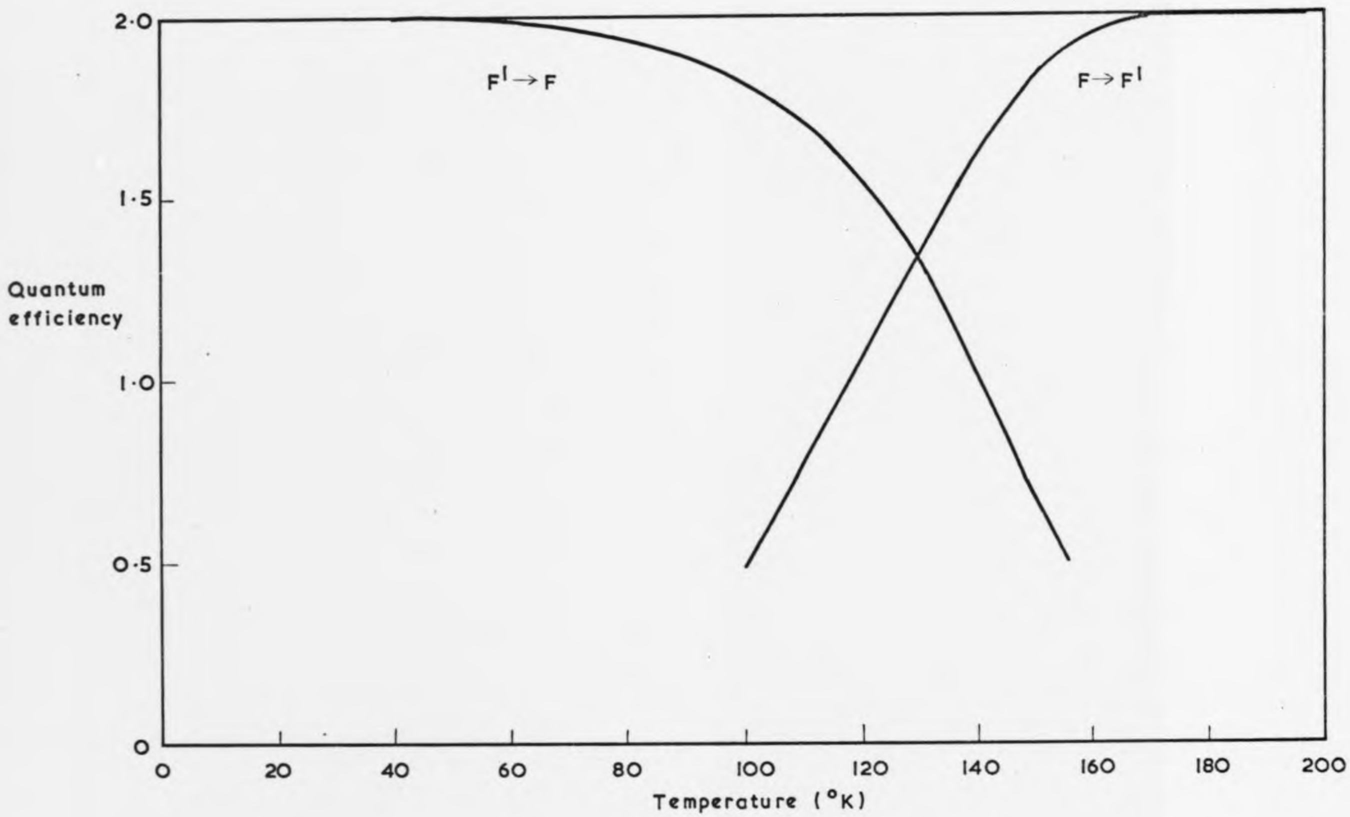

FIG. 5.2. QUANTUM EFFICIENCY TEMPERATURE VARIATION OF THE $F \rightleftharpoons F^{I}$ PROCESS.

another F centre. Hence the maximum allowable quantum efficiency is two, which is the case at $80^{\circ}K$, however at higher temperatures, F centres tend to trap free electrons with greater ease than do anion vacancies and the efficiency of the process decreases. For the F $\rightarrow$ F' reaction the process takes place via an F centre excited state just below the conduction band. Again the maximum permissible quantum efficiency is two since two F centres are destroyed per incident light quanta to provide both the free electron and trapping F centre. As the crystal is cooled below $170^{\circ}K$ thermal ionisation of the electron from the excited state becomes more improbable and the quantum efficiency of the F $\rightarrow$ F' process decreases.

Initially it was thought that holograms formed by bleaching the F band at $170^{\circ}K$ could be readout non-destructively at a lower temperature where the F $\rightarrow$ F' quantum efficiency is virtually zero. However this can not be realised experimentally, because of the overlapping F and F' bands as seen in Fig. 5.1. Destructive readout occurs by bleaching of the induced F' centre concentration by the interrogating F band light.

5.2.2. Crystal Preparation

Additive colouration of potassium chloride was achieved by a process similar to that originally reported by Van Doorn [4,5]. This essentially consists of the modified bomb calorimeter shown in Fig. 5.3. The crystal mounted in a nickel container is heated to $700^{\circ}C$ in an atmosphere of potassium vapour which is cycled around the calorimeter. Above the volume of potassium vapour which is contained by the cooling water jacket is a volume of argon. Since the two gases are in equilibrium it is possible to alter the pressure of the potassium vapour by careful control of the argon pressure without changing the temperature of the crystal. The induced F centre concentration can be varied by alteration of the argon pressure and by experiment it was found that pressures of 600 mTorr were required at a temperature of $700^{\circ}C$ for a period of thirty minutes to produce a suitable F centre concentration of typically 10^{17} - 10^{18} per cm^3.

At the end of the colouration period the calorimeter was plunged into liquid nitrogen in order to cool rapidly the coloured crystal and prevent the excess formation of aggregate centres. Because of the inevitable presence of aggregate centres formed during storage, the crystals after being

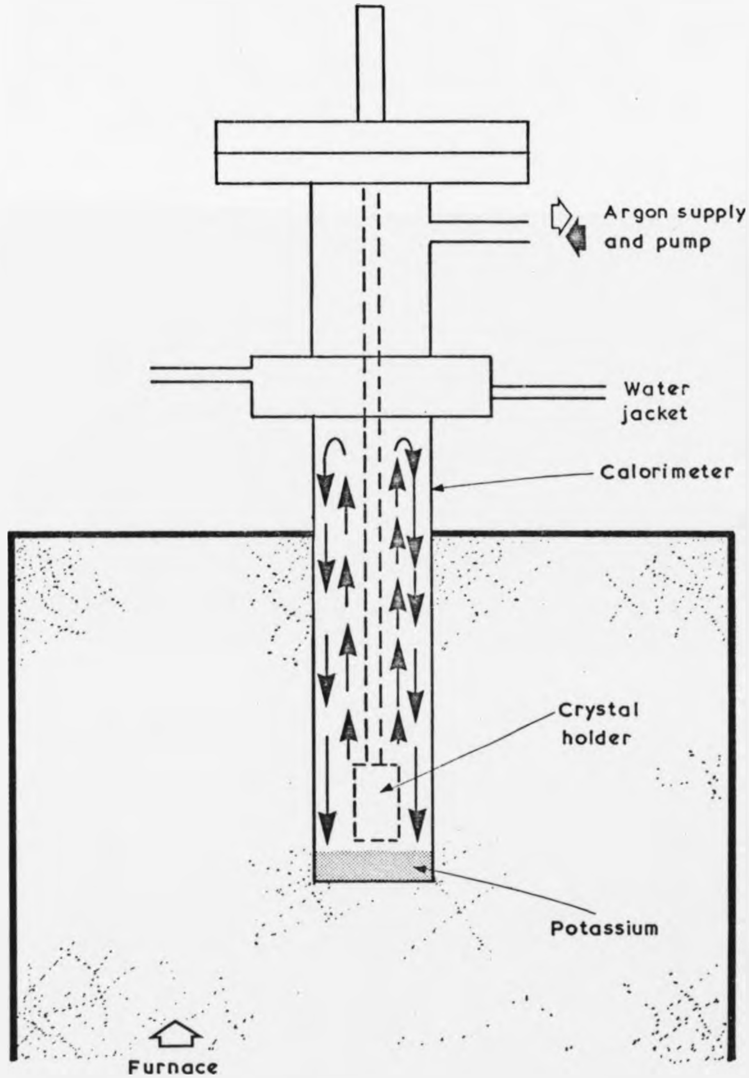

FIG. 5.3. ADDITIVE COLORATION OF POTASSIUM CHLORIDE

cleaved to size for mounting were annealed at 500°C in a red (F' band) safe light. This has the effect of dissociating aggregate centres which would otherwise inhibit the F $\rightarrow$ F' reaction by electron trapping.

5.3.1. Holography using the F — F' Photochromic Process

Holograms were recorded at low temperature in additively coloured potassium chloride using the optical arrangement of Fig. 5.4 which is essentially that used previously. An F' band light source in this case a helium neon laser, is included to be coincident with one of the interfering beams. An exploded schematic of the crystal holder is shown in Fig. 5.5 (the reason for the design of the crystal holder will be fully explained in section 5.4.2. where it is used for the electrophotochromic experiments). Cleaved crystals of size 6 mm.x 6 mm.x $\frac{1}{2}$ mm.were mounted into the low temperature cryostat after annealment. The cryostat is evacuated by means of the diffusion - rotary - adsorption pump arrangement, as used in chapter three, for low temperature vibrationless holography on electron irradiated potassium chloride. Only when the crystal - cryostat assembly has been cooled below 200°K can the crystal be safely exposed to green F band light without fear of damage to the F $\rightleftharpoons$ F' process.

Since non-destructive readout was not possible by cooling, holographic recording was performed at 140°K, where the quantum efficiencies of the F $\rightarrow$ F' and F' $\rightarrow$ F processes are equal. Initially the crystal is given a prolonged F' band exposure to maximise the F centre concentration. The hologram was then written in using either the 514.5 nm.or 488 nm.argon ion laser lines and then interrogated at the same wavelength. Destructive readout decay with time is shown in Fig. 5.6 with the diffracted signal displayed as a negative voltage. For this example an initial holographic exposure of 125 msec was given with an incident intensity of 12 mWatts/cm^2 per beam. Fig 5.6. shows the diffraction with time (the oscillograph time base was 200 msec/cm), and it can be seen that it falls to approximately one tenth of its initial value after a readout exposure of 5 mJoules/cm^2.

For a series of holographic exposures the initial readout diffraction efficiency was determined and is shown in Fig. 5.7(a) for read/write cycling at 514.5 nm. In these experiments the F band equilibrium optical density at 514.5 nm was 1.0. Also shown in Fig. 5.7(b) are the results of the equivalent

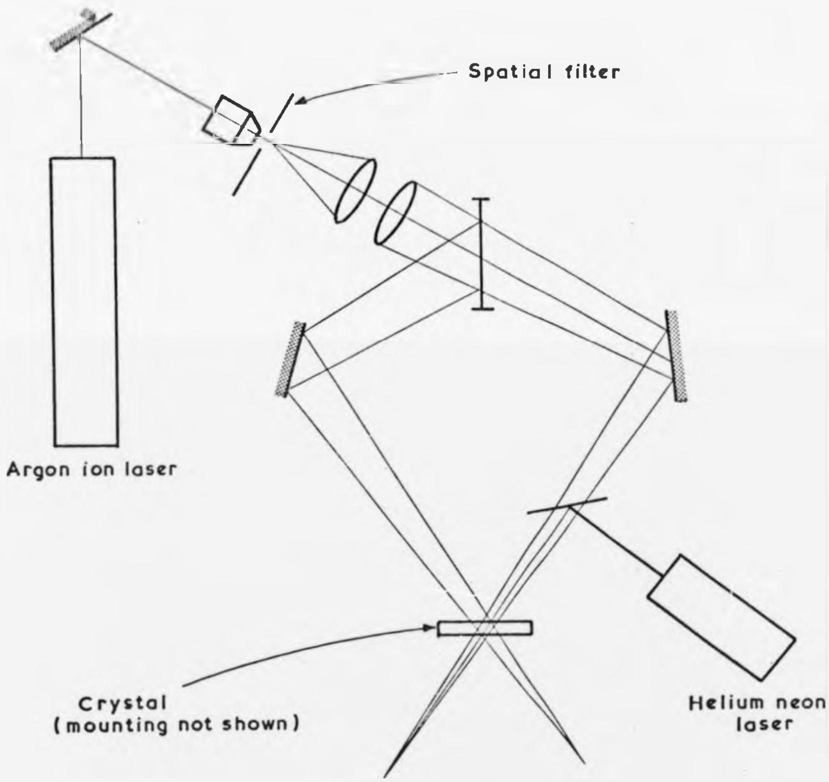

FIG. 5.4. THE HOLOGRAPHIC ARRANGEMENT

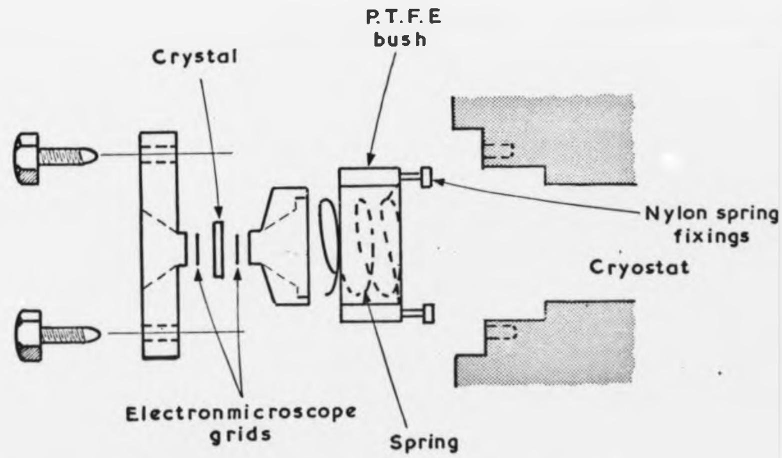

FIG. 5.5. CRYSTAL MOUNTING SHOWING HIGH VOLTAGE ELECTRODE ASSEMBLY

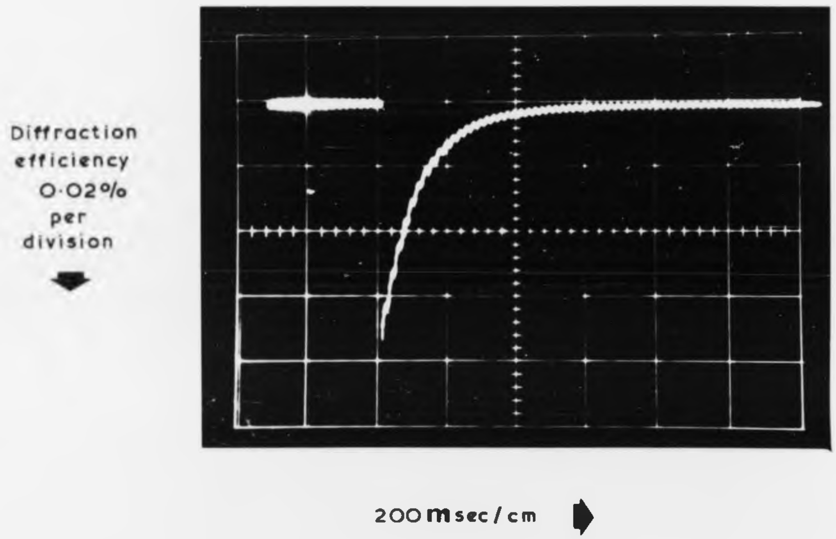

FIG. 5.6 DESTRUCTIVE READOUT OF A HOLOGRAM RECORDED IN ADDITIVELY COLOURED KCℓ

Diffraction efficiency 0·02% per division

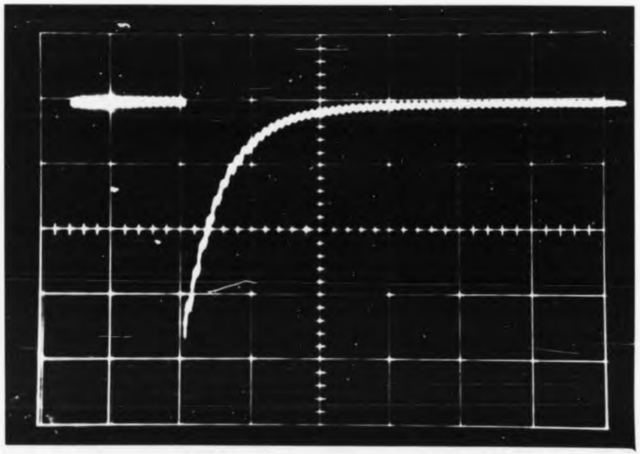

200 msec/cm

FIG 5.6 DESTRUCTIVE READOUT OF A HOLOGRAM RECORDED IN ADDITIVELY COLOURED KCl

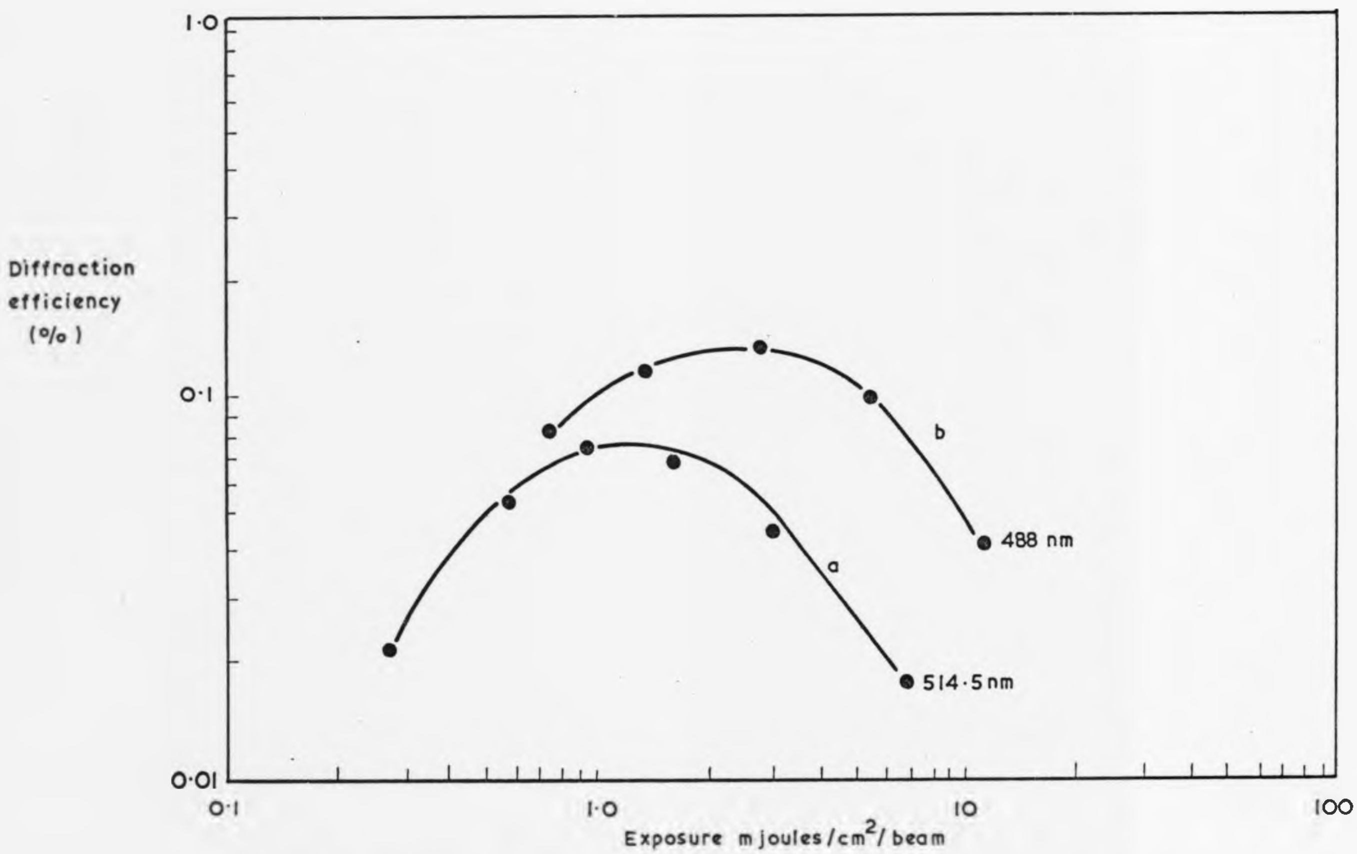

FIG. 5.7. DIFFRACTION EFFICIENCY AS A FUNCTION OF EXPOSURE FOR WRITE/ READ WAVELENGTHS 514·5nm AND 488 nm.

experiment performed at 488 nm.

Maximum diffraction efficiencies of 0.1% were observed for incident exposure of 1 mJoule/cm^2 per beam, at 514.5 nm. Whereas at 488 nm slightly larger efficiencies where seen for incident exposures of 2.5 mJoules/cm per beam. Because of the fixed residual absorption shown in Fig. 5.1 it would not be possible to achieve particularly high diffraction efficiencies, and this is experienced in practice.

5.4.1. An Electrophotochromic System : Introduction

In the photochromic process described previously the F $\rightarrow$ F' process is most efficient at 170°K. This is because of the ionisation of the F centre via an excited state below the conduction band. Thermal energy is required to finally ionise the electron from the excited state. At liquid nitrogen temperatures as explained in section 5.2.1. there is insufficient thermal energy, however here the F $\rightarrow$ F' conversion can be achieved by an electric field induced ionisation [6,7]. Originally it was thought that a non-destructive readout system could be devised with a fast cycle time in the following way. Writing is achieved at liquid nitrogen temperature (L.N.T.) by the application of the electric field and readout effected with the field removed also at L.N.T. where the F $\rightarrow$ F' process is very inefficient. However it was found that non-destructive readout was impracticable due to the overlapping F and F' bands. Induced F' centre concentrations were converted back to F centres due to the favourable F' $\rightarrow$ F process at L.N.T. In spite of this, the electrophotochromic system was investigated as a fast holographic recording medium with destructive readout.

5.4.2. Experimental Operation

Field induced ionisation, known as the Schottky effect, above 20°K occurs because of a reduction in the potential barrier that retains the electron within the negative ion vacancy, resulting in a lowering of the thermal activation energy. At temperatures below 20°K where the effect of field assisted ionisation still occurs tunnelling takes place and this requires a larger field. In the region of temperatures in which the Schottky effect is active the thermal activation is field dependent. For the following experiments at 90°K an electric field of 2. 10^5 volts/cm was necessary to give an F $\rightarrow$ F' quantum efficiency of two.

To investigate electrophotochromic additively coloured potassium chloride as a fast storage, medium high speed write/read experiments were carried out an are reported in the following subsection. Initially in order to determine the read stability 'single shot' experiments were performed. The cryogenic arrangement was identical to that previously reported in this chapter and a full explanation of the special crystal holder and electrode assembly shown in Fig. 5.5. is now given. The crystal is held between the outer copper clamp shown on the lefthand side of the diagram and the spring loaded copper insert to its right. Application of the electric field is achieved by two x 100 electron microscope grids, which are glued to the two clamping apertures with silicone grease prior to crystal loading. The righthand clamp is electrically insulated from the surrounding copper tail of the cryostat by means of the P.T.F.E. bush into which is also fitted the spring's retaining screws. Crystals of thicknesses between 250 μm. and 500 μm were freshly cleaved and mounted as before under safe light conditions and voltages between 5kV. and 10 kV. applied to the grid mesh electrodes to provide fields of 2×10^5 volts/cm. across the crystal. The grid-crystal sandwich had an active area corresponding to the grid size which was 2 mm. in diameter. Maintaining the crystal constantly at 90^{o}K an initial prolonged F band exposure was given using 514.5 nm laser light in the presence of the electric field. This corresponds to the write mode and results in an F' centre concentration increase with a corresponding F band transmission increase. The light, and then field are removed and the crystal reinterrogated with green light. Fig. 5.8. shows the F band transmission as a negative signal after the shutter is re-opened for the read mode. Since the crystal is at a temperature of 90^{o}K the F centre concentration should be stable, however this is not the case in practice. Because of the presence of F' centre absorption at 514.5 nm, F' centres are bleached back to F centres and the F band transmission alters to a new value corresponding to the steady state level on the far right of the oscillograph in Fig. 5.8. The initial part of the trace, which has a time base of 100 msec/cm. indicates the zero light level. Final 'readout' interrogating intensity was 5 mWatts/cm^2 giving an allowable readout exposure of 0.5 mJoule/cm^2 before total decay. Because of the relative sensitivity of the material its high speed operation was examined and fatigue measurements were also made, as part of a general programme of characterisation for possible application to read/write holographic information storage and this is continued in the following section.

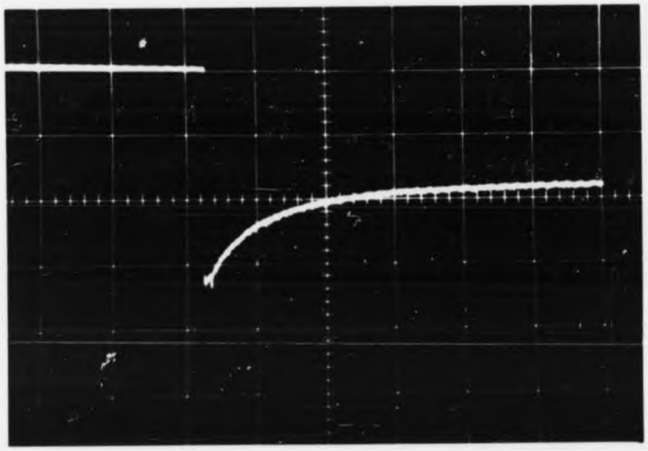

FIG. 5.8. DESTRUCTIVE READOUT OF ELECTRO-PHOTOCHROMIC ADDITIVELY COLOURED KCℓ (Time base 100m sec/cm).

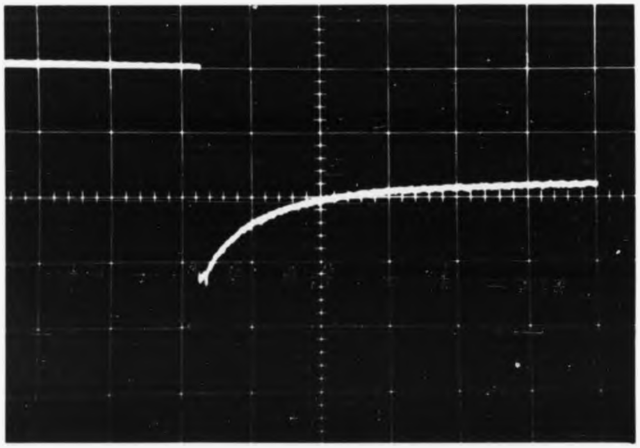

FIG 5.8. DESTRUCTIVE READOUT OF ELECTRO-PHOTOCHROMIC ADDITIVELY COLOURED KCℓ (Time base 100m sec/cm).

5.5.1. High Speed Operation

This section deals with the electrophotochromic effect observed at low temperature in additively coloured potassium chloride cycled in a write-read mode at high speed. Physically the process is as that reported for the 'single shot' experiments in the previous section. High speed cycling was considered necessary in an effort to determine the system's performance under conditions that prevail in a fast read/write optical storage element. A Pockels Cell light modulator was used to provide green 514.5 nm. write/read light pulses at speeds of up to 10 kHz and synchronised to this was a fast rise time transistorised high voltage pulse generator to provide the necessary write conditions. The experimental arrangement was such that it was possible to alter the time duration and relative phase of both the light and E.H.T. pulses. Because of the destructive readout during the read pulse no arrangement for erasure was necessary.

Shown in Fig. 5.9 is the schematic experimental arrangement, the light modulator in this instance providing light pulses of duration 150 μsec with a contrast ratio of 100:1. The incident light intensity was 20 Watts/cm^2. and write pulses occurred when the E.H.T. pulse was applied to the first 80 μsec of the light pulse. Illustrated in Fig. 5.10a is the transmitted light through the crystal as a function of time and this must be compared to the E.H.T. pulse shown in the upper trace of Fig. 5.10b. During the write pulse the F band transmission increases and then decreases due to the destructive readout in the latter part of the light pulse. The lower trace of Fig. 5.10b shows a monitor from the light modulator amplifier and enables a direction comparison of light and E.H.T. pulses. Fig. 5.10c gives the light transmission when the E.H.T. is removed. Each oscillograph has a time base of 100 μsec/cm. and clearly show that induced transmission changes of 50% are possible in 80 μsec with no marked reciprocity failure. The high voltage switch [8] could provide 5 kV pulses with a rise time of better that 10 μsec. Difficulty was experienced in cleaving 250 μm. thick coloured crystals necessary to achieve the correct field strength of 2. 10^5 volts/cm. Although the dielectric strength should increase with decreasing thickness because of impact ionisation [9] this was not found to be the case for cleaved samples. No crystal exceeded 1 hour of continuous cycling without breakdown. However this represents a fatigue test of approximately 2. 10^7 write and read cycles. During this time no noticeable deterioration was observed in the switchable amount of light transmission.

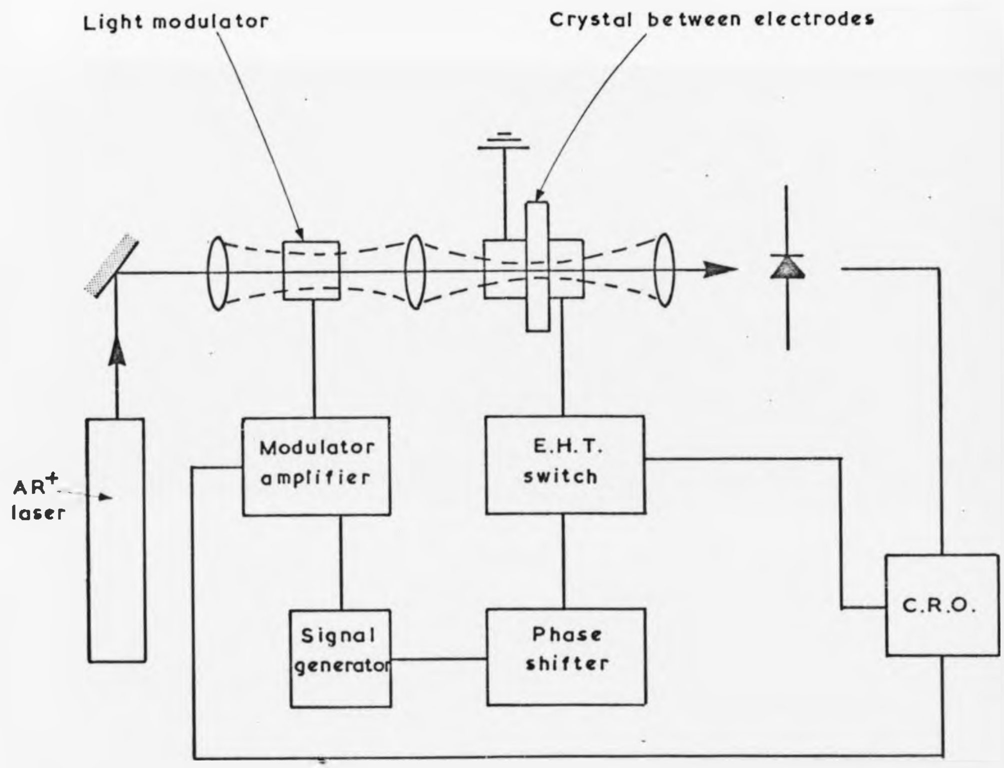

FIG. 5.9. HIGH SPEED OPERATION OF THE ELECTROPHOTOCHROMIC

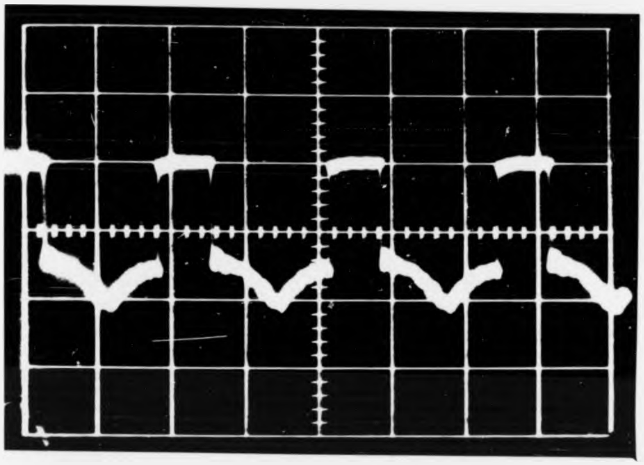

FIG. 5.10(a).

(LIGHT INTENSITY AS A NEGATIVE SIGNAL)

TIME BASE
100 μsec / cm.

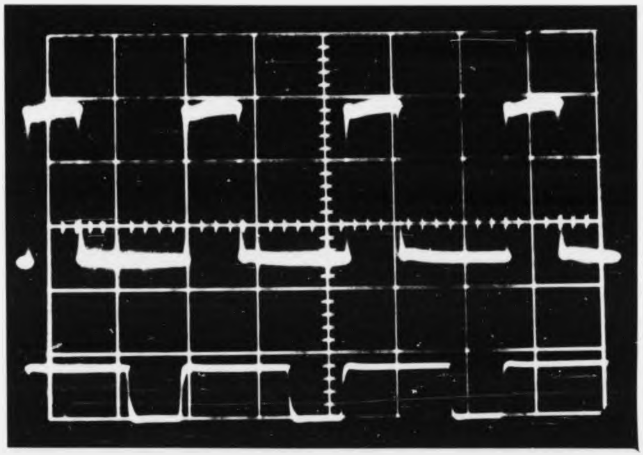

FIG. 5.10 (b).

TIME BASE
100 μsec / cm.

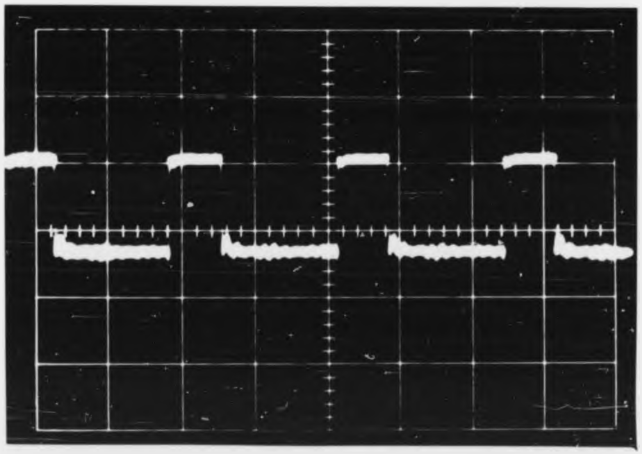

FIG. 5.10 (c).

TIME BASE
100 μsec / cm

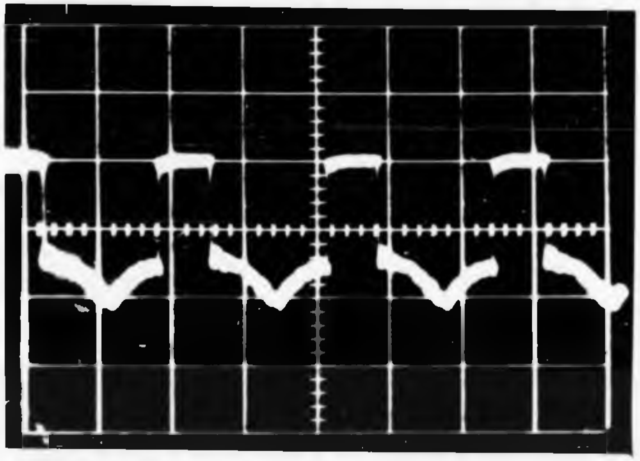

FIG. 5.10(a).
(LIGHT INTENSITY AS A NEGATIVE SIGNAL)
TIME BASE
100μsec/cm.

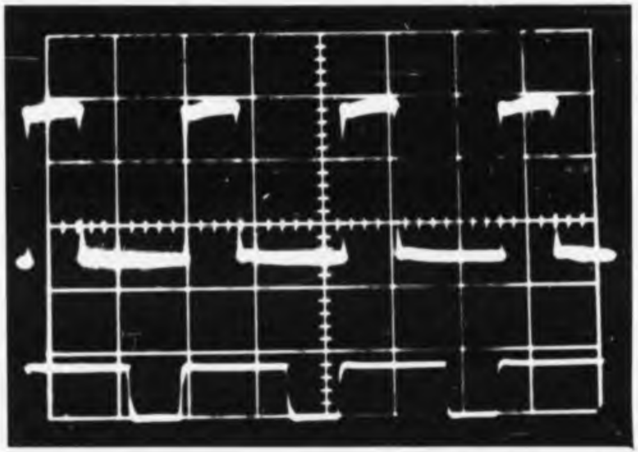

FIG. 5.10 (b).

TIME BASE
100 μsec/cm.

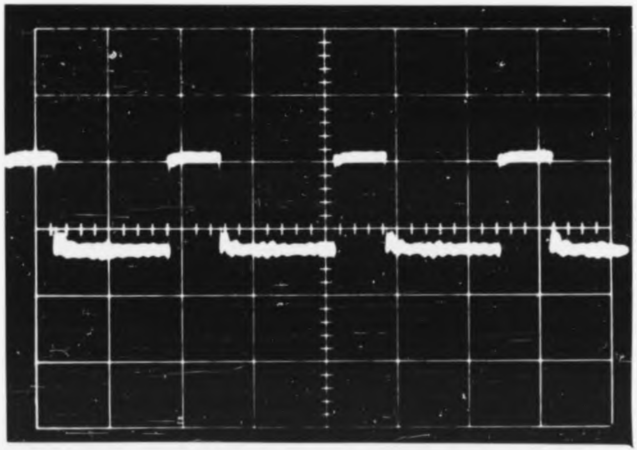

FIG. 5.10 (c).
TIME BASE
100μsec/cm

5.6.1. Conclusion

In summary both photochromic and electrophotochromic F $\rightarrow$ F' systems have been examined for possible application to either direct or holographic reversible information storage. Although in each case the sensitivity approaches that expected from an ideal photochromic, severe destructive readout is experienced for an incident read intensity of only 1 mJoule/cm^2. Additional disadvantages are the necessary operation at liquid nitrogen temperature and the difficulty in obtaining large active areas.

REFERENCES

[1] H. Pick, Nnovo Cimento, V11 Serx. No. 2, 498.

2 Colour Centres in Solids : Schulman and Compton: Pergamon.

3 M.K. Tubbs, D.K. Wright : Phy. Stat. Sol. (a) 7, 155.

4 C.Z. Van Doorn, Philips Res. Rep.; Suppl. No. 4.

5 C.Z. Van Doorn, Rev. Sci. Instr. 32, 755.

6 G. Spinolo, W.B. Fowler : Phys. Rev. Vol. 138 No. 2A, 661.

7 Physics of Colour Centres : Edited by W.B. Fowler : Academic Press.

8 M.D. Lee : Techn. Proc. of Brighton Electro-optics Conf., 207.

9 G.A. Vorob'ev, I.S. Pikalova : Solid State Soviet Physics, Vol 9, No. 4, 755.

CHAPTER SIX

COMPARISON OF RECYCLABLE HOLOGRAPHIC RECORDING MEDIA

6.1. Introduction

This chapter summarises the present 'state of the art' for all forms of reversible holographic recording mediums that require no development. The literature contains many excellent review articles on the subject [1,2]. A short subsection is devoted to each of the many recyclable holographic storage media and this includes other photochromics which were not acknowledged in chapter one's review of recording in coloured alkali halide crystals. All these materials have a possible application to holographic information storage and optical processing systems. Of secondary importance are the display applications. A comprehensive comparison chart is given listing the relative merits and this includes the photochromic and cathodochromics studies in the previous chapters. In this way an assessment of holographic recording in coloured alkali halides can be made.

6.2.1. Inorganic Photochromic Storage Media [3,4,5,6,7 and 8]

There has been particular interest for some time, in the photochromic properties of calcium fluoride doped with Rare Earths and strontium (or calcium) titanate doubly doped with Transistion Metals. Colouration of CaF_2 is difficult unless the crystal has previously been doped with a Rare Earth (e.g. lanthium or cerium). In the case of CaF_2:La a thermally stable absorption is produced in the visible due to a La^{2+}:F centre complex when the crystal is additively coloured. This visible absorption is increased on ultra violet exposure since this results in an electron transfer between the Ca^{2+}:F centre and a La^{3+} ion in a cubic site. The new absorption state is due to both the ionised La^{2+}:F centre and newly created La^{2+} centre. Reduction of the new absorption is possible with red light and holograms have been recorded in this photochromic using a helium neon laser. Reported diffraction efficiencies of 0.4% have been achieved for an incident exposure of 0.2 Joules/cm^2 and these holograms show destructive readout. Thermal relaxation of the induced colouration occurs in CaF_2:La and recorded holograms have lifetimes of no more than 24 hours. For Ce doped CaF_2 lifetimes of 1 week have been achieved; however this material is less sensitive in the recording stage.

Strontium titanate doubly doped with Fe and Mo exhibits photochromism again by a charge transfer process, between the dopants. Holograms have been recorded to 1.2% diffraction efficiency but have short thermal lifetimes of approximately 10–15 minutes.

6.2.2. Thermoplastic Recording [9,10 and 11]

Holograms have been recorded in transparent thermoplastic film. The photosensitive device consists of a combined film structure of thermoplastic and photoconductor as shown in Fig. 6.1. Initially (prior to exposure) the device is sensitized in the dark by the application of an electrostatic charge onto the thermoplastic surface as shown in stage I of Fig. 6.1. Light exposure onto the photoconductor results in a spatially varying discharge of the photoductor as in stage II of Fig. 6.1. The electric field across the thermoplastic remains constant since the charge density remains unchanged. In the third step the device is recharged and the potential of the device restored to its original value, and this results in a spatial variation of the electric field. Stage IV shows the development stage and this requires heating the device, which deforms accordingly, to the attraction of the electric field variations. The phase hologram formed is permanent and may be read non-destructively. Erasure is achieved by reheating the device whereby surface tension effects remove the thickness variations, and return the thermoplastic to its original shape. Diffraction efficiencies of 40% have been reported [10] and although in the writing mode the device has good optical sensitivity (as determined by the photoconductor) the main disadvantage for rapid read/write applications is the long erasure time of typically 20 seconds.

An alternative technique consists of a deformable photoconductor elastomer device [11] which requires no heating but is dependent on the electric field remaining fixed. The lifetime is limited to a few hours with the applied field which when removed automatically erases the stored pattern.

6.2.3. Curie Point Writing of Magnetic Holograms [12,13,14]

Manganese bismuth is a ferromagnetic compound with a large magneto-optic effect and relatively low Curie point at 360°C. Direct [13] and holographic [12] storage has been reported in this medium using a thermomagnetic effect and readout is accomplished by either the Faraday effect in transmission or Kerr effect in reflection. Extremely low diffraction efficiencies have been measured although writing speeds are necessarily fast to prevent thermal

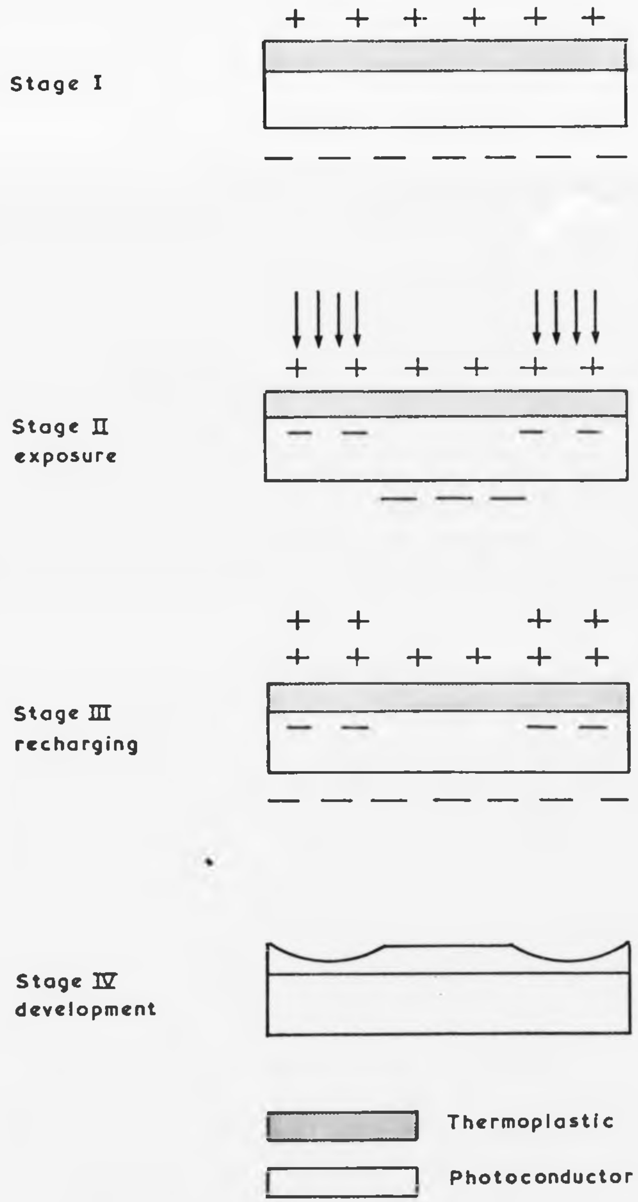

FIG. 6.1. THERMOPLASTIC HOLOGRAPHIC RECORDING.

spreading effects. Locally induced laser heating (corresponding to the holographic interference pattern) causes selective reversal of magnetisation. Regions heated above the curie point, on cooling in the presence of adjacent demagnetising fields of unheated regions become magnetised in the opposite direction. To read the information in transmission use is made of the Faraday rotation effect. Erasure is achieved by the application of a large external saturation magnetic field. Holograms have also been demonstrated in EuO [14] although here the curie point is 69^{o}K and liquid helium operation is necessary.

The main advantage of these materials is that there is non-destructive readout and that they have an indefinite shelf life, however difficulty has been experienced in avoiding hole burning effects in the films which are typically only 1000 Å thick.

6.2.4. Ferroelectric - Photoconductor Devices [15,16]

Ferroelectric Bismuth titanate $Bi_4Ti_3O_{12}$ has an a axis and c axis component of remanent polarisation. The c axis component is switchable by the application of an electric field in the c direction and corresponding to the two states are two orientations of the optical index ellipsoid. The photo - sensitive device consists of a semi transparent electrode - photoconductor - ferroelectric - electrode film structure to which is applied a biasing voltage. Selective exposure onto the photoconductor provides a spatial variation of field across the ferroelectric enabling selective switching of the ferroelectric, copying the incident light interference pattern. Because of changes in the index ellipsoid in the region where there was high intensity incident light it is possible to readout the hologram between two crossed polarisers. Also reported [15] is the possibility of phase readout and this has improved the diffraction efficiency by a factor of ten. Non-destructive readout is achieved by removal of the applied electric field and erasure accomplished by field reversal. Only low diffraction efficiency holograms have been reported and resolution problems are still to be solved.

6.2.5. Electro-optic 'Laser Damage' Holographic Recording [17,18,19,20]

Lithium Niobate is a rhombohedral ferroelectric crystal which exhibits a large electro-optic effect. Although holograms have been recorded in several types of electro-optic materials lithium niobate has been found to be the most promising. The recording process is thought to involve a space charge field effect. Intense parts of the spatial light pattern produces carriers which are then trapped in regions of low light intensity. A charge distribution results corresponding to the original interference pattern, and the space charge field produced modulates the refractive index via the electro-optic effect to generate a phase diffraction grating. Use of doped crystals of $LiNiO_3$ (particularly with Fe) increases the sensitivity because of the increased presence of traps and carriers. Sensitivies of 12 mJoules/cm^2 have been reported [20] to achieve a diffraction efficiency of 0.1%. Although it is possible to produce efficiencies of greater than 40% at the expense of longer exposure times. Permanent fixing of the hologram is possible by heating. This occurs because of the relative mobility of the lattice at higher temperatures while the trapped electronic charge distribution remains unaffected. The ions drift in this field to form an equal and opposite field distribution which on cooling the crystal becomes 'frozen in'.

Recently holographic recording has been reported in a ferroelectric ceramic called P.L.Z.T. (lead-lanthanum titano-zirconate) [21,22], although the relative sensitivity of this material is considerably less than that of $LiNiO_3$ one of the main advantages of this ceramic is the ease with which large area devices can be manufactured.

6.2.6. Miscellaneous Recording Devices

The previous subsections have dealt individually with various recording mediums, in this subsection a brief survey is given of other miscellaneous recording devices that are reversible.

Reversible holographic recording has been reported in certain photochromic organic compounds an example of which is α_2 salicylidene aniline [23] although thermal fading is a severe problem with these types of photochromics. Diffraction efficiencies of 0.14% have been reported with incident green light sensitivities of 20 mJoules/cm^2, and recolouration is achieved by ultra violet exposure. A similar process is that using photochromic glasses [24,25,26] but here again thermal fatigue appears to be an insurmountable problem.

Thin Bismuth films [27] provide an alternative method of recording. Here by using high power pulsed lasers evaporation of the film alters its transmission properties. Cycling is made possible by operation of the evaporant within two surfaces in close proximity. Erasure is achieved by redistribution of the evaporant, uniformly over one surface by exposure to a uniform light intensity.

Other holographic recording materials include chalcogenide glasses where transmission changes occur between the amorphous and crystalline states, and thermochromics where a change of reflectivity is observed when a phase change is induced by heating.

6.3.1. Comparison Chart

This section provides a comparison chart of most known cycleable holographic recording media with particular emphasis on the alkali halides which are treated separately. In the case of other recording mediums only the best known figures are given.

It is customary at this stage to indicate a figure of merit for each material but no attempt will be made here because of uncertainty in its definition.

Medium	Inorganic Photochromic	Thermoplastic	MnBi Film	Ferroelectric Photoconductor	Laser Damage
Write process	Optically induced charge transfer	Electric field induced deformation	Curie point writing	Reorientation of remanent polarisation	Electro-optic effect
Write sensitivity m Joules/cm^2	100 mJoules/cm^2		10	1.0	100 mJ/cm^2
N.D.R.O. non-destructive readout readout process D.R.O. destructive readout	D.R.O.	N.D.R.O. after cooling	N.D.R.O.	N.D.R.O.	Thermal fixing
Erase Process	Same as write	Surface tension effects with heat	External field	Field reversal	Optical redistribution of charge
Erase sensitivity	100 mJoules/cm^2	Allow 20 seconds for cooling	Application of external magnetic field	By field reversal	equal to write sensitivity
Fatigue (maximum cycling number reported)	Indefinite	Tested to 100 times			
Maximum Observed diffraction efficiency	1.2%	40%	0.01% Reflection 0.001% transmission	0.01% in phase 0.001% in birefringence	80%
Material resolution lines/mm (observed)	10^4	4×10^3	3×10^3	800	10^3
Thermal stability	Not very good	Very good	Very good		Quite good
Comments		Difficulty to resolve low spatial frequency		Not very good resolution	
References	3,4,5,6,7,8	9,10,11	12,13,14	15,16	17,18,19,20

Electron Coloured NaCl	Electron Coloured KBr	Electron Coloured KCl	F — X Conversion in KCl + KBr	Dichroic FA Centre Absorption	U Centres in KBr
Electron Colouration					
bleached at 476nm	bleached at 630nm	bleached at 515nm	bleached at higher temperature	reorientation of FA centres	F — U conversion
29 mJ/cm^2	2.10^5 mJ/cm^2	7.10^5 mJ/cm^2	KCl 72 J/cm^2 KBr 36 J/cm^2	5 mJ/cm^2	
R band Readout N.D.R.O	D.R.O. reduced at low temperature	D.R.O. reduced at low temperature	N.D.R.O. after cooling	low temperature N.D.R.O. at 60^oK	N.D.R.O. at 632.8nm
Recolouration			reheating	reorientation	heating
electron dose rate of $10^{15}eV/cm^2$ sec for 2 sec	electron dose rate of $10^{17}eV/cm$ sec for 5 mins				
5.0	no measurement	no measurement			
0.04%	2%	4%	KCl 0.29% KBr 0.28%	0.15%	
at least 10^3 (observed)	at least 10^3 (observed)	at least 10^3 (observed)	at least 10^3 (observed)		
good	achieved by cooling	achieved by cooling	good	achieved by cooling	good
$\bar{e}$ beam damage to surface - lost of resolution			storage retained after 3 years		very insensitive

Dichroism of M centres in NaF	F' — F conversion in KCl
reorientation	electron transfer
100 mJ/cm^2	1 mJ/cm^2
N.D.R.O. probable by cooling	D.R.O.
reorientation	electron transfer
approximately 100 mJ/cm^2	1 mJ/cm^2
	10^5 measured
	0.1%
at least 10^3 (observed)	at least 10^3 (observed)
good	good
loss of M centre concentration on cycling	fast D.R.O. operation at 77^{o}K

6.4.1. Conclusion

This thesis has characterised the holographic recording performance of coloured alkali halide single crystals. These materials show extremely good resolution properties. It has been shown in chapters three and four, both experimentally and theoretically, that there is a phase contribution to the diffraction efficiency and this manifests itself in a characteristic M shaped wavelength sensitivity. The main disadvantage of the electron coloured and additively coloured systems considered here is that destructive readout occurs. Although this effect is almost completely eliminated in dichroic M centre recording as reported in chapter Four. Cathodochromic materials have been shown to be inherently low in sensitivity; however for the F $\longrightarrow$ F' system studied in chapter Five, the sensitivity approaches that of an ideal photochromic. Obviously these materials cannot complete, in sensitivity, with photographic emulsions where gain occurs during the development stage.

The photochromics and cathodochromics studied in the experimental chapters of this thesis compare very favourably with other alkali halide recording mediums. At present it is clear from consideration of the chart in section 6.3.1. that there exists no ideal reversible holographic recording medium. However it is likely that each of the before mentioned mediums has a potential application in holographic recording.

REFERENCES

[1] J. Bordogna, S.A. Keneman, J.J. Amodei, R.C.A. review Vol. 33, No. 1, 227.
2 M.R. Tubbs, Optics and Laser Techn., Aug. 1973, 155.
3 R.C. Duncan, R.C.A. review, Vol. 33, No. 1, 248.
4 Z.J. Kiss, I.E.E.E., J. Quan. Elect. Q.E.5, No. 1, 12.
5 J.J. Amodei, D.R. Bosomworth: App. Opt. Vol. 8, No. 12, 2473.
6 R.C. Duncan Jr., B.W. Faughnan, W. Phillips: App. Opt. Vol.9, No. 10, 2236.
7 D.R. Bosomworth, H.J. Gerritsen, App. Opt. Vol. 7 No. 1, 95.
8 M. Chomat, M. Miler, I. Gregora: Opto. Com. Vol. 4, No. 3, 243.
9 L.H. Lin, H.L. Beaucham: App. Opt. Vol. 9, No. 9, 2088.
10 T.L. Credelle, F.W. Spong: R.C.A. review, Vol. 33, No. 1, 206.
11 N.K. Sheridon: I.E.E. electron devices meeting, Oct. 1970.
12 R.S. Mezrich: App. Phys. Letts. Vol 14, No.4, 132.
13 R.W. Cohen, R.S. Mezrich: R.C.A. review, Vol. 33, No. 1, 54.
14 G. Fan, K. Pennington, J. Greiner: Journal of App. Phy. Vol. 40, No. 3, 974.

15 S.A. Keneman et al, App. Opt. Vol. 9, No. 10, 2279.

16 S.A. Keneman et al, App. Phys. Lett. 17, 173.

17 J.J. Amodei, D.L. Staebler: R.C.A. review, Vol. 33, No. 1, 71.

18 W. Phillips, J.J. Amodei, D.L. Staebler: R.C.A. review, Vol. 33, No. 1, 94.

19 F.S. Chen, App. Phys. Letts. Vol 13, 223.

20 D.L. Staebler, W. Phillips, Apps. Opts. Vol. 13, No. 4, 788.

21 F. Micheron, C. Mayeux, J.C. Trotier: App. Opts. Vol. 13, No. 4, 784.

22 F. Micheron, G. Bismuth: I.E.E.E. Meeting on Optical Storage of Digital Data March 1973, MB3-1.

23 D.S. Lo, D.M. Manikowski, M.M. Hanson: App. Opts. Vol. 10, No. 4, 978.

24 G.K. Megla: App.Opt. Vol. 5, No. 10, 945.

25 V.I. Sukhanov, D.N. Sitnik, I.V. Tuuimanova, V.A. Tsekhomskiy, Optical Techn. Vol. 37, No.12, 796.

26 G.K. Megla, Optics and Laser Tech. Vol. 6, No. 2, 49.

ACKNOWLEDGEMENT

I would like to thank Professor A.J. Forty and the department of Physics (University of Warwick) for making this research possible. Also the Science Research Council and The Plessey Company for financial support. In particular I would like to thank Dr. M.R. Tubbs and Mr. P. Waterworth my University and Industrial supervisors. Finally I would like to mention Mr. M.D. Lee (Plessey) for provision of the E.H.T. transistor switch used for the electrophotochromic experiments and Mr. D.C.J. Reid (Plessey) for useful discussions on holographic techniques.

THICK HOLOGRAMS BY KBr SINGLE CRYSTALS CONTAINING COLOUR CENTRES

G.E. SCRIVENER and M.R. TUBBS
Department of Physics, University of Warwick, Coventry CV4 7AL, UK

Received 16 August 1972

A helium–neon laser has been used to record holograms in KBr single crystals containing colour centres introduced by electron irradiation. Holograms recorded in crystals with coloured layers between 6 and 500 μm thick have diffraction efficiencies up to 2.3% and show marked orientation sensitivity.

1. Introduction

Recent experiments have shown that coloured alkali halide crystals containing F-centres (electrons trapped at negative ion vacancies) can be used for graphic or digital optical information storage [1]. A page organised optical information store with data stored as holograms would have advantages over a store using direct digital recording. The holographic store would have a larger capacity, higher data rate and better immunity to defects on the storage plane. Reversible holographic storage on alkali halide crystals has been reported previously [2, 3] but the measured diffraction efficiencies were only of order 0.01% so that coloured crystals have not seriously been considered for holographic storage applications. We wish to report some experiments on holographic recording in coloured KBr single crystals which have given diffraction efficiencies of 2 to 3%. These efficiencies are approximately two orders of magnitude larger than those reported previously for colour centre holograms [2, 3] and nearly one order of magnitude larger than the efficiencies obtained with photochromic CaF_2 crystals [4, 5].

2. Photochromic KBr crystals

A holographic grating recorded on a photochromic material gives a high diffraction efficiency only if a large modulation can be achieved (i.e., a large optical density difference between bright and dark fringes). This requirement is only partially met by CaF_2:La crystals in which the maximum and minimum optical densities are 0.7 and 0.4 [4] or KCl crystals containing F_A centres with values 1.7 and 1.15 respectively [2]. The optical density of KBr crystals which have been electron irradiated at room temperature (RT) can only be reduced from 1.4 to 0.65 after extended illumination [6]. However, if a KBr single crystal is irradiated at liquid-nitrogen temperature (LNT) and warmed to room temperature in the dark, its response is very different; illumination in the F-band (at 625 nm) with 6328 Å light from a He/Ne laser steadily reduces the F-band optical density to zero from initial values of 1.5 or more. This behaviour occurs because illumination induces vacancy/interstitial recombination [6]. Illumination of a crystal irradiated at room temperature, on the other hand, leads only to vacancy aggregation because the increased mobility of interstitials during irradiation at room temperature enables them to form stable complexes which are unable to recombine with vacancies or F-centres. The vacancy aggregate centres formed in this case have absorption bands in the F-band region so that it is not possible to reduce the optical density at the F-band by more than 50–60%.

The photochromic response at RT of a KBr crystal which has been coloured by electron irradiation at LNT is illustrated in fig. 1 (curve a) which shows the

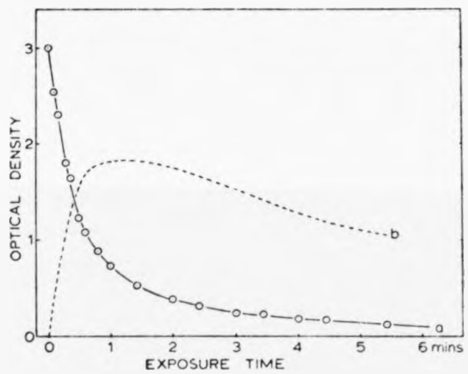

Fig. 1. The photochromic response of a coloured KBr crystal. The variation of optical density with time of exposure (to 350 mW cm^{-2} of 6328 Å) is shown in curve (a) and the variation of the modulation with time (for β = 0.1) in curve (b).

variation of F-band absorbance with exposure to 25 mW He/Ne laser illumination. Previous work [6] has shown that the optical density varies only with the absorbed energy (intensity × exposure time) for a wide range of intensities. This kinetic behaviour leads to some interesting consequences. If two regions of a crystal are simultaneously illuminated, one with an intensity I and the second with a lower intensity, βI, then the difference in optical density between the two regions initially increases but then remains approximately constant. This behaviour is illustrated by curve b of fig. 1 which shows the time dependence of the density difference (calculated from a) for a 10:1 intensity ratio (β=0.1). The density difference increases rapidly at first but then remains constant with a slow decrease after long exposures. The constant density difference will be determined by the value of β and will be approximately proportional to $\log(1/\beta)$ since the reduction in optical density is proportional to log(absorbed energy) [6]. A large difference in optical density can only be achieved with a small value of β.

3. Experimental arrangement

Potassium bromide single crystals obtained from Rank Precision Industries are cleaved, mounted in a low-temperature cryostat and irradiated a LNT with fast electrons from a 20–400 keV Van de Graaff electron accelerator. A coloured crystal is then warmed to room temperature in the dark and mounted in a cell containing index matching liquid. The irradiated crystals are coloured only in a thin surface layer; the thickness of this layer varies from 6 μm at 20 keV to 500 μm at 350 keV. The coloration depth for low-energy electrons (E<50 kV) is given by the formula of Shul'man and Gel [7] but this relationship leads to a severe over-estimate of the coloration depth for higher electron energies. There is a non-linear variation of colour density through the coloured layer and we have obtained the best results by illuminating coloured crystal plates oriented with the coloured surface facing away from the incident light beams.

Hologram gratings are recorded on coloured crystals using a standard arrangement in which light from a 25 mW helium–neon laser passes through a spatial filter, beam expander and a beam splitter and the two beams recombine at the sample plane, each beam being inclined at an angle of approximately 15° to the normal to the crystal surface. More complex holograms have been recorded by placing transparencies in one of the two beams. Holograms are "read" by illuminating them with the reference beam only at reduced intensity to minimize erasure. The read stability can be greatly increased by cooling the crystal and holograms can readily be erased by an extended exposure to uniform read light and by re-irradiation with fast electrons.

4. Results

The variation of diffraction efficiency with exposure time for a deeply coloured KBr crystal illuminated with an intensity of 80 mW cm^{-2} during the formation of a hologram grating is illustrated in fig. 2. The diffraction efficiency (defined as the ratio of diffracted to incident intensity) increases rapidly at first, reaches a maximum efficiency of 2.33% and then decreases more slowly. The peak diffraction efficiency appears to be larger for samples with large initial optical densities. The peak efficiencies and initial optical densities for a number of crystals coloured

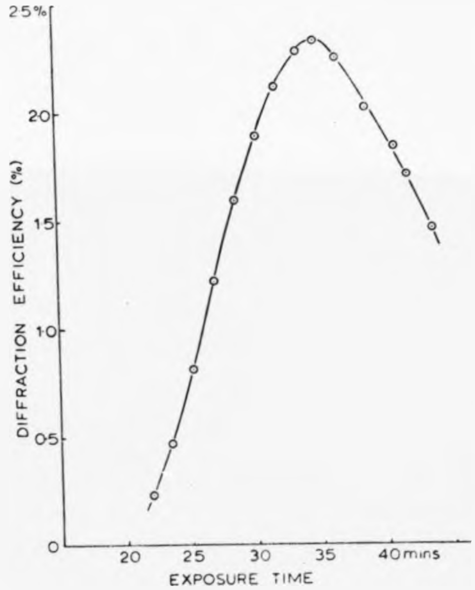

Fig. 2. The variation of the diffraction efficiency of a KBr hologram grating with time of exposure (to 80 mW cm^{-2} of 6328 Å).

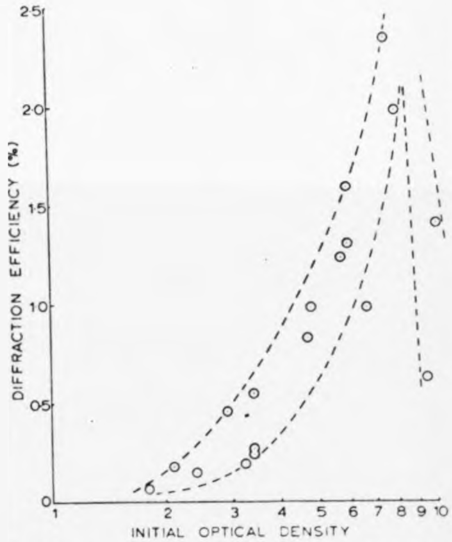

Fig. 3. The peak diffraction efficiencies of KBr hologram gratings recorded on crystals with various initial F-band optical densities.

at approximately 350 keV are plotted in fig. 3: the peak efficiency does not appear to continue increasing for initial optical densities exceeding 7.0 to 8.0. This might be associated with the effects of vibration which are more important for the longer exposure times needed for heavily coloured crystals.

More complex holograms have been recorded on KBr crystals and fig. 4a shows a transparent object seen through a KBr crystal while fig. 4b shows an image of this transparency reconstructed from a KBr hologram.

The coloration depth is sufficiently large for KBr holograms to show the marked angular sensitivity characteristic of thick holograms. The variation of diffraction efficiency with angular deviation from the Bragg setting – the rocking curve – is illustrated in fig. 5 for a crystal with a coloured layer 122 ± 6 μm thick. A relatively thin coloured layer was chosen so that the angular width of the peak was much greater than the beam divergence. The relative efficiency has dropped to one half of its peak value for an angular deviation of approximately 33 minutes of arc. If one assumes that the orientation sensitivity varies as $\mathrm{sinc}^2 x$ [4] the data for fig. 5 (with all parameters corrected to their values in the crystal) predict a grating thickness of 90 μm, rather less than the measured coloration depth.

5. Discussion

The efficiency (η) of an absorption grating hologram at Bragg incidence is

$$\eta = \exp[-2D_0/\cos\theta_0] \sinh^2[\tfrac{1}{2}D_1 \cos\theta_0] ,$$

where θ_0 is the angle of incidence in the medium, D_0 is proportional to the average optical density and D_1 to the optical density modulation [8]. Our coloured

(a) (b)

Fig. 4. (a) An object transparency photographed through a KBr crystal. (b) A photograph of the image reconstructed from a KBr hologram.

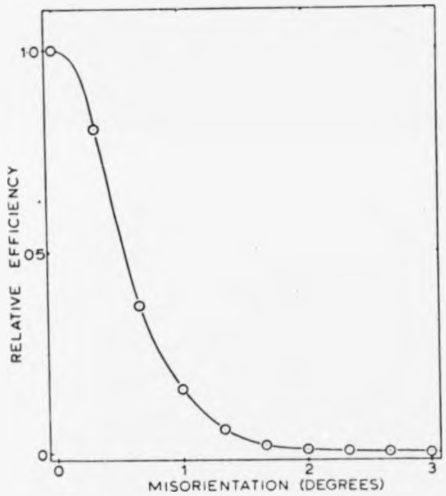

Fig. 5. The variation of the diffraction efficiency of a KBr hologram (coloured layer 120 μm thick) with angular deviation from the Bragg condition.

KBr crystals are exposed to a grating pattern with an intensity I at the bright fringes and βI at the dark fringes ($\beta<1$). The diffraction efficiency will initially increase rapidly as D_1 increases and will continue to increase after D_1 reaches its constant value (determined by the value of β) since D_0 continues to decrease. After an extended exposure, D_1 will gradually decrease, D_0 will also decrease but the efficiency will decrease because the $\sinh^2$ term varies more rapidly than the exponential; the efficiency may also be reduced after long exposures by the effects of vibration. Crystals with large initial optical densities may well have larger efficiencies because the effective value of β will be smaller for that part of the crystal furthest from the incident light.

The maximum diffraction efficiency of 2.33% obtained so far with KBr is less than the maximum of 3.7% predicted for a perfect absorption grating [8]. The dispersion relations predict that a refractive index or phase modulation will be associated with the absorption modulation and will contribute to the measured diffraction efficiency. We estimate that the phase grating contributes less than one quarter of the total efficiency of our KBr gratings. We hope to unambiguously demonstrate the presence of a phase contribution in other materials where the laser wavelength is further from the peak of the colour centre absorption band and efficiencies exceeding 3.7% should be attainable.

The rocking curve for thick KBr holograms (fig. 5) differs from the expected sinc^2 distribution in that there are no secondary maxima. The secondary maxima are seen for gratings in CaF_2:La [4] but are not well defined because the gaussian laser beam cross section has been convoluted with the sinc^2 intensity variation and this modifies the rocking curve to give a finite intensity at the position of the first "zero" and reduces the visibility of the secondary maxima [9]. The secondary maxima do not appear at all in our rocking curves because the grating contrast varies throughout the thickness of the coloured layer as β is effectively larger at the illuminated surface. There is a Fourier transform relationship between $f(z)$, the variation of fringe contrast with depth in the crystal and the variation of diffracted light with angle, $g(\theta)$ which was first noted for the diffraction of light by acoustic waves [10]. Thus, if $f(z)$ has a gaussian or exponential form, the secondary maxima in $g(\theta)$ will disappear. The effective width of $g(\theta)$ will also be increased and this explains why the grating thickness calculated from fig. 4 (assuming a sinc^2 intensity variation) is less than the coloration depth.

6. Conclusion

Thick volume holograms with diffraction efficiencies between 2 and 3% have been recorded at room temperature on KBr single crystals coloured by electron irradiation at low temperature. The variation of grating contrast with depth in these thick holograms leads to a characteristic modification of the rocking curve and the absence of secondary maxima. Colour centre materials will offer considerable advantages for reversible holographic recording if the high diffraction efficiencies and good angular sensitivity described in this paper can be combined with the high photochromic sensitivities reported previously [1].

Acknowledgement

One of us (G.S.) wishes to thank the Science Research Council for the award of a research studentship.

References

[1] M.R. Tubbs and D.K. Wright, Phys. Stat. Sol. A7 (1971) 155.
[2] F. Lanzl, V. Röder and W. Waidelich, Appl. Phys. Letters 18 (1971) 56.
[3] A.S. Macklin, Appl. Opt. 9 (1970) 1658.
[4] D.R. Bosomworth and H.J. Gerritsen, Appl. Opt. 7 (1971) 95.
[5] M. Chomat, M. Miler and I. Gregora, Opt. Commun. 4 (1971) 243.
[6] M.J. Redman and M.R. Tubbs, Phil. Mag. 24 (1971) 1059.
[7] A.R. Shul'man and E.P. Gel, Fiz. Tverd. Tela 2 (1960) 524.
[8] H. Kogelnik, Bell Syst. Tech. J. 48 (1969) 2909.
[9] G.L. Francois and A.E. Siegman, Phys. Rev. 139A (1965) 4.
[10] C.F. Quate, C.D.W. Wilkinson and D.K. Winslow, Proc. IEEE 53 (1965) 1604.

THICK PHASE HOLOGRAMS IN COLOUR CENTRE MATERIALS

G.E. SCRIVENER and M.R. TUBBS
Department of Physics, University of Warwick, Coventry CV4 7AL, UK

Received 18 October 1973

Thick holograms have been recorded in single crystals of KCl and NaF containing colour centres introduced by electron irradiation. Diffraction efficiencies up to 4.2% are reported and near an absorption band there is a characteristic 'M' shaped variation of efficiency with wavelength. These observations show that there is a strong phase contribution to the diffraction efficiency and a simple model is used to describe the properties of such mixed holograms.

1. Introduction

Thich or volume holograms with diffraction efficiencies between 2 and 3% can be recorded with a He–Ne laser in KBr single crystals which have been suitably coloured by electron irradiation [1]. In this case the visible coloration is caused by F-centres and the F-band peaks at 625 nm, close to the He–Ne line at 632.8 nm. These KBr holograms are thus absorption holograms and readout is achieved largely by diffraction from spatial variations of optical density. The measured variation of diffraction efficiency with angular deviation from the Bragg condition (the 'rocking curve') does not show the usual secondary maxima because of the way in which the modulation varies with depth. The refractive index of a crystal varies in the neighbourhood of a strong absorption band in such a way that the change in index is very small near the absorption peak but reaches a maximum near the half-power points of the absorption band. We have thus studied the characteristics of holographic gratings formed in coloured KCl and NaF where laser lines are available to explore the diffraction efficiency at several wavelengths spread over the region of absorption. These measurements reveal that there are both phase and absorption contributions to the efficiency and show that the phase contribution dominates at wavelengths away from the absorption peak. A single classical oscillator model for a colour centre absorption band is used to predict the positions of peak diffraction efficiency for holograms with various modulation depths and background absorption levels.

2. Mixed holograms gratings

The diffraction efficiency of a mixed, unslanted, thick transmission hologram grating is [2]

$$\eta = \left\{ \sin^2\left(\frac{\pi n_1 d}{\lambda \cos\theta_0}\right) + \sinh^2\left(\frac{2.3 D_1}{4\cos\theta_0}\right)\right\} \times \exp\left\{-\frac{2.3 D_0}{\cos\theta_0}\right\}, \tag{1}$$

where θ_0 is the Bragg angle, d the hologram thickness, and n_1 and D_1 are the amplitudes of the modulation of the refractive index and optical density respectively while D_0 is the average optical density. The first and second terms in this expression refer to the phase and absorption contributions to the diffraction efficiency respectively. There are two ways in which one may demonstrate experimentally that a substantial phase contribution is present. The first is to note that, if $n_1 = 0$, the absorption term in (1) predicts a maximum diffraction efficiency $\eta_m = 3.7\%$ when $D_0 = D_1$ and $D_1/\cos\theta_0 = 0.95$. A measured efficiency greater than 3.7% would thus indicate the presence of a phase contribution. However, this conclusion is only strictly valid for sinusoidal gratings and, if a recording material has a substantially non-linear exposure characteristic, an efficiency greater than 3.7% might be possible. Indeed, if one compares sine wave and square wave gratings of the same amplitude, the fundamental Fourier component of the square wave grating will have an amplitude which exceeds that of the sine wave grating. One would thus expect a peak efficiency exceeding 6% for a square wave absorption grating. Experiments with photographic emulsions have given efficiencies exceeding 5% but it is not clear that these gratings had a square wave profile or that no phase contribution was present [3]. A characteristic variation of diffraction efficiency with wavelength provides the second method of identifying a phase contribution. For example, a hologram grating may be formed by exposing the material to a laser wavelength lying at the absorption peak until maximum efficiency is reached (i.e. the modulation is large and the background absorption small). The diffraction efficiency will then be lower for other wavelengths if only the absorption term of 1 is important. However, if the phase term contributes, there will be an 'M' shaped variation of efficiency with wavelength over the absorption band since the phase term is large near the half power points of the absorption band. This characterisitc 'M' shape could only be obtained for a pure absorption hologram if the initial exposure was chosen to give maximum efficiency at a wavelength near the half power point since D_0 and D_1 would then have values which were too large or too small for wavelengths on either side of this.

3. Mixed holograms for a single oscillator absorption

It is useful to consider the diffraction efficiency for a mixed grating when n_1 is simply related to D_1 in eq. (1). The single classical oscillator is a convenient example where the absorption and phase vary with wavelength as follows:

$$D_x = \frac{D_{max}}{4x^2+1}; \qquad \frac{2\pi d \delta n}{\lambda} = 2.3\, x D_x, \tag{2}$$

where $x = \delta\omega/W$ with $\delta\omega$ the frequency difference between the peak and that frequency at which the optical density is D_x, W the half-width (fwhh) of the absorption band, d the thickness of the coloured layer and δn the difference between the index at x and that of the crystal in the absence of any absorption. We have assumed that W is much less than the peak absorption frequency and in the following we will assume $\lambda \approx \lambda_{max}$. The variation of optical density and of normalized path difference $\delta n d/\lambda_{max}$ with wavelength for this single oscillator are illustrated in fig. 1. We note that $\delta n d \lambda_{max}^{-1}$ has a maximum value of 0.092 D_{max} at $x = \frac{1}{2}$ and that the optical path is changed by $\lambda/2$ for $D_{max} \approx 5.5$. If we assume that the optical density of the hologram grating varies from D_0 in exposed regions to $D_0 + 2D$ in unexposed regions, we can combine (1) and (2) to give

$$\eta = \left\{ \sinh^2\left(\frac{B}{4(4x^2+1)}\right) + \sin^2\left(\frac{Bx}{2(4x^2+1)}\right)\right\} \times \exp\left\{-\frac{B(1+b)}{(4x^2+1)}\right\}, \tag{3}$$

where $B = 2.3D/\cos\theta_0$ and $D_0 = bD$. For diffraction efficiencies of a few percent (i.e. for most colour centre materials) we can take $\sinh z \approx \sin z \approx z$ and show that the peaks in the 'M' shaped plot of efficiency versus frequency will occur for

$$x = \left(\frac{B(1+b)-1}{4}\right)^{1/2}, \tag{4}$$

and for observation at a specific wavelength $x = a$ we expect peak efficiency for an optical density given by

$$B \approx \frac{2(4a^2+1)}{1+b}.$$

The efficiency at the peak in each case initially varies as $(4x^2+1)(1+b)^{-2}$. The values of x at which the peaks in the curve of efficiency versus wavelength occur for various B are shown by the dotted lines in fig. 1 for $b=0$ and $b=1$; $\sin z$ and z differ by 10% when $x = 1.5$ for $b=0$ and $x=3$ for $b=1$. The dash-dot line indicates the approximate value of B needed to achieve maximum efficiency at that x for $b=0$. When $b=0$ we find peak efficiencies for $x = \pm\frac{1}{2}$ with $B \approx 2$ (or an optical density modulation of 0.87 for θ_0 small); at $x = \pm 1$ one requires $B \approx 5$ (or $D \approx 2.2$). High diffraction efficiencies are clearly obtained at large x and for small values of b. The reason for this is apparent from fig. 1 where the phase change is seen to decrease much more slowly than the optical density as one moves out from $x = 0.5$. The argument of the sin term in (3) needs to be multiplied by λ_{max}/λ when one can no longer assume $\lambda_{max} \approx \lambda$. The efficiency is thus multiplied by $1+4(\lambda_{max}/\lambda)^2$ near $x=1$ and this alters the symmetry of the 'M' shaped variation of efficiency with wavelength. The long-wave portion has a distinctly lower peak efficiency than the short wave part for $x \gtrsim 1$. The efficiencies differ from the mean by some

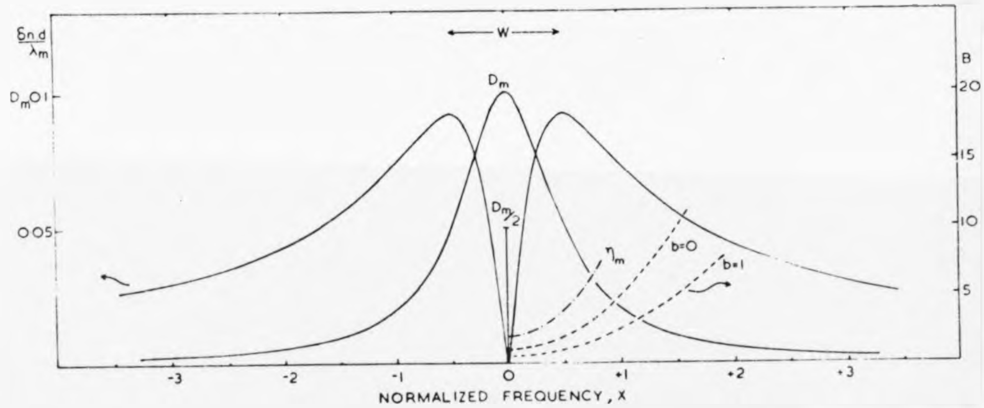

Fig. 1. The variations of optical density and optical thickness ($\delta n d \lambda_{max}^{-1}$) with normalized photon energy (x) for a single classical oscillator (full lines). The position of peak holographic diffraction efficiency for various modulation depths (denoted by B) is given for two values of the background absorption parameter b by the dotted lines. The dash dot line shows the value of B required for maximum efficiency at any x. The curves would be symmetrical about $x = 0$.

16% when λ_x differs from λ_{max} by 10%. For large efficiencies or more complex absorption structures it is necessary to compute the variation of efficiency with wavelength using (1) with the observed $D(\lambda)$ and $n_1(\lambda)$ calculated from $D(\lambda)$ via the dispersion relations.

4. Experimental results

The growth of diffraction efficiency with exposure time for a grating recorded on photo-cathodochromic KCl at room temperature is illustrated in fig. 2. This sample was coloured by electron irradiation at liquid nitrogen temperature using the technique described previously for KBr [1]. The hologram grating was recorded and interrogated using the 514.5 nm argon laser line. This wavelength is close to the half power point of the F-band in KCl. The peak efficiency in this case was 4% and an efficiency of 4.2% has been achieved at 502 nm. These figures compare with a maximum efficiency of 2.3% for KBr [1] and suggest the presence of a phase contribution to the efficiency in KCl.

The photodichroic absorption spectrum of an electron coloured NaF single crystal is shown in fig. 3. This sample contained a large concentration of M centres which absorb in the green (507 nm) for electric vector along the centre axis [which must lie in a (110) direction] and which can be reoriented to another (110) direction by light absorbed near 350 nm and below (absorption active for electric vector perpendicular to the centre axis) [4]. The absorption spectra of fig. 3 show that a large proportion of M centres can be oriented so that they absorb in the green for light polarized along one (110) direction in the plane of the crystal but not in the perpendicular

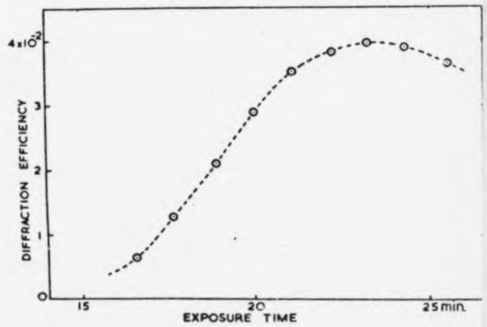

Fig. 2. The variation of diffraction efficiency with exposure time for a holographic grating recorded on photocathodochromic KCl.

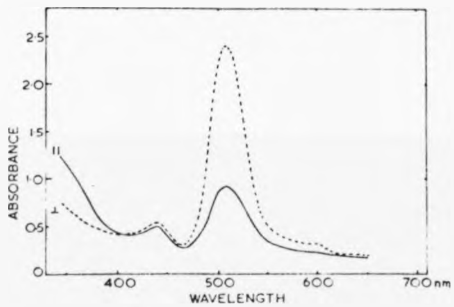

Fig. 3. The photodichroic absorption spectrum of a coloured NaF crystal containing M-centres.

(110) direction; the situation is reversed in the ultraviolet. A hologram grating was recorded on a coloured NaF crystal with the 350.7 nm krypton laser line until an efficiency near maximum was obtained at 514.5 nm; the efficiency was then monitored non-destructively at other wavelengths near the absorption band with the crystal oriented for maximum efficiency in each case. The results are shown in fig. 4 and clearly follow the characteristic 'M' shape expected for a phase hologram. We note that peak efficiency occurs for $x \approx 0.83$ and, using $b = 1$, $B \approx 1.7$ (as suggested by fig 3), we would expect $x \approx 0.8$ from eq. (4). The agreement is satisfactory. The peak efficiency predicted by (3) for $x = 0.8$, $B = 1.7$, $b = 1$ is 1.9% with the phase term being substantially larger than the absorption term: we have observed efficiencies up to 0.8%. It is usual

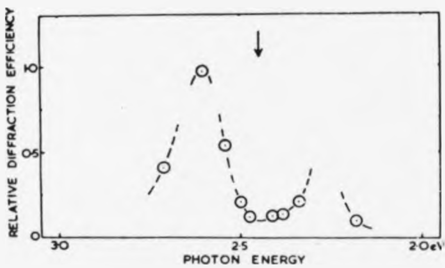

Fig. 4. The variation of diffraction efficiency with photon energy for a hologram grating on coloured NaF. The arrow indicates the peak of the M-band.

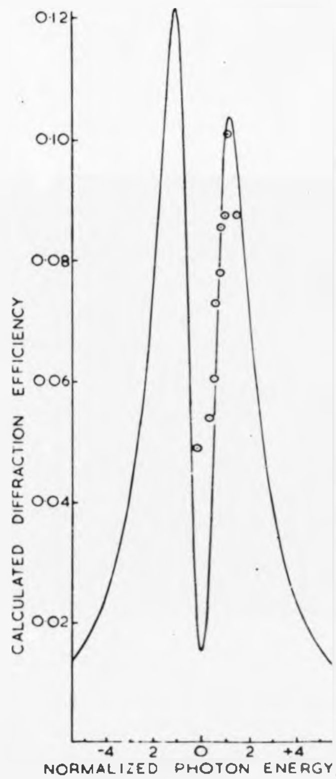

Fig. 5. The variation of diffraction efficiency with photon energy for a hologram grating on coloured KCl. The full line is the computed variation while the circles are normalized experimental points.

for practical efficiencies to be only some 50% of the theoretical maximum.

Experimental measurements of the variation of efficiency with wavelength for holograms recorded at 514.5 nm on photocathodochromic KCl are represented by the circles in fig. 5. The full line shows the variation of diffraction efficiency with wavelength computed via (1), with a lorentzian approximation to the F-absorption band which does not involve the assumptions $\delta w \ll W$, $\lambda \approx \lambda_{max}$ used to obtain (3). The computed variation of η with x shows the characteristic

'M' shape with the expected asymmetry between the efficiency at the two peaks; the experimental points (normalized to peak efficiency) follow this line quite well. We note that peak efficiency occurs at 476.5 nm or $x \approx 1$ while (4) would predict $x = 1$ for $b = 0.1$ and $B = 4.6$ (values suggested by bleaching experiments carried out to indicate the magnitudes of the modulation and background absorption for our KCl samples). An efficiency of about 11% is predicted by (3) for $x = 1$, $B = 4.6$, $b = 0.1$ (with a correction for $\lambda_{max} = \lambda$) while efficiencies up to 4.2% have been obtained in practice. The phase contribution is much larger than the absorption one under these conditions. Indeed, it would not be possible to explain the observations without a phase contribution both in view of the large observed efficiencies and, particularly, since with recording at 514.5 nm one could not obtain a variation of η with x which peaked at 476.5 nm rather than 514.5 nm (the possibility described at the end of section 2).

5. Conclusions

Experimental results have been described which show that there is a substantial phase contribution to the holographic diffraction efficiency of photochromic colour centre materials which leads to peak efficiencies exceeding 4% and to a characteristic 'M' shaped variation of efficiency with wavelength. A single oscillator model for a colour centre absorption enables one to predict the wavelength at which peak efficiency will occur for various combinations of background absorption and modulation depth. Diffraction efficiencies of several percent can be obtained at wavelengths well removed from the absorption band. This can simplify the design of opto-electronic devices using colour centre or photochromic holographic materials since one can select a read-out wavelength from those laser lines available in a substantial frequency range near the absorption band. This is particularly useful for holograpl storage devices [5] where an intense laser line may not quite coincide with a particularly useful colour centre absorption band or where one wishes to reduce the separation of 'write' and 'read' wavelengths in devices using thick storage page holograms.

Acknowledgements

We wish to thank the Science Research Council for a generous grant towards the apparatus used for this work and one of us (G.E.S.) acknowledges the award of an S.R.C. Studentship.

Note added in proof

The referee has kindly drawn our attention to a paper by H. Nassenstein and J. Eggers [6] who report that a hologram with a coloured interference structure recorded in a photographic emulsion also shows a wave length selective reconstruction with peak diffraction efficiency occurring at wavelengths on either side of the absorption band. This is also attributed to the presence of phase modulation.

References

[1] G.E. Scrivener and M.R. Tubbs, Opt. Commun. 6 (1972) 242.
[2] H. Kogelnik, Bell Syst. Tech. J. 48 (1969) 2909.
[3] C.R. Bendall, B.D. Guenther and R.L. Hartman, Appl. Opt. 11 (1972) 2992.
[4] I. Schneider, M. Marrone and M.N. Kabler, Appl. Opt. 9 (1970) 1163.
[5] M.R. Tubbs, Optics and Laser Tech. 5 (1973) 155.
[6] H. Nassenstein and J. Eggers, Phys. Letters 28a (1968) 141.